MSc in Water and Environmental Engineering

Effects of increased wastewater discharge

Hjørring wastewater treatment plant

Tautvydas Butenas and Philipp Meier

June 2020

Tautvydas Butenas and Philipp Meier

Effects of increased wastewater discharge. Hjørring wastewater treatment plant

MSc in Water and Environmental Engineering, June 2020

Supervisor: Associate Professor Asbjørn Haaning Nielsen

Aalborg University

The Faculty of Engineering and Science

"Why can't a tree be called Pluplusch?"

Hugo Ball, 1916
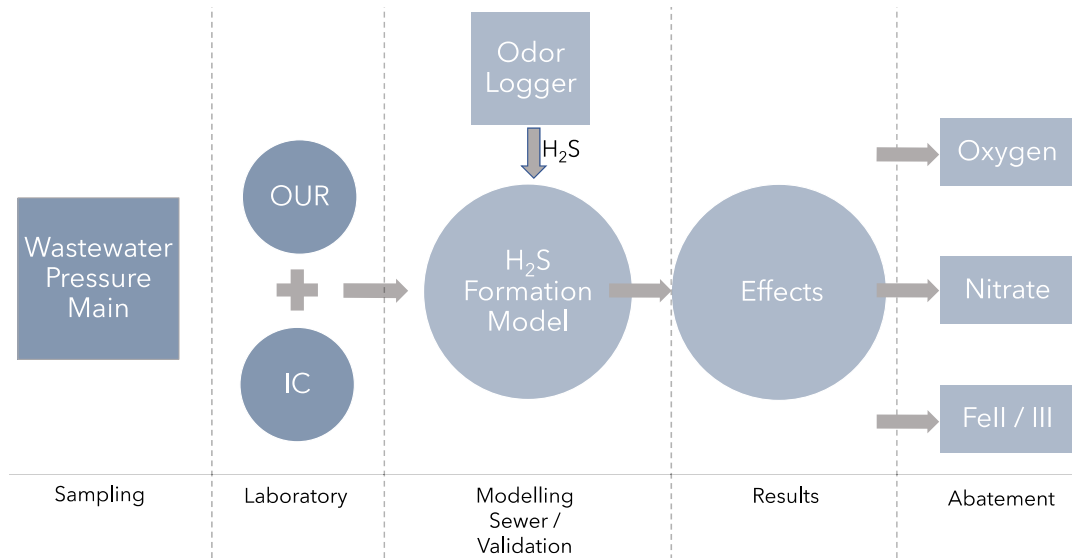
Preface

This report is a result of the master program at 4th semester of Water and Environmental Engineering to fulfill the requirements for obtaining a Master of Science (M.Sc.) degree. The thesis deals with the effects of increased wastewater load on the wastewater treatment plant in Hjørring, Denmark.

Aalborg, Denmark, June 2020

Abstract

The Master thesis deals with effects of increased wastewater loading on Hjørring Wastewater Treatment Plant and the interactions between long force mains in the sewer system and wastewater treatment processes. The goal of the thesis is to investigate both, positive and negative, effects of this increase. The Master thesis is carried out in several steps. First, the wastewater influent is characterized in terms of composition and biodegradability. This includes volatile fat acids (VFA) measurements on wastewater samples, which were done in the laboratory. Furthermore, respirometry experiments were carried out to measure oxygen uptake rate (OUR). The aim of this is to characterize the wastewater organic matter composition, that accounts for possible sulfide formation and investigate sulfide abatement methods. For this case two experimental wastewater treatment reactors were constructed. In addition, negative impacts of sulfide generation in the sewer system were quantified by placing an odor sensor at the inlet to the wastewater treatment plant (WWTP) to measure volatilized sulfides. Laboratory data serves as a basis for setting up models describing wastewater transformations. Models were used to simulate wastewater transformations with wide array of parameters. Sulfide abatement methods were implemented into mathematical models to investigate possible sulfide control methods that would be

applicable in the site of the thesis. Monte Carlo simulations were carried out to account for uncertainties. After laboratory experiments, measurement campaign and simulations were completed, results were discussed in a report and conclusions were drawn. Visual abstract above illustrates workflow throughout this master thesis.

Contents

List of Figures

List of Tables

Symbol Reference

Symbol	Description	Unit
μ_H	Maximum specific growth rate of X_{BW}	d^{-1}
$k_{h,fast}$	Hydrolysis rate constant of $X_{S,fast}$	d^{-1}
$k_{h,slow}$	Hydrolysis rate constant of $X_{S,slow}$	d^{-1}
K_S	Saturation constant of S_S	g COD m^{-3}
$K_{X,fast}$	Saturation constant, hydrolysis of $X_{S,fast}$	g COD g COD^{-1}
$K_{X,slow}$	Saturation constant, hydrolysis of $X_{S,slow}$	g COD g COD^{-1}
q_m	Maintenance energy requirement rate constant	d^{-1}
S_S	Readily biodegradable substrate	g COD m^{-3}
S_f	Fermentable substrate	g COD m^{-3}
S_A	Fermentation products	g COD m^{-3}
S_O	Dissolved oxygen	g O$_2$ m^{-3}
X_{Hw}	Heterotrophic biomass in water phase	g COD m^{-3}
$X_{S,fast}$	Fast hydrolysable substrate	g COD m^{-3}
$X_{S,slow}$	Slowly hydrolysable substrate	g COD m^{-3}
Y_H	Yield constant of X_{BW}	g COD g COD^{-1}
BOD_5	Biological oxygen demand	g O$_2$m^{-3}
COD	Chemical oxygen demand	g O$_2$m^{-3}
COD_{sol}	Chemical oxygen demand (solved)	g O$_2$m^{-3}
T	Temperature	°C
r	Hydraulic radius	m
a	Coefficient for sulfide production	-
rH$_2$S	Rate of H$_2$S transfer	g S m^{-2}h^{-1}
k$_L$a	Mass transfer rate	d^{-1}
H$_2$S$_{aq}$	Dissolved H$_2$S in liquid phase	g S m^{-3}
H$_2$S$_{aq}^*$	Equilibrium H$_2$S$_{aq}$ Concentration	g S m^{-3}
H$_2$S$_T$	Fraction of total dissolved H$_2$S concentration	g S m^{-3}
pKa	Dissociation constant	-
Y_{HW}	Suspended biomass yield constant for heterotrophics	g COD g COD^{-1}
K_O	Saturation constant for dissolved oxygen	g O$_2$ m^{-3}
α_W	Temperature coefficient in water phase	-
$k_{1/2}$	1/2 order rate constant	g O$_2^{0.5}$ m$^{-0.5}d^{-1}$
Y_{HF}	Biofilms yield constant for heterotrophics	g COD g COD^{-1}

Symbol	Description	Unit
S_{H_2S}	Dissolved sulfide	g S m^{-3}
K_{SF}	Saturation constant for readily biodegradable substrate	g COD m^{-3}
ϵ	Efficiency constant for biofilm biomass	-
α_F	Temperature coefficient in the biofilm	-
h_{fe}	Anaerobic hydrolysis reduction rate	-
q_{fe}	Maximum rate for fermentation	d^{-1}
K_{Fe}	Saturation constant for fermentation	g COD g COD^{-1}
k_{H2S}	H$_2$S production rate constant	g S m^{-2} h^{-1}
α_S	Temperature coefficient for H$_2$S production	-
i	sulfide oxidation rate	[g S m^{-3} day^{-1}]
$k_{S(-II)}$	Rate constant for chemical oxidation of H2S	(g S m^{-3})$^{1-mc}$(g O$_2$ m^{-3})$^{-nc}$ day^{-1}
$m \, and \, n$	Reaction order	-
i_c	Chemical sulfide oxidation rate	g S m^{-3} day^{-1}
i_b	Biological sulfide oxidation rate	g S m^{-3} day^{-1}
k_{H_2Sc}	Rate constant for chemical oxidation of H2S	(g S m^{-3})$^{1-m}$(g O$_2$ m^{-3})$^{-n}$ day^{-1}
k_{HS^-c}	Rate constant for chemical oxidation of HS-	(g S m^{-3})$^{1-m}$(g O$_2$ m^{-3})$^{-n}$ day^{-1}
$k_{S(-II)b}$	Rate constant for biological sulfide oxidation	(g S m^{-3})$^{1-m}$(g O$_2$ m^{-3})$^{-n}$ day^{-1}
K_{a1}	First dissociation constant for sulfide	-
$\omega_{S(-II)b}$	Optimum pH range for heterotrophic processes	-
μ_{H,NO_3}	Maximum specific growth rate	d^{-1}
Y_{NO_3}	Yield constant for heterotrophic biomass	mol e-eq (mol e-eq)$^{-1}$
K_{S,NO_3}	Saturation constant for S_S	g NO$_3$-N m^{-3}
μ_{H,NO_2}	Maximum specific growth rate	d^{-1}
Y_{NO_2}	Yield constant for heterotrophic biomass	mol e-eq (mol e-eq)$^{-1}$
K_{S,NO_2}	Saturation constant for S_S	g NO$_3$-N m^{-3}
f_n	Fraction of nitrate reducing biomass	-
X_{HVN}	Heterotrophic biomass under anoxic conditions	g COD m^{-3}
k_{anoxic}	Maximum sulfide anoxic oxidation rate	g S m^{-3} h^{-1}
$K_{s,anoxic}$	Saturation constant for anoxic sulfide oxidation	g S m^{-3}
$[S(-II)_{t=0}]$	Concentration of total dissolved sulfide at t=0	µM S
$[S(-II)_{end}]$	Sulfide concentration at equilibrium	µM S
α_{obs}	Observed reaction order	-
$k_{obs,20}$	Observed rate constant	(µM S)$^{(1-\alpha_{obs})}$ s^{-1}
OUR	Oxygen uptake rate	g L^{-1} h^{-1}
q_{O_2}	Specific oxygen uptake rate	g g^{-1} h^{-1}

Introduction

The purpose of a functional wastewater treatment plant (WWTP) is the production of clean effluent via removal of nutrients, organic matter, metals and other pollutants present in wastewater. These components would eventually cause oxygen depletion and thereby provoke negative impacts for flora and fauna in the receiving waters. After the first water action plan in 1987, WWTPs in Denmark constantly undergo considerable upgrades and nowadays most of the wastewater in Denmark is treated at the biggest and most modern WWTPs in the country (Niero et al., 2014). In this context modern unavoidably means economically viable, which, consequently leads to the fact, that, at least for now, most advanced wastewater treatment solutions lies with centralisation of WWTPs (Henze, 1997; Libralato et al., 2012). This conclusion is especially viable in developed countries, where sewer infrastructure is prevalent and well established, therefore centralisation is relatively inexpensive, because there is no need for a completely new sewer systems.

Such is the case with WWTP in the city of Hjørring, located in Northern part of Denmark. The WWTP, which treats wastewater from the municipality, recently received substantial additional inflow of various industrial wastewater. This addition by itself does not seem to be problematic. On the contrary: this industrial wastewater is rich in easily biodegradable substrate, which only enhances performance of WWTP. However, transportation of wastewater can be problematic. The long force mains, which are used for transportation of wastewater, are a suitable environment for the formation of hydrogen sulfide, which is not only characterised by unpleasant smell, but also acts a a corrosive agent and is toxic at higher concentrations.

With this Master Thesis, small scale positive and negative effects of centralisation of wastewater treatment are investigated based on a case study of Hjørring WWTP. Investigation in the thesis also goes beyond WWTP and looks into interactions between long force main in the sewer system and wastewater treatment processes. Afterwards, possible sulfide abatement methods are investigated and evaluated in respect to Hjørring WWTP.

Research questions

<div style="text-align: right">2</div>

The focus of this Master Thesis lies in the understanding and analyses of complex relations between wastewater treatment efficiency, increased wastewater loads and transformation processes of wastewater. Challenges in understanding these relations rises not only from intricate composition of wastewater, domestic as well as industrial, but also in the microbial transformations wastewater undergoes in long force mains as well as in WWTP. The case of Hjørring WWTP is selected for this research, because this treatment plant recently started to receive wastewater from different industries from the city of Vrå. Here the largest amount of wastewater is generated from a laundry, hatchery and a marmalade industry. Previously the resulting wastewater from this industries were treated in Lyngby WWTP. While Hjørring WWTP is still able to treat influent wastewater efficiently, changes in dynamics of wastewater transportation and treatment processes undoubtedly develops.

The aim of this study is to investigate the interactions between the long force main in the sewer system and wastewater treatment processes at increased loads of VFA rich wastewater. In addition to the identification of hydrogen sulfide causing factors, the concentrations of hydrogen sulfide at the inlet structure of WWTP is of major interest, as well as its consequences for further treatment. After the transformations of wastewater with and emphasis on sulfide formation are defined, possible sulfide abatement methods are investigated and modeled to represent the problem at hand as well as possible solutions.

In order to solve the aforementioned problem, a strategy consisting of three main stages is devised. Firstly, a literature review is carried out, section 3. Afterwards, laboratory experiments are done in order to describe wastewater and its transformations, section 4. Where laboratory work proofs to be insufficient, mathematical models to describe wastewater transformations are introduced, section 4, section 6. These models are used to simulate wastewater transformations with a wide array of variable wastewater quality parameters continuously. After all laboratory work and modeling is complete, results are discussed and conclusions are drawn.

In the laboratory influent wastewater is characterized in terms of composition and biodegradability, presented in section 5. This includes volatile fatty acids (VFA) on wastewater samples. Measurements are

done by employing methods of ion chromatography. Furthermore, respirometry experiments are carried out to measure oxygen uptake rate (OUR). The aim of this is to characterize wastewaters organic matter composition. For this case, a couple of experimental wastewater treatment reactors are assembled and tested. Finally, sludge tests are performed to investigate the direct impact of the inflowing wastewater on WWTP. In addition, negative impacts of sulfide generation in the sewer system are quantified by placing a hydrogen sulfide gas sensor at the inlet to the wastewater treatment plant (WWTP), which provides continuous in-situ data of hydrogen sulfide concentration in gas phase. Experiments also serve as a basis for setting up mathematical models for simulations of wastewater transformations under a continues prolonged time interval with variable wastewater quality parameters. Models also serve as a tool to introduce, investigate and evaluate possible sulfide abatement methods in a pressure main from Vrå to Hjørring. Data from simulation runs is presented in section 7. The thesis is rounded up with a discussion section 8, where acquired laboratory data and modeling results are implement together with data provided by Hjørring WWTP in order to present a comprehensive analysis of problem at hand.

Overview of in-sewer transformations, role of sulfide. Hjørring WWTP

<div align="right">

3

</div>

This part contains a general overview of wastewater transformations in the sewers with an emphasis on presence of sulfide. A glimpse to the historical evolution in understanding sulfide role in sewer system is made, which, to an extent, is reflected throughout the thesis. Analysis of Hjørring WWTP and its operational data is carried out. The chapter serves as preparation for the methodical analysis of the problem in question and as a basis for further detailed investigations and laboratory work.

3.1 In-sewer wastewater transformations with presence of sulfide

Sulfur is unavoidably present in sewage. As part of the organic substance in living cells (e.g. thiol proteins, amino acids), sulfur contributes 1% to the organisms dry matter. In terms of sulfur presence in wastewater, potable water contains 4 g S/(Person $\cdot$ d). The vast majority is present as sulfate, which promotes the H_2S formation under anaerobic conditions. The input from domestic sources can be determined with approximately 7 g S/(Person $\cdot$ d), Table 3.1. However, sewage from industries can contain high sulfate concentrations (for example industrial cleaning products with sulfuric acid) and, occasionally, sulfide can be present as well. Table 3.1 illustrates, that sulfur with its variety of different forms (ions) is a integral part everyday life and, therefore, is always present in wastewater.

In-sewer transformations

Wastewater is a product of domestic and industrial activities. While domestic wastewater mostly consists of washing water with human excreta, hygiene products and additional substances, such as detergents,

Table 3.1: Person equivalent total sulfide in domestic sewage, adapted from (Frey, 2008)

Origin	Total Sulfur g Person^{-1} d^{-1}	
	Koppe/Strozek (1999)	Barjenbruch (2005)
Urine	1.3	1.3
Faeces	0.2	0.2
Detergent		
Na$_2$SO$_4$ sulfide	3.0	0.5–1
Tenside sulfide	0.5	0.15–0.5
Kitchen waste	0.2	0.2
Freshwater	4.0	3.4
Sum raw sewage	9.2	5.8–6.6

oils, etc., composition of industrial wastewater varies immensely depending on the type of industry. All wastewater is disposed into sewers, where it flows (possibly with addition of rainwater and infiltration) towards the wastewater treatment plant. Wastewater is transported through gravity and pressure sewers with occasional pumping stations in between. Wastewater in gravity sewers is exposed to the sewer atmosphere, therefore aerobic (and in some cases anoxic) processes takes place there, whereas in pressure pipes anaerobic processes develop, Table 3.2. Under aerobic conditions, organic matter is mainly transformed into inorganic carbon as CO_2, nitrogen and phosphorus from the organic matter are eventually released as inorganic ammonia and phosphates, and the energy produced in these processes is used by biomass for growth and maintenance (Hvitved-Jacobsen *et al.*, 2013). Anaerobic wastewater transformations could be classified into fermentation, sulfate reduction (respiration) and methanogenesis. Fermentation is a type of energy production, which results in readily degradable organic by-products, such as VFAs and alcohols (Hvitved-Jacobsen *et al.*, 2013). Sulfate reduction, for example Equation 3.1, results in sulfide compounds, such as H_2S and HS$^-$, and takes place in biofilm and sediments (Hvitved-Jacobsen *et al.*, 2013).

$$SO_4^{2-} + C_{org} \rightarrow HCO_3^- + H_2S \tag{3.1}$$

Methanogenesis is also a metabolic process, which takes place in deeper anaerobic layers of biofilm and sediments. During methanogenesis VFA's are consumed and methane is created as a by-product. However, methanogenesis is not investigated in this report. Transformations as well as formation of sulfide are reviewed in more detail in the following.

Table 3.2: An overview of the integrated aerobic, anoxic and anaerobic processes and corresponding air/water interactions and gas phase processes included in the WATS sewer process model valid for any type of sewer, from Hvitved-Jacobsen *et al.*, 2005 Table 5

	Process	Electron Donors	Electron Acceptors
Water phase (aerobic)	Biomass growth Biomass maintanance Hydrolysis Sulfide oxidation Transport	Fermentable substrate Fermentation products Hydrolysable substrate (2–3 fractions) Sulfide	Dissolved oxygen
Water phase (anoxic)	Biomass growth Biomass maintenance Hydrolysis Transport	Fermentable substrate Fermentation products Hydrolysable substrate (2–3 fractions) Sulfide	Nitrate Nitrite
Water phase (anaerobic)	Hydrolysis Fermentation Transport	Fermentable substrate Fermentation products Hydrolysable substrate (2–3 fractions)	-
Biofilm (aerobic)	Biofilm growth Sulfide oxidation (chemical and biological)	Fermentable substrate Fermentation products Sulfide	Dissolved oxygen
Biofilm (anoxic)	Biofilm growth	Fermentable substrate Fermentation products Sulfide	Nitrate Nitrite
Biofilm (anerobic)	Sulfate reduction	Fermentable substrate Fermentation products	Sulfate
Air-water exchange	Reaeration Hydrogen sulfide emission	-	-
Water phase/ solid phase	Sulfide precipitation	-	-
Gas phase/ solid phase	Hydrogen sulfide oxidation (corrosion) Horizontal transport	Sulfide	Dissolved oxygen

Sulfide in wastewater

It was established in the previous section, that sulfide is the result of sulfate reduction during the anaerobic respiration of biomass in wastewater. The entire sulfide cycle in sewers is illustrated below, Figure 3.1. The sulfide cycle starts with reduction of sulfate. Main source of the sulfate in wastewater is
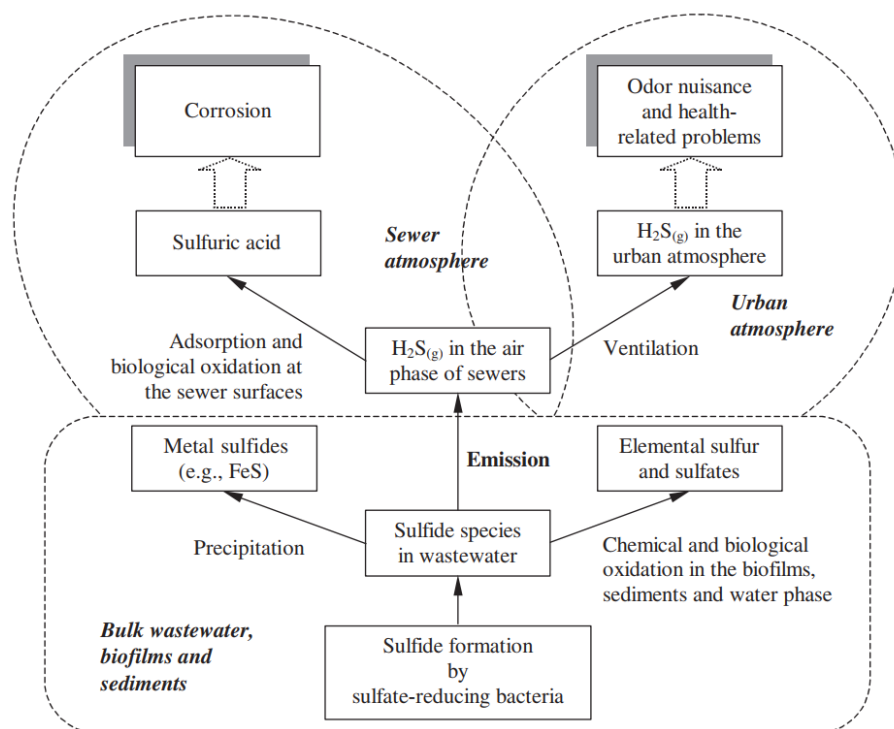
Figure 3.1: Sulfide cycle in sewers, sewer atmosphere and urban/WWTP atmosphere, from Yongsiri et al., 2003

drinking water. Volatile organic compounds (VOCs) containing sulfur are not important quantitatively in sulfide production, even though organic carbon is used as an energy source (electron donor) for sulfate reduction (Hvitved-Jacobsen et al., 2013). Sulfide types, that are found in sewage are usually summarized to H_2S, HS^- and S^{2-}. Primarily H_2S and HS^- are present in wastewater and from these two only H_2S can pass the wastewater - atmosphere barrier. More recent studies disproves the presence of S^{2-} in aqueous solution, (May et al., 2018). And even according to older literature it is described as only present in low concentrations at very high pH. Naturally, it shall not be taken into account here. The significance of H_2S in sewer atmosphere lies in its negative effects, mainly malodour and corrosion of sewer pipes, as well as health issues to people exposed. Sulfide effects to human health are illustrated in the Table 3.3. In terms of usually reported problems, sulfide concentration can be considered as low 0.5 g S m^{-3}, medium 3.0 g S m^{-3} and high 10 g S m^{-3}, but in countries with long pressure mains or where high wastewater temperatures are likely, significantly higher concentrations of sulfide can occur (Hvitved-Jacobsen et al., 2000). Sometimes, even though other chemical compounds cause similar

problems, sulfide is wrongly suspected as causative substance. In this report only sulfide is considered, since it is the most widely discussed, investigated and occurring compound with such properties.

Table 3.3: H_2S effects on human health, from U.S. Department of Labor, 2020

Concentration (ppm)	Symptoms/Effects
0.00011–0.00033	Typical background concentrations
0.01–1.5	Odor threshold (rotten egg smell first noticeable)
10	Eye irritation
20	Headache, dizziness
100–150	Loss of smell (olfactory fatigue or paralysis)
500–700	Staggering, collapse in 5 minutes. Death after 30–60 minutes
1000–2000	Instant death

H_2S transportation between water and gas phase depends on pH, temperature, hydraulic conditions of the sewer flow and ventilation of the sewer atmosphere (Yongsiri *et al.*, 2003). The transfer from hydrogen sulfide in the water phase to the sewer atmosphere shows significant dependency on pH. Rate of this transfer can be calculated as (Sudarjanto *et al.*, 2011):

$$rH_2S = k_L a(H_2S_{aq} - H_2S_{aq}^*) \tag{3.2}$$

Aqueous H_2S depends on pH and represents a fraction of total dissolved sulfides (H_2S_T), as described below:

$$H_2S_{aq} = \frac{H_2S_T}{1 + 10^{(pH - pKa)}} \tag{3.3}$$

At 25°C the pKa for H_2S_{aq} is 7.0, which describes, that at a pH of 7.0, 50% remains as HS^-, while the other 50% occur as H_2S in gas phase, as illustrated in Figure 3.2, key parameters from Equation 3.3 are displayed in the Figure 3.2 (Sudarjanto *et al.*, 2011). The dissociation changes the H_2S fraction with increasing pH value; e.g. at pH 8 only 10% off the total amount are H_2S. pH also influences the sulfate reduction - production of H_2S. Sharma *et al.*, 2014 shows, that the highest H_2S production takes place from 5.5 to 8.0 pH. Like most biological processes, H_2S production is highly temperature dependent. In normal sewer temperatures, production increases with increase in temperature, factor 3.4 per 10 °C (temperature coefficient α=1.13) (Hvitved-Jacobsen *et al.*, 2013). Similar process is present in H_2S release into sewer atmosphere, where rise in temperature increases the emission of H_2S by approximately 2% every 1°C. (Hydrogen Sulphide Corrosion in Sewerage Works (Australia), 1989).

H_2S has ideal conditions to form in pressure mains. One of the most common characteristics of pressure mains is, that its wastewater is anaerobic, which means that biomass reduces sulfate to sulfide. Pressure mains are usually at least few kilometers long and collect relatively high amounts of wastewater, which, in most cases, leads to readily biodegradable and hydrolysable substrate rich wastewater. Hydrolysable
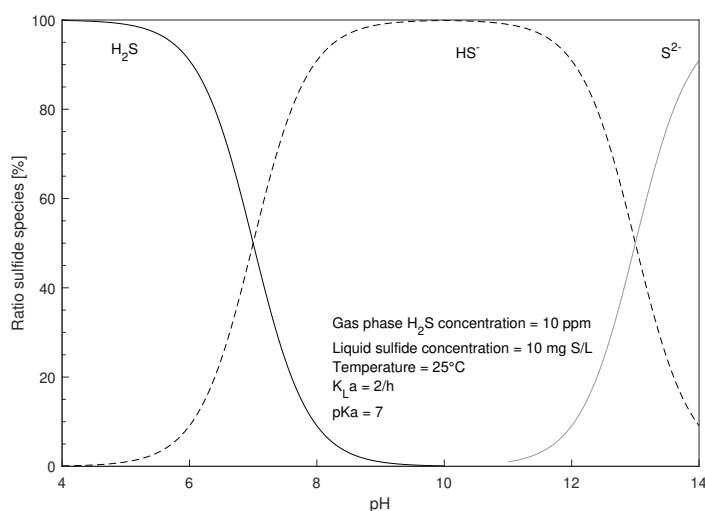
Figure 3.2: Wastewater pH and its impact on sulfide transfer rate; pH=4 is taken as 100% transfer rate of H_2S. S^{2-} is displayed in grey, since more recent research argues against its existence (May *et al.*, 2018).

substrate is used in complex fermentation processes which delivers bi-products of readily biodegradable substrate (VFAs). This means that if the wastewater is rich enough with easily hydrolysable substrate and force main is long enough, VFAs can become non-limiting factor in sulfate reduction, even though in regular wastewater transformations they are the most crucial limiting factor.

Since dissolved H_2S concentration can become very high in such sewers, at the outlet of force main to manholes or pump stations H_2S is released rapidly due to an increased water – air interface surface from turbulence (Yongsiri *et al.*, 2003). Because of its chemical properties, as well as its practical analyse methods and low human odor threshold, sulfide is considered as indicator for corrosion problems in pressure mains. Corrosion rates in full scale experiments up to 10 mm per year are found Appendix Table 11.1. It is interesting to note, that special concrete types (e.g. calcium aluminate cement, geopolymer) have a reducing effect on corrosion rates. In Frejlev pilot scale reactor indicated corrosion rates of 3.1 mm per year (Vollertsen *et al.*, 2008). Wastewater from Frejlev is also used in this report for testing the experimental setup.

Sulfide production can be estimated by different equations, as presented by various authors in Table 3.4. Temperature is considered a major factor, because at higher temperatures, more sulfide is formed, meanwhile the solubility of oxygen decreases, illustrated in Appendix 11.5. With less oxygen present in the water phase - anaerobic conditions occur and H_2S starts to form. This exacerbates with water saving measures (e.g. water saving toilets), due to reduced sewege quantity at constant pollution load. Due to the many parameters (temperature, force main geometry and length, hydraulic gradient, etc.) which contributes to H_2S formation, the applicability of the presented equations is limited and should be always reviewed for every single situation.

Equation (1), (2) and (3) calculating maximum production rates; Equation (4) also adds biodegradability of wastewater by applying a correction factor a. Tanaka and Hvitved-Jacobsen, 2001 proves, that Equation (4) applies for Danish sewers. The resulting production rates are shown in Figure 3.3. Here three different types of variable biodegradable wastewater, characterized by COD contents (domestic, mixed and industrial) show an increasing trend, with the highest rates for industrial sewage. However, it can be seen, that the exact determination of factor a is crucial for further considerations.

Table 3.4: Overview different calculations of sulfide production, adapted from Matsché *et al.*, 2005

Calculation method	Equation
(1) Boon and Lister, 1975	$r_s = 0.228 \cdot 10^{-3} \cdot COD \cdot 1.07^{(T-20)}$
(2) Pomeroy and Parkhurst, 1978	$r_s = 1 \cdot 10^{-3} \cdot BOD_5 \cdot 1.07^{(T-20)}$
(3) Thistlethwayte, 1972	$r_s = 0.5 \cdot 10^{-3} \cdot u \cdot BOD_5^{0.8} \cdot [SO_4]^{0.4} \cdot 1.139^{(T-20)}$
(4) Nielsen *et al.*, 1998	$r_s = a \cdot (COD_{sol} - 50)^{0.5} \cdot 1.03^{T-20}$
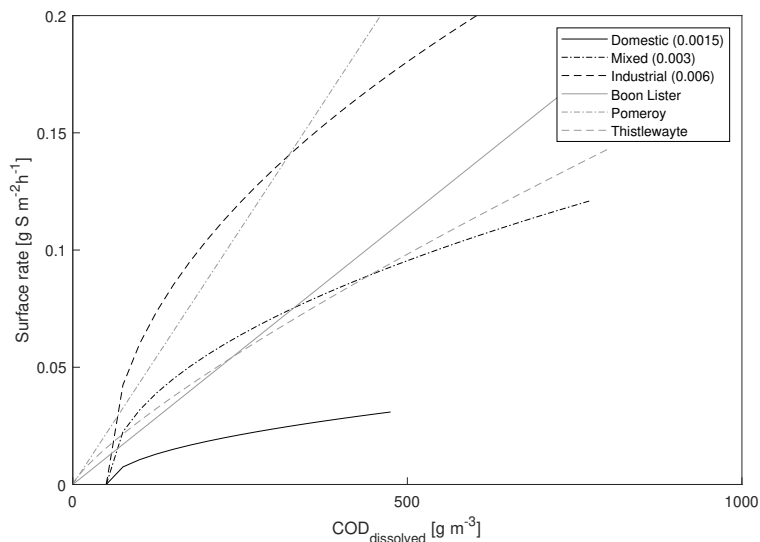
Figure 3.3: Production rate of H_2S in force mains with Equations from table 3.4 and varying a for Nielsen *et al.* (1998)

Besides the already mentioned effects of corrosion and odor, presence of sulfide in the process of WWTPs has negative effects on the floc stability. This is explained by a increased shear stress sensitivity - or weakened floc strength - in the sludge flocs, due to the reduction of Fe(III) ions and precipitation to FeS. This leads to particle release and particle floc disintegration, which consequently impairs dewatering and thickening of sludge as well as a reduction in removal efficiency, as reported in Nielsen and Keiding, 1998 and Hydrogen Sulphide Corrosion in Sewerage Works (Australia), 1989.

3.2 Historical background of sulfide in sewers

1900 – 1940, Sulfide related corrosion is realized In the beginning of the last century Olmstead and Hamlin, 1900 investigate the corrosion of concrete sewer pipes, which is often considered as first study regarding this topic. They observed, that the mortar, brickwork and iron which was used for construction of the Los Angeles sea outfall was disintegrating and "rusting badly" accordingly. After concrete was analysed, they found that it has lost 80% of its lime content. They also precisely mentioned different effects that occur, e.g. stages of corrosion at pressure drops in the sewer infrastructure or the composition of cement, but did not find – or at least did not mentioned – hydrogen sulfide. Instead the loss of concrete was related only to sulphuric acid from the "gases given off by sewage".

The connection between sulfuric acid and H_2S in sewer atmosphere was first found 30 years later in the studies by Bowlus and Banta, 1932. The published results promote chlorination, which back then was the most reliable sulfide control. It also improved the cleaning efficiency in the treatment plant. They applied design criteria to define a minimum flow velocity through the sewer, which in relation to the time, solved the corrosion quite sufficient. Later in 1932 regular trunk sewer cleaning was tried the fist time, which "brought sulfides under fair control". Still, the corrosion process was assumed to be fully chemical through a possible series of chemical reactions (Lea and Desch, 1936), with only non-biological H_2S oxidation. In 1939 the districts of Los Angeles study corrosion broadly and to a much deeper extend. They analysed over sixty thousand samples, as reported later by Pomeroy and Bowlus (1946), which was back then enabled with the newly invented rapid methylene blue method (Pomeroy, 1936) for determining the total sulphide content in sewage.

1940 – 1945, boundaries and parameters are discovered Corrosion inducing microoganisms (*thiobacillus concretivorus*), where first described by Parker, 1945 and Parker already mentions corrosion of sewers as world wide phenomena in, for example, Cairo, Cape Town and Melbourne. Pomeroy and Bowlus, 1946 found the valid concept of H_2S formation. They summarize the effects of temperature, pH, sewer velocity and sewage age (retention time), slimes (biofilm) and sewage strength ("bacterial nutrients"). And also give proper design advises, e.g. scouring the channels, reaeration and calculate flow velocities.

With a newly introduced parameter *Effective BOD* they summarize temperature and sewage strength. And with a new formula they presented a way to estimate minimum velocities required to prevent sulphide formation: Effective BOD = BOD $\cdot$ 55 v^2. Of course this equation is rather simple and ignores some other factors, but nevertheless the underlying reactions were discovered. They concluded, that "[...] sulfide generation can be expected in completely filled lines. Force mains therefore should be kept to a minimum" (p. 615).

1945 – 1995, sulfide formation prediction models Different equations were established after 1945. Most are empirical equations, some of them already presented in section 3. They are outcomes of experiments, as well as field experiments. As shown in Figure 3.3, the results vary. This is explained by the highly individual experimental setup and limits the results for the particular experiment only. Hvitved-Jacobsen *et al.*, 2005 proposed to group these models in three types, regarding their increasing complexity:

- Type I: Simple models for gravity sewers for "Risk models"
- Type II: Models for gravity sewers and force mains; Prediction of sulfide in water phase with 3–6 parameters
- Type III: Models that include the sulfur cycle with additional sinks of sulfide in gas phase and concrete corrosion. Consecutive calculation steps with a multitude of equations

Most found reports from the last decades and larger field surveys to compare different abatement methods today use Typ I and II models, for example in Matsché *et al.*, 2005; Frey, 2008. This can be explained by the easy application and good comparability of results in different locations. Hvitved-Jacobsen *et al.* described Type III models as problematic, in regards to too high complexity and mathematical equations which can not depict real situations.

In the 1970s the H_2S formation and resulting consequences were excessively examined; the most known published articles are from Thistlethwayte, 1972; Boon and Lister, 1975; Pomeroy and Parkhurst, 1978. Here factors, boundary conditions and detailed chemistry reactions for sulfur conversion in sewers were examined around the globe. Most of the findings from this period were included and summarized in various technical design manuals, for example EPA, 1992 and Hydrogen Sulphide Corrosion in Sewerage Works (Australia), 1989. All these models belong to Type II. It can be seen that they work for both gravity and pressure sewers, and main parameters are wastewater strength (BOD or COD), hydraulic conditions (flow rate, surface area) and network boundaries (e.g. diameter, length, slope). Even though they need relatively small amount of data as an input, these factors contain much more derivated information. For example pipe slope or network conditions can indicate reaeration. All of these articles are easy accessible, which also contributes to the wide spreading of these models worldwide, e.g. US, UK, Denmark, Germany, Portugal. A review of studies containing various sulfide emission control methods is presented by Zhang *et al.*, 2008.

Since 1995, Modeling sulfur cycle in sewers In 1994, Aalborg, the first IAWQ Specialized Conference on The Sewer as a Physical, Chemical and Biological Reactor took place and cases in sewers and possible solutions were presented and later published (e.g. Boon, 1995, Kyeoung-Suk and Mori, 1995).

New studies approach a more detailed understanding of corrosion conditions, such as gas-phase temperature (Jiang *et al.*, 2015). O'connell *et al.*, 2010 concluded, that there are three major study fields:

- Biological corrosion processes (sulfate-reducing and sulfur-oxidising bacteria)
- Chemical Concrete analyses with sulfates and sulfuric acid
- Laboratory concrete experiments, especially incorporating biological corrosion.

Nowadays modeling of wastewater processes serves as an integral part in understanding wastewater transformations and estimating the scope of outcomes, which allows to account for possible complications and future development of these processes. Hvitved-Jacobsen *et al.*, 2000 created the framework of conceptual understanding of organic matter transformations in wastewater in regard to sulfide. Based on this concept, models of wastewater transformations and sulfide production in sewers were created and integrated with Wastewater Aerobic/anaerobic Transformations in Sewers (WATS) model. Nielsen *et al.*, 2006 investigated and defined kinetics and stoichiometry of aerobic sulfide oxidation and determined rate equations that can be integrated into the model. Abdul-Talib *et al.*, 2002; Yang *et al.*, 2004 researched anoxic transformation of wastewater organic matter. A process concept is devised and process kinetics are established based on two-step denitrification reactions, which mainly describes denitrification in sewer systems. Yang *et al.*, 2005 investigated anoxic oxidation of sulfide. It was found that anoxic sulfide oxidation in sewer systems is almost completely biological. Yang *et al.*, 2004; Yang *et al.*, 2005 defined rate equations for anoxic processes that can be integrated into wastewater models. Kiilerich *et al.*, 2018 discusses the outlook of sulfide precipitation with iron, where precipitation with Fe(III) is more rapid than with Fe(II). Also, iron to sulfide ratios are redefined according to stoichiometry as well as precipitation efficiency. Sulfide precipitation rate equations are defined. All proposed rate equations - aerobic sulfide oxidation, anoxic wastewater processes and anaerobic sulfide precipitation with iron - can be integrated into WATS process model to deliver comprehensive and comparable simulations of wastewater transformations.

3.3 Hjørring wastewater treatment plant

Figure 3.4: Aerial view of Hjørring WWTP. Photo from Hjørring Kommunes Spildevandsplan, 2020

The WWTP, Figure 3.4, in the city of Hjørring (Denmark) treats municipal wastewater from Hjørring and several towns, villages and industrial wastewater from small companies. Industrial wastewater from Vrå was recently attached via long force main to WWTP, Figure 3.5. Biggest wastewater discharging industries here are a laundry, chicken hatchery and and marmalade factory, Appendix Figure 11.3. Even though its only three industries, they contribute approximately 40% to the water consumption of the city Appendix Figure 11.4. The capacity of WWTP is determined to be 160 000 person equivalents (PE), Hjørring Vandselskab A/S, 2020, and the plant is currently loaded with an 85% percentile of approximately 81 000 PE. The plant was established in 1970 and extended in 1992. The treatment includes mechanical, biological and chemical processes.

After sand and oil is removed, wastewater is treated in a primary settling tank, where with first mechanical purification some amount of organic matter and phosphorous are removed. Additional iron chloride can be applied. In the following anaerobic process tank, biological phosphorus removal happens. Afterwards wastewater flows into the biological process tanks, where active sludge removes the remaining nitrogen and organic matter with the help of microorganisms. Biomass has to be supplied with oxygen during the nitrification process, where ammonia is converted to nitrate. Additionally most

organic matter is removed here. In the denitrification processes, oxygen supply is terminated, and nitrate is transformed to free nitrogen, which is released into the atmosphere. In the following four settling clarifiers water is separated from sludge and phosphorus removal is supplemented with iron chloride addition to ensure low phosphorous concentrations in the effluent.
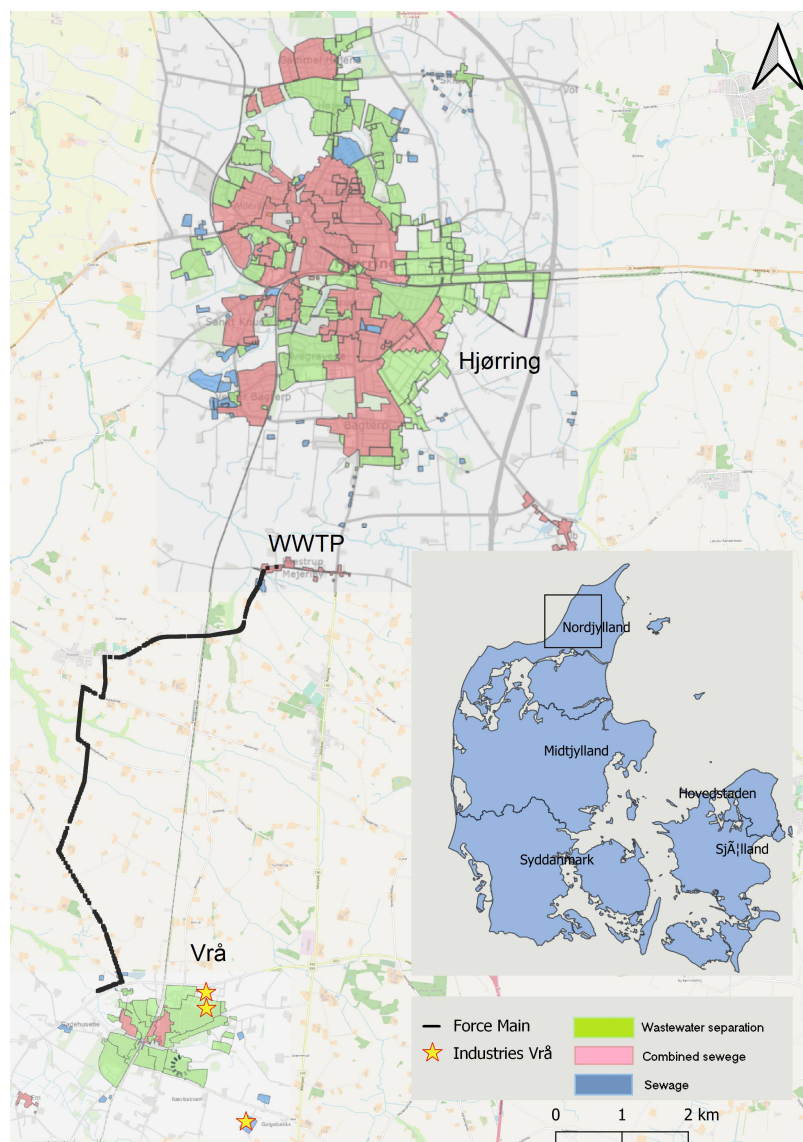
Figure 3.5: Map of location, sewer types and force main in Vrå and Hjørring, □ is detail view. Data from Hjørring Kommunes Spildevandsplan, 2020. Vrå catchment map in Appendix Figure 11.3

Daily operational data (January – December 2019) from WWTP is used to evaluate general status of the plant, Table 3.5. Daily wastewater load and COD are shown in Figure 3.6. The daily treated sewage is approximately $15\,200$ m^3d^{-1}. It has to be mentioned, that Hjørring WWTP measures COD not regularly, also smaller gaps are present in inflow data, as seen in Figure 3.6. Therefore the 85% percentile was calculated to establish statistically correct load values, as shown in Appendix 11.1. The average and the 85% percentile inflow loads and resulting PE from Hjørring WWTP are shown in Table 3.6 and are

Table 3.5: Mean values of raw wastewater from Hjørring WWTP for 2019/2020. Standard deviation as range variation, number of samples in brackets.

Parameter	Unit	Influent
Inflow	m^3 day^{-1}	$15{,}256 \pm 7{,}490$ (384)
pH	-	7.41 ± 0.32 (97)
Temperature	°C	12.2 ± 3.5 (382)
COD	mg l^{-1}	880 ± 425 (97)
N$_{tot}$	mg l^{-1}	44.5 ± 20.9 (98)
P$_{tot}$	mg l^{-1}	6.9 ± 2.9 (71)

calculated as follows: total daily load of COD is calculated from daily flow average and COD average, Equation 3.4. Afterwards, Population Equivalent (PE) is calculated with Equation 3.5.
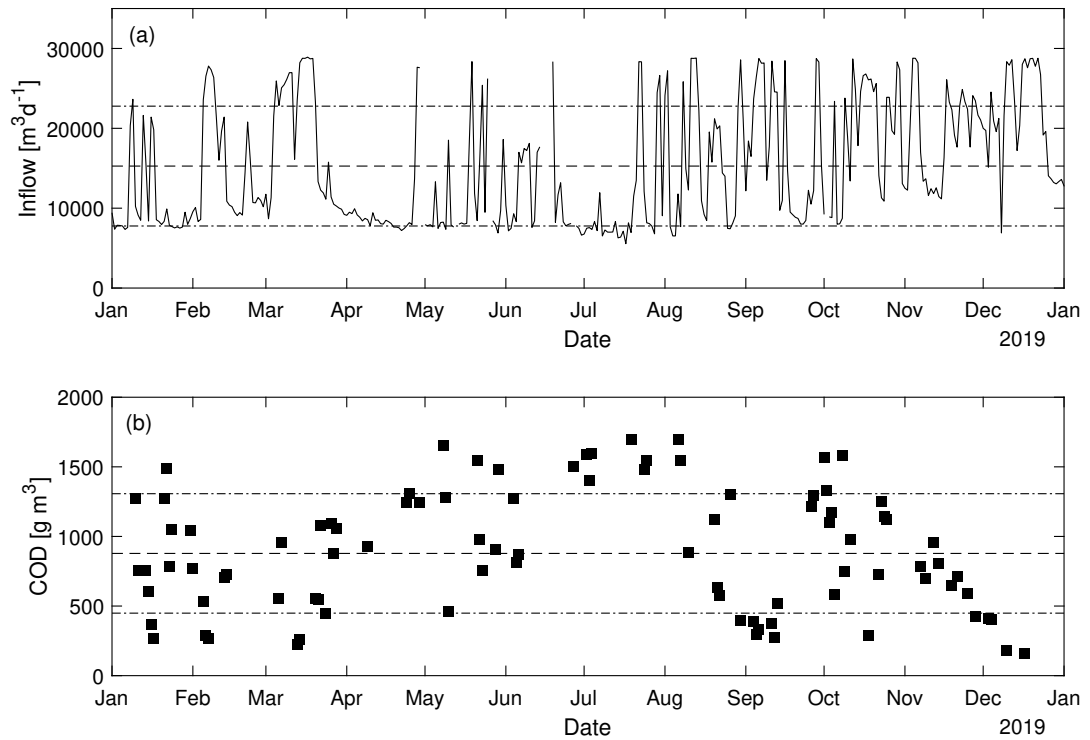
Figure 3.6: Hjørring WWTP yearly variation from 2019 of daily inflow (a) and COD (b). COD is measured occasionally. −− indicates average mean, −· standard deviation. Data provided from Hjørring Treatment plant.

$$Load = \overline{Q_{Inflow}} \cdot \overline{COD} \tag{3.4}$$

$$Population\ Equivalent\ (PE) = \frac{\overline{Q_{inflow}} \cdot \overline{COD}}{120g\ d^{-1}} = \frac{Load}{120g\ d^{-1}} \tag{3.5}$$

Table 3.6: Daily load and Population Equivalent (mean and 85%-percentile) from Hjørring WWTP. *Values from Jan 2019 to Jan 2020. Calculating Factors: COD = 120 g PE d^{-1}, N = 11 g PE d^{-1}.

Parameter	Mean load [*] kg d^{-1}	Mean load Average PE	85% Percentile load [*] kg d^{-1}	85% Percentile PE
COD	13 410	111 742	22 847	190392
N$_{tot}$	677	61 570	1 154	104906

By comparing the the 85% percentile load to the intended load of 160 000 PE, it can be concluded that the WWTP does operate over full capacity; at least for COD removal.
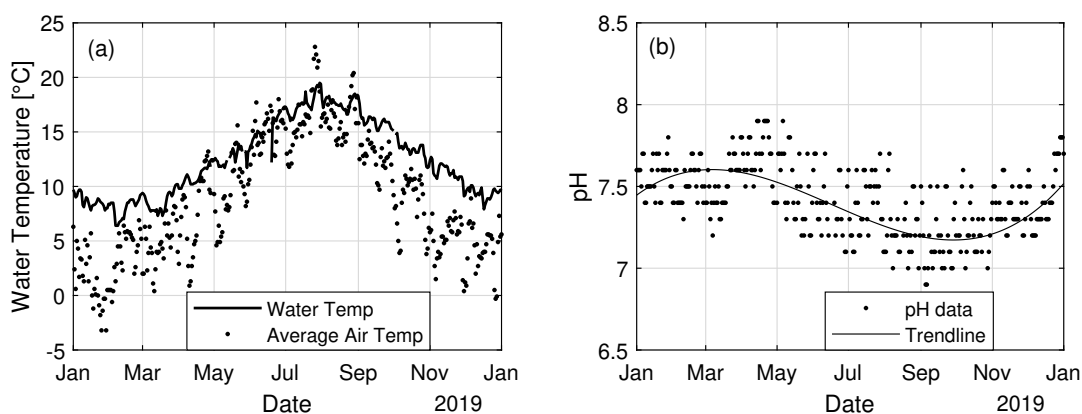
Figure 3.7: Yearly variation of influent to WWTP Hjørring for 2019 . Water temperature (a) and pH measurements and applied 4th order polynomial trend line (b). Data supplied from the WWTP of Hjørring.

Water temperature and average air temperature, as well as effluent pH are shown in Figure 3.7. Water temperature shows annual fluctuation, with warmer water in summer month. High variations during the month are explained by daily air temperature variations, as well as rain events, which is confirmed by Pearson correlation coefficient $r = 0.89$ between air temperature and wastewater temperature. Measured pH vary from 7 to 8, with few acidic events. For full data, refer to Appendix Figure 11.2. At lower temperatures (March), the pH is higher and drops then during the warmer spring and summer time. This is presented as a trendline through the pH data set. The pH drop could be explained by the increased rate of H$_2$S formation, as well as the fermentation producing VFAs due to the increase in temperature.

In the past, additional readily degradable substrate had to be added to Hjørring WWTP in order to increase the efficiency of the plant, by increasing the nutrient removal. However, since the introduction of additional organic matter rich wastewater from Vrå, this addition became unnecessary. It indicates, that industrial wastewater inflowing into WWTP is rich in readily biodegradable substrate, most likely - in VFAs. As already mentioned, VFAs tend to form in pressure mains, which is the case here, as wastewater from the industries is fed to WWTP via long pressure main, Table 3.7 and appendix Figure 11.6. In section 3.1 it was described that such conditions - long force mains with organics rich wastewater -

are suitable for formation of H_2S. Nature of organic mater in wastewater incoming to Hjørring WWTP, transformation rates and possible formation of H_2S, as well as its effects on WWTP processes are further investigated throughout the thesis.

Table 3.7: Characteristics of force main from Vrå to Hjørring. Flow is calculated from total water consumption in the town of Vrå data

Lenght	Diameter	Flow	Volume
m	mm	$m^3 d^{-1}$	m^3
9 541	197	565	290.7

Pressure main from Vrå to Hjørring, being on of the key interest throughout the thesis, has to be investigated further, since it provides the medium for wastewater processes to develop. In Table 3.7 main parameters describing physical characteristics of wastewater flow are provided. Since wastewater flow in pressure main is not constant (pumping station does not run constantly), the most straightforward evaluation is averaging wastewater velocity in the pipe from potable water consumption in Vrå. It is assumed that water consumption (565 $m^3 d^{-1}$) is equal to wastewater produced in the dry season of the year, which means, that average velocity of wastewater is 0.05 m s^{-1} and total retention time is 51.0 h. Data analysis is carried out on Figure 3.8 to determine wet flow in the pressure main. The figure demonstrates, that most intensive rainfall months have approximately 6 times more precipitation than least intensive months, while highest wastewater inflow to Hjørring WWTP is two times larger than the lowest inflow. It is decided to stick with WWTP inflow data for estimation of wet flow conditions in the force main. Total wastewater flow during wet season is assumed to be two times larger, with average velocity of 0.10 m s^{-1} and total retention time of 26.5 h.
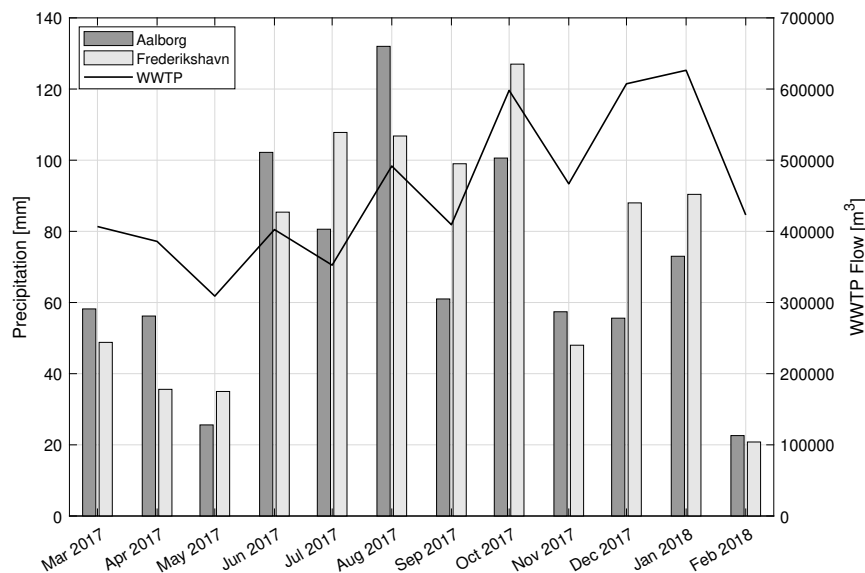
Figure 3.8: Accumulated monthly precipitation from Aalborg and Frederikshavn against inflow WWTP Hjørring 2017, rain data provided from WWTP Frederikshavn (Centralrenseanlæg) and Aalborg West (Vest)

Methodology for in-sewer process evaluation

In this chapter methods for investigating transformations of wastewater are presented. These methods consists of experimental methods, modelling and in-situ testing. Laboratory work consist of OUR experiments and measurements of VFA via ion chromatography. Furthermore, modeling microbial transformations of wastewater and H_2S formation in the sewers is carried out. In-situ measurements of H_2S odor logger at the inlet of WWTP are done to measure H_2S concentration in the gas phase.

The methodological part of the thesis starts with OUR experiments and modelling, which provides crude wastewater parameters at the inlet of WWTP. To specify wastewater composition further, IC tests are conducted on filtered wastewater. The main purpose of these tests is to quantify VFAs in water phase. To quantify the total amount of H_2S (water and gas phases), the H_2S production aerobic/anaerobic model is set up. The model allows simulating virtually unlimited number of scenarios of H_2S production with varying temperature, wastewater composition, etc. To validate the model, H_2S measurements from an odor logger and IC are used.

4.1   Sampling and preparation of samples

Wastewater sampling was done to carry out the experiments in a laboratory setting as well as to test laboratory equipment. For testing the reactor (OUR) setup wastewater samples from Frejlev monitoring station were used. Frejlev is characterised as a small, rather steep catchment with a conveyance time from the source to the sampling station of approximately 30 min (Kiilerich $et\ al.$, 2017). Samples from Frejlev were collected at 2nd November 2019.

A wastewater sample from Hjørring was collected at 20th January 2020. Sampling in Hjørring was done to retrieve samples for OUR experiment, where wastewater is acquired without filtration. Another type of sampling was done for IC experiments for quantification of VFA's, where the sample was filtered.

4.2 Respirometry for OUR rate determination

The determination of the rate of the biological consumption of oxygen (or other inorganic electron acceptors) is defined as respirometry. Biochemically, respiration is the adenosine triphosphate (ATP) generating process. ATP is used as energy carrier in the cells and is used for cell growth, maintenance and reproduction (Loosdrecht *et al.*, 2016). Energy, which is produced by respiration is therefore directly linked to this processes. High cell process rates are indicated by high respiration rates. Since oxygen dissolves rather poorly in water and large amounts of oxygen needed at high cell densities, the oxygen supply is considered as one of the most important and therefore limiting process values at aerobic cell respiration. Two major types of information can be extracted from respirometry experiments: first the direct activity of the biomass, e.g. aerobic respiration rate. And second, the indirect deviated information from these results, e.g. substrate concentration, microorganism concentration and kinetic parameters.

In this study, indirect results from oxygen uptake rate (OUR) measurements were used to estimate wastewater parameters, for example, fractions of COD, as proposed by Vollertsen and Hvitved-Jacobsen, 2002. OUR is defined as the product from the specific oxygen uptake rate q_{O_2} (which varies for different populations of microorganism) and the biomass concentration c_x.

$$OUR = q_{O_2} \cdot c_x \tag{4.1}$$

Where:

OUR	Oxygen uptake rate	$\mathrm{g\,L^{-1}\,h^{-1}}$
q_{O_2}	specific oxygen uptake rate	$\mathrm{g\,g^{-1}\,h^{-1}}$

The enrichment with oxygen in bioreactors can be described by surface renewal, penetration model or two-phase theory (Lewis and Whitman, 1924). The latter is most used (Chmiel, 2011). The liquid phase limits the transport of oxygen. For achieving optimal productivity in aerobic processes, oxygen has to be supplied. In this experimental setup, reactors with aeration and air control were used to provide a controlled environment.

For measurement of OUR, two independent stainless steel batch reactors, with a volume of 2.4 liters were set up, as shown in Figure 4.1 and Figure 4.2. Respirometry experiments were conducted immediately after the sampling, at the Department of Chemistry and Bioscience, Aalborg University, to prevent degradation of fast degradable substrate and limit uncontrolled growth of biomass. After 24 h, $60\,\mathrm{mg\,L^{-1}}$ COD (88 µl 96% ethanol equivalent) was added to the reactors to validate the model. These reactors run in parallel in order to confirm the experimental results. Through permanent stirring with a magnetic

stirrer, particles were kept in suspension and oxygen was distributed evenly. Water temperature was kept at room temperature $20°C \pm 0.5°C$, without additional temperature control. Dissolved Oxygen (DO) concentration was measured in the liquid phase with an oxygen probe. The oxygen sensor was calibrated before the actual test setup.
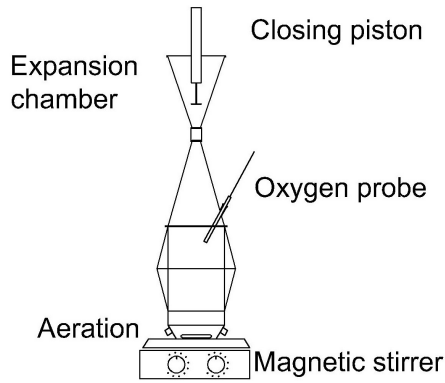
Figure 4.1: Sketch of Experimental OUR Reactor   Figure 4.2: Photo of OUR Reactor Setup

When the DO concentration was below 6 mg O_2 L^{-1}, aeration was applied with compressed air in the bottom of a reactor until a DO concentration of 8.8 mg O_2 L^{-1} was reached. Expansion volume was partly filled with wastewater for inhibiting reaeration through surrounded air. For the same reason a closing piston was installed in the upper expansion part. The piston is open during the reaeration procedure in order to avoid pressure build up in the system. After the reaeration the piston closes to avoid reaeration from the surrounding atmosphere. Reaeration from the atmosphere is negligible, due to the low solubility of oxygen in water phase. However, it might be enough to set off the results of OUR experiment and therefore proper procedure to avoid this must be followed.

OUR was calculated as the change of oxygen concentration over time. Periods of pumping are excluded from the calculation. For smoothing results a moving average was used, to filter out high variations and noise. The average is taken over 15 consecutive time steps, Equation 4.2.

$$OUR_i = \frac{1}{15} \sum_{j=i}^{i+15-1} \frac{\partial s_O}{\partial t}_j \qquad (4.2)$$

Results of OUR experiments are illustrated in respirograms, Figure 4.3a and Figure 4.3b. Here, wastewater transformations reveals an initial peak in microorganism activity. This results from the oxidation of readily biodegradable substrate, S_S, which is being used by microorganism for growth and respiration. Area of S_S is followed by an area representing fast hydrolysable substrate $X_{S,fast}$ and afterwards the

(a) OUR from Unspecified Test Data

(b) OUR from Frejlev Research and Monitoring Station 2-11-2019
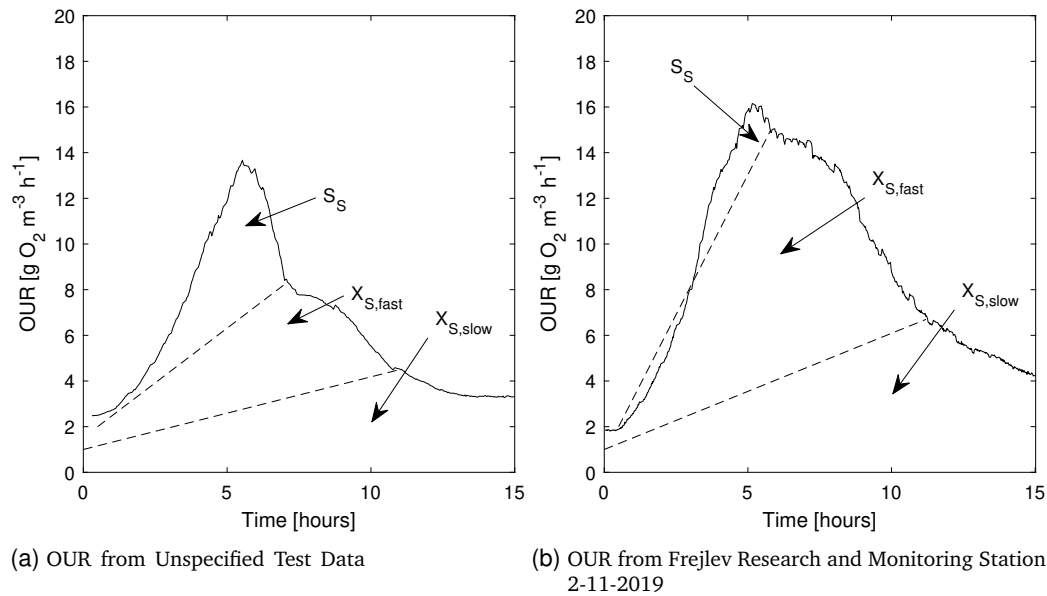
Figure 4.3: Oxygen Uptake Rate (OUR) for two different sewer waters. (a) test data, (b) Frejlev. Interpretation of compartments S_S, $X_{S,fast}$ and $X_{S,slow}$; Straight dividing lines ($--$) are exponential in reality.

slowly hydrolysable substrate $X_{S,slow}$. Reason for gradual consumption of different fractions of substrate lies in differences of chemical composition of these fractions. S_S is composed of soluble compounds, like short chain volatile fatty acids. It is degraded fast and explain the fast oxygen uptake response at the beginning of the experiment. $X_{S,fast}$ and $X_{S,slow}$ consist of organic compounds with longer chains, therefore $X_{S,fast}$ and $X_{S,slow}$ have to be hydrolysed before this fraction can be consumed by microorganisms. OUR from Figure 4.3b shows a small area of S_S, which is explained as a fresh wastewater sample, collected close to the catchment. OUR from Figure 4.3a in comparison results in a much greater S_S area, which indicates older sewage. This process is explained in a way, that in older sewage $X_{S,fast}$ and $X_{S,slow}$ are hydrolysed into S_S, therefore quantity of S_S increases in long force mains.

A numerical model describing the experiment is set up. The reason behind modeling OUR experiment is that the model enables extraction of wastewater parameters from the OUR data. The Model is set up according to the Vollertsen and Hvitved-Jacobsen, 1999; Hvitved-Jacobsen *et al.*, 2013 and it is based on wastewater transformations described by Activated Sludge Model (ASM No.1). Main differences between ASM No.1 and OUR models are that OUR model proposes several fractions of hydrolysable substrate and that decay of biomass into substrate and inert particles is absent and biomass maintenance energy requirements are introduced (Vollertsen and Hvitved-Jacobsen, 1999). The OUR model concept is presented in Table 4.1 and it works as regular ASM model: parameter is calculated as a sum of processes multiplied by their corresponding rates. For example, S_S is calculated as follows, Equation 4.3:

Table 4.1: Matrix formulation of aerobic microbial transformations of organic matter in an OUR batch experiment with nonseeded wastewater, (Hvitved-Jacobsen *et al.*, 2013)

	S_S	X_{S1}	X_{S2}	X_{HW}	$-S_O$	Rate
Biomass Growth	-1/Y_{HW}			1	(1-Y_{HW})/Y_{HW}	Equation a
Maintenance energy	-1			-1*	1	Eq. b
Hydrolysis (fast)	1	-1				Eq. c, n = 1
Hydrolysis (slow)	1		-1			Eq. c, n = 2

* *If S_S is not present in sufficient concentration, X_{HW} is used for endogenous respiration.*

Equation a: $\mu_H \cdot \frac{S_S}{K_{SW}+S_S} \cdot X_{Hw}$
Equation b: $q_m \cdot X_{Hw}$
Equation c: $k_{hn} \cdot \frac{X_{Sn}/X_{Hw}}{K_{Xn}+X_{Sn}/X_{Hw}} \cdot X_{Hw}$

$$\frac{S_S}{dt} = \frac{-1}{Y_{HW}} \cdot a + (-1 \cdot b) + 1 \cdot c_1 + 1 \cdot c_2 \tag{4.3}$$
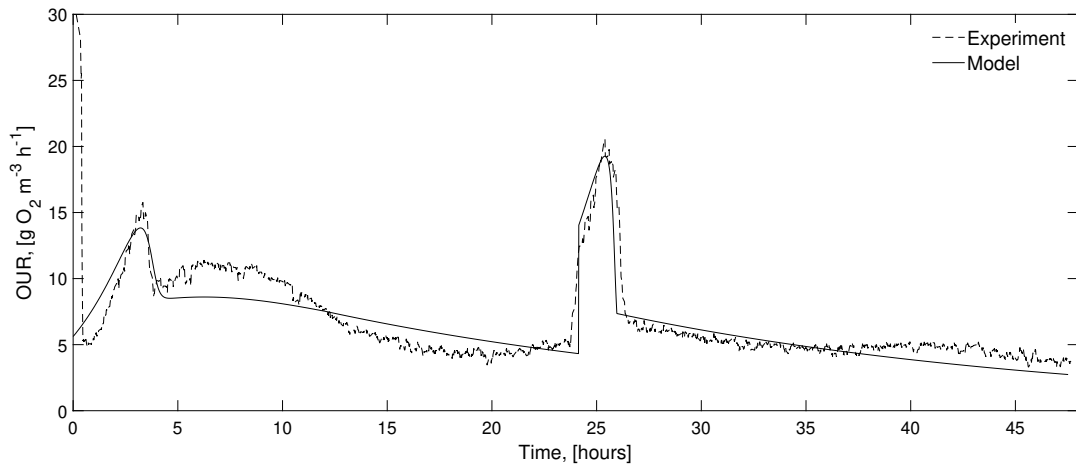
Figure 4.4: OUR experiment data, end of force main, Hjørring WWTP, 2020-20-01

Model parameters describing wastewater composition are evaluated from the initial wastewater transformations, as illustrated in Figure 4.3. Parameters such as maximum specific growth rate (μ_H), saturation constant of S_S (K_S), maintenance energy requirement rate (q_m), and yield constant (Y_H) are derived from addition of readily biodegradable substrate after 24h, as described above in section 4.2. This addition is clearly visible in Figure 4.4. Aerobic microorganisms immediately reacts to the addition of S_S with a significant increase in OUR, which illustrates increased activity and growth rate of X_{Hw}. In Table 4.2, the parameters used for model simulation of OUR experiment are presented. Initial realistic parameters for model set up are taken from Hvitved-Jacobsen *et al.*, 2013. Afterwards, iterative process of model calibration by trial-and-error is carried out. Parameters of a calibrated model are presented

in Table 4.2. As already mentioned, during the OUR experiment the temperature is nearly constant, therefore temperature factors are voided from the model.

Table 4.2: Initial values for describing aerobic microbial transformations of organic matter in an OUR batch experiment with nonseeded wastewater, from Hvitved-Jacobsen *et al.*, 2013. Values used in model illustrated in Figure 4.4. Numbers in brackets are literature values

Symbol	Description	Value	Unit
μ_H	Maximum specific growth rate	9.0 (4.0–8.0)	d^{-1}
$k_{h,fast}$	Hydrolysis rate constant	8.0 (5.0)	d^{-1}
$k_{h,slow}$	Hydrolysis rate constant	0.5 (0.5)	d^{-1}
q_m	maintenance energy requirement rate constant	2.2 (0.5–2.0)	d^{-1}
K_S	Saturation constant for S_S	4.0 (0.5–2.0)	g COD m^{-3}
$K_{X,fast}$	Saturation constant for hydrolysis	1.5 (1.5)	g COD g COD^{-1}
$K_{X,slow}$	Saturation constant for hydrolysis	0.5 (0.5)	g COD g COD^{-1}
Y_H	Yield constant for heterotrophs	0.63 (0.5–0.6)	g COD g COD^{-1}
S_S	Readily biodegradable substrate	50 (0–40)	g COD m^{-3}
X_{Hw}	Heterotrophic biomass	19 (20–100)	g COD m^{-3}
$X_{S,fast}$	Hydrolysable substrate	140 (50–100)	g COD m^{-3}
$X_{S,slow}^*$	Hydrolysable substrate	391 (300–450)	g COD m^{-3}

$* X_{S,slow} = COD_{Total} - S_S - X_{S,fast} - X_{Hw}$

Despite OUR model matrix in Table 4.1 being relatively compact, the estimation of model parameters is complicated. Even though there is no - or no significant - correlation between model parameters, some parameters in the model concept are not independent (Vollertsen and Hvitved-Jacobsen, 1999). Furthermore, biomass can be substrate selective, as in specific type of microorganism might prefer one type of substrate to another. In order to avoid error due to selective substrate consumption by biomass, substrate containing a wide range of readily biodegradable organics (e.g. molasses, beer etc) can be added instead of ethanol.

Results from OUR experiment together with OUR model allows characterisation wastewater quality as well as quantity of different fractions of biodegradable matter. Establishing composition of wastewater is a first step in understanding processes happening not only at the inlet to the WWTP, but also in the pressure main. Results of OUR experiments, together with IC measurements and in-situ data logging, creates the foundation for estimating hydrogen sulfide production processes as well as understanding full extent of effects of inflow from Vrå on pressure main and Hjørring WWTP.

4.3 Ion Chromatography for VFA and sulfide measurements in wastewater

Composition of wastewater is determined with OUR experiment and modelling. However, OUR delivers only rough composition and it is not enough to accurately quantify sulfate redox reactions. Especially, when readily biodegradable substrate is concerned, mainly - acetate. Acetate is a typical by-product of fermentation processes during sulfate reduction. Even though acetate is a VFA, it is not a preferred substrate for biomass in sewers. For these two reasons, acetate serves as a good indicator for possible sulfate reduction processes in the sewer.

Ion Chromatography (IC) Figure 4.5, is described as a separation method, which divides loaded inorganic and organic molecules into molecule classes (Weiss, 2004; Michalski, 2018). These classes can be identified and quantified to identify compounds in liquid phases, such as wastewater. Loaded functional groups are attached to a polymeric matrix, which allow the cations from the mobile phase to bound. The tests in this study are conducted with a Dionex ICS-1000, with auto samplers, as shown in Figure 4.6 and Appendix Figure 11.9, to detect the amount of VFA. Following VFA can be detected, but only acetate is used in this report:

- Formic acid (CH_2O_2)
- Acetic acid (CH_3COOH)
- Propionic acid ($C_3H_6O_2$)
- Isobutyric acid ($C_4H_8O_2$)

- Butyric acid ($C_5H_{10}O_2$)
- Isovaleric acid ($C_3H_6O_2$)
- Valeric acid ($C_5H_9O_2$)
- Caproic acid ($C_6H_{12}O_2$)
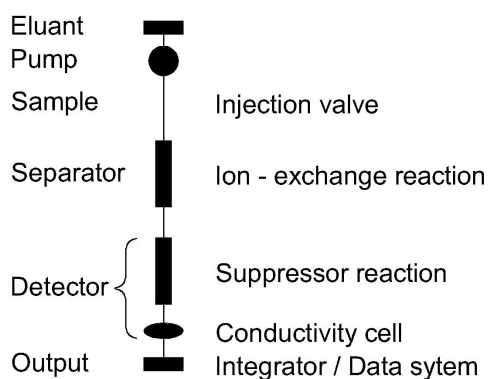

Figure 4.5: Basic components of an ion chromatograph, from Weiss, 2004

Figure 4.6: Ion Chromatograph Dionex ICS 2100: (4) central unit, (1) Auto Sampler, (2) Efluent, (3) Regenerent

Detection of VFAs were conducted with a IonPac ICE-AS6 separator column 9 x 250 mm from Dionex (Sunnyvale, USA) as stationary phase. Samples were filtered through a 0.45 μm membrane filter after collection. For calibration, solutions with four different concentrations of a standard were tested to obtain a calibration curve (concentration versus peak area), according to Figure 4.7. Slope of the linear regression equals the correction factor for the analytes compound. The analyte concentration should lie among the calibrated concentrations, to ensure correct interpolation of the analyte. Extrapolation should not be executed, due to the unknown function outside the investigated range. Weiss, 2004 and Barnett *et al.*, 2013 state, that a relative precision of 0.3% and 0.26% respectively can be be achieved. Analysed wastewater inlet from Hjørring displays a detected acetate peak after 15min detection time, Figure 4.8. For this figure the same sample was tested three times. The high reproducibility is visible in the sub-figure.
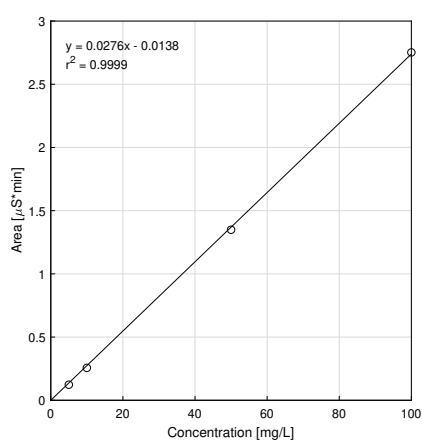
Figure 4.7: External standard calibration for acetate with concentrations of 5, 10, 50 and 100 mg/l and resulting peak area response linearity
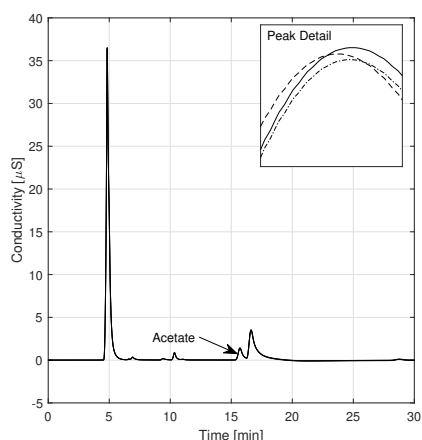
Figure 4.8: Chromatogram. Three runs with a sample from Hjørring 2020-01-20

The eluent was 0.4 mM heptafluorobutyric acid for minimum background conductivity. Flow rate was 1.0 mL min^{-1} and the background eluent conductivity was suppressed with an AMMS-ICE suppressor. Hence, the separation method was suppressed conductivity. Injection volume was 25 μL. This procedure and technical design was kept unaltered during the sampling campaign.

However, in case of this thesis, VFA measurement in water phase are not consistent nor very accurate in a sense, that wastewater from pressure main varies a lot in time while sampling is momentary. It is impossible to estimate when and how big the surge of VFA (consequently - H_2S) rich wastewater reaches WWTP, ergo the sampling and IC tests most likely illustrates only short time period average wastewater characteristics at the outlet of pressure main. To obtain continuous in-situ data - a H_2S gas sensor (Odalog^{TM}) is set up at the inlet of WWTP.

4.4 Odor measurement of volatilized sulfides

Odors from sewer at the inlet of WWTP, especially inorganic gases, such as hydrogen sulfide can be measured with an odor sensor, Figure 4.9(a). It has to be mentioned, that this technique only allows determination of gas phase concentration. Measurements of sulfide in the liquid phase requires additional experiments. An odor sensor is a reliable tool to measure hydrogen sulfide in the atmosphere. These measurements are important, because hydrogen sulfide is most noticeable in the gas phase. An odor sensor is placed above the pressure main outlet at the Hjørring WWTP, as illustrated in Figure 4.9(b) from May 7th to 14th, 2020.

(a) OdaLog^{TM} (b) OdaLog^{TM} installation in inlet structure

Figure 4.9: Logger and Installation

Measurements of sulfides in gas phase at the pressure mains outlet to WWTP serves as a tool not only to quantify hydrogen sulfide in the gas phase, but also to estimate a full extent of hydrogen sulfide formation in the pressure main from Vrå to Hjørring. The sensor is continually logging data for seven days, which allows to capture possible diurnal variations in hydrogen sulfide production. The sensor also captures surges in hydrogen sulfide production due to the increase in readily biodegradable substrate rich wastewater from the industries. In this case, the sensor is the only reliable way to quantify these surges, because continuous sampling of wastewater from the pressure main is impossible.

4.5 Modelling sulfide formation under aerobic/anaerobic conditions in sewers

In-situ hydrogen sulfide assessment in WWTP provides continuous results, but due to the construction of the inlet structure, significant underestimations are possible. Laboratory experiments, while very informative, heavily relies on sampling, which is extremely limited in time therefore - in wastewater composition. In order to simulate higher variety of scenarios, a model of sulfide formation under aerobic/anaerobic conditions is build. This model is constructed based on Hvitved-Jacobsen *et al.*, 2000; Tanaka and Hvitved-Jacobsen, 2001. The underlying matrix is presented in Table 4.3. Matrix in this section works in the same way as the matrix presented in section 4.2. However, model parameters presented in Table 4.2 and Table 4.4 are not fully interchangeable, because they describe different experiments/situations. However, wastewater composition values at the inflow to WWTP, estimated with OUR experiments, are used to reverse-engineer wastewater composition at the beginning of the pressure main.

As in most wastewater processes, limiting factor here is availability of biodegradable substrate. In this model, biodegradable substrate consists of fermentable substrate, S_F, fermentation products, S_A and hydrolysable substrate, X_S. S_F, and S_A make up S_S. Slowly biodegradable substrate, X_{S2}, is calculated as follows: $X_{S2} = COD_{tot} - (S_F + S_A) - X_{S1} - X_{BW}$, (Tanaka and Hvitved-Jacobsen, 2001). Hydrogen sulfide production rate here is modelled based on equation 4 in Table 3.4, where soluble COD value is used to calculate content of sulfide. However, in the model soluble COD is changed into the content of $S_F + S_A + X_{S1}$, as seen in the equation g, Table 4.3, since soluble COD value is not a direct part of the matrix. Also, such change makes sense from theoretical, experimental and modeling point of view (Hvitved-Jacobsen *et al.*, 2000). The model takes aerobic and anaerobic conditions into account, therefore it can be used for gravity sewers as well as for pressure mains. Oxygen content in wastewater in this model is described by three statements: oxygen consumption by biomass in bulk water as well as in biofilm, oxygen consumption for maintenance energy and oxygen increase in the system by reaeration. Other equations and used parameters are presented in Table 4.3 and Table 4.4.

Table 4.3: Matrix formulation of aerobic/anaerobic sulfide formation in sewers, (Hvitved-Jacobsen *et al.*, 2000)

	S_F	S_A	X_{S1}	X_{S2}	X_{HW}	S_{H2S}	$-S_O$	Rate
Aerobic growth in bulk water	$-1/Y_{HW}$				1		$(1-Y_{HW})/Y_{HW}$	Eq. a
Aerobic growth in biofilm	$-1/Y_{HF}$				1		$(1-Y_{HF})/Y_{HF}$	Eq. b
Maitanence energy requirement	-1						1	Eq. c
Aerobic hydrolysis, fast	1		-1					Eq. d, n=1
Aerobic hydrolysis, slow	1			-1				Eq. d, n=2
Anaerobic hydrolysis, fast	1		-1					Eq. e, n=1
Anaerobic hydrolysis, slow	1			-1				Eq. e, n=2
Fermentation	-1	1						Eq. f
H$_2$S production						1		Eq. g
Reaeration							-1	Eq. h

Equation a: $\mu_H \cdot \frac{S_F+S_A}{K_{SW}+(S_F+S_A)} \cdot \frac{S_O}{(K_O+S_O)} \cdot X_{HW} \cdot \alpha_W^{(T-20)}$

Equation b: $k_{1/2} \cdot S_O^{0.5} \cdot \frac{Y_{HF}}{(1-Y_{HF})A/V(S_F+S_A)/(K_{SF}+(S_F+S_A))} \cdot \alpha_F^{(T-20)}$

Equation c: $q_m \cdot \frac{S_O}{(K_O+S_O)} \cdot X_{HW} \cdot \alpha_W^{(T-20)}$

Equation d: $k_{hn} \cdot \frac{(X_{Sn}/X_{BW})}{K_{Xn}+(X_{Sn}/X_{BW})} \cdot \frac{S_O}{(K_O+S_O)} \cdot (X_{BW} + \epsilon X_{BF} \cdot A/V) \cdot \alpha_W^{(T-20)}$

Equation e: $h_{fe} \cdot k_{hn} \cdot \frac{(X_{Sn}/X_{BW})}{K_{Xn}+(X_{Sn}/X_{BW})} \cdot \frac{K_O}{(S_O+K_O)} \cdot (X_{BW} + \epsilon X_{BF} \cdot A/V) \cdot \alpha_W^{(T-20)}$

Equation f: $q_{fe} \cdot \frac{S_F}{K_{fe}+S_F} \cdot \frac{K_O}{(S_O+K_O)} \cdot (X_{BW} + \epsilon X_{BF} \cdot A/V) \cdot \alpha_W^{(T-20)}$

Equation g: $k_{H2S} \cdot 24 \cdot 10^{-3} \cdot (S_F + S_A + X_{S1})^{0.5} \cdot a_S^{(T-20)} \cdot \frac{K_O}{(S_O+K_O)} \cdot A/V$

Equation h: $K_L \cdot 24 \cdot (S_{OS} - S_O)$, where $K_{La} = 0.86 \cdot (1 + 0.20F^2) \cdot (s \cdot u)^{3/8} \cdot d_m^{-1} \cdot \alpha_r^{(T-20)}$

Table 4.4: Values used in hydrogen sulfide formation in the sewers model described in Table 4.3 (Hvitved-Jacobsen *et al.*, 2000)

Symbol	Description	Value	Unit
μ_H	Maximum specific growth rate	6.3	d^{-1}
Y_{HW}	Suspended biomass yield constant for heterotrophics	0.63	g COD g COD^{-1}
K_S	Saturation constant for readily biodegradable substrate	1.0	g COD m^{-3}
K_O	Saturation constant for dissolved oxygen	0.05	g O$_2$ m^{-3}
α_W	Temperature coefficient in water phase	1.07	-
q_m	maintenance energy requirement rate constant	1.0	d^{-1}
$k_{1/2}$	1/2 order rate constant	4.0	g O$_2^{0.5}$ m$^{-0.5}d^{-1}$
Y_{HF}	Biofilms yield constant for heterotrophics	0.55	g COD g COD^{-1}
K_{SF}	Saturation constant for readily biodegradable substrate	5.0	g COD m^{-3}
ϵ	Efficiency constant for biofilm biomass	0.15	-
α_F	Temperature coefficient in the biofilm	1.05	-
$k_{h,fast}$	Hydrolysis rate constant	5.0	d^{-1}
$k_{h,slow}$	Hydrolysis rate constant	0.5	d^{-1}
$K_{X,fast}$	Saturation constant for hydrolysis	1.5	g COD g COD^{-1}
$K_{X,slow}$	Saturation constant for hydrolysis	0.5	g COD g COD^{-1}
h_{fe}	Anaerobic hydrolysis reduction rate	0.14	-
q_{fe}	Maximum rate for fermentation	3.0	d^{-1}
K_{Fe}	Saturation constant for fermentation	20.0	g COD g COD^{-1}
k_{H2S}	H$_2$S production rate constant	2	g S^{2-}m^{-2} h^{-1}
α_S	Temperature coefficient for hydrogen sulfide production	1.030	-

It is clear from the matrix Table 4.3, that H_2S production is mainly dependent on wastewater characteristics (S_F, X_{S1}, etc), wastewater temperature and oxygen content in wastewater. Biodegradable substrate is required for growth and maintenance of microorganisms. Temperature determines the rate of processes, where with increasing temperature rate of H_2S production increases, whereas oxygen acts as inhibiting factor: H_2S production is possible only under anaerobic conditions. These changes are illustrated in Figure 4.10, where changes of wastewater composition are presented, and H_2S formation dependency on temperature is illustrated at Figure 4.11. As soon as oxygen in the bulk water is depleted, H_2S production begins. During the wastewater conveyance in the anaerobic pressure main, H_2S production is further increased.
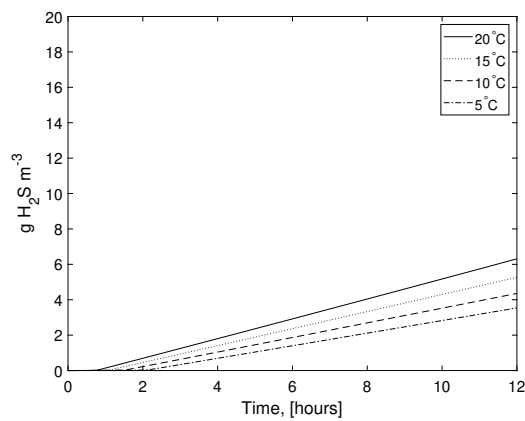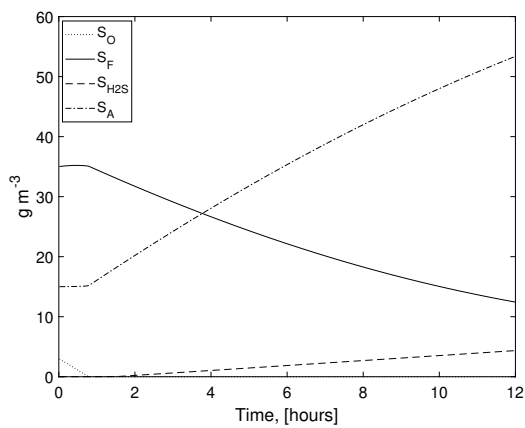
Figure 4.10: Wastewater composition during aerobic/anaerobic processes in pressure main, 10°C

Figure 4.11: H_2S formation dependency on wastewater temperature and retention time

During aerobic heterotrophic growth of biomass, S_F is rapidly consumed. However, it is not noticeable in Figure 4.10 due to the low X_{HW} concentration in the wastewater, which leads to biomass growth rate being lower than hydrolysis rate. Simulation with increased value of X_{HW} (X_{HW} = 35 COD g m^{-3}) is done to illustrate the concept (presented in Figure 11.10 and Figure 11.11). It illustrates, that with increased X_{HW} readily biodegradable substrate is rapidly consumed.

Figure 4.11 illustrates, that H_2S production is highly dependant on wastewater temperature as well as residence time in the sewer. Since temperature of wastewater in Hjørring has an amplitude of at least 15 °C, as illustrated in Figure 3.7, and wastewater flow is highly varying as well, Figure 3.6, capability of modelling a vast amount of possible scenarios is crucial in a comprehensive understanding in processes related to hydrogen sulfide production in sewers.

Results of in-sewer process evaluation

<div style="text-align: right">5</div>

In section 5 results of experiments carried out during this master thesis are presented together with sulfide formation in sewers model results. Results are presented as follows: results from OUR experiments, results from IC experiment for VFAs, results from in-situ odor sensor and finally - modeled sulfide formation in the pressure main data. Comparative analysis of the results as well as discussion are presented in section 8.

5.1 Oxygen uptake rate (OUR) and ion chromatography (IC)

Procedure of OUR experiment is described in section 4. Experiments are carried out in order to describe and quantify composition of wastewater as well as to estimate kinetic processes of biomass. Two parallel OUR experiments on Hjørring wastewater samples were carried out in order ensure replicability of the experiment. Parallel experiments proved to be very similar, therefore one data set is used for analysis. Experiment, illustrated in Figure 5.1, is used as the basis of wastewater composition description. The first 24 hours of experiment are used to estimate composition of wastewater in regard of biodegradable matter and quantity of biomass. Time period after addition of ethanol (24h–48h), illustrated in previous chapter, Figure 4.4, allows to select appropriate constants describing wastewater transformations.

Data used in this OUR experiment is fully described in previous chapter, Table 4.2. Wastewater composition in regard to COD parts is of major interest here. With OUR experiments highly active parts of COD were estimates as follows: S_S = 50 gCOD m^{-3}, X_{Hw} = 19 gCOD m^{-3}, $X_{S,fast}$ = 140 gCOD m^{-3}. This wastewater quality data fits the narrative described throughout the thesis. Long pressure main from Vrå to Hjørring receives high inflow of readily biodegradable matter rich wastewater, therefore S_S and $X_{S,fast}$ values are high.
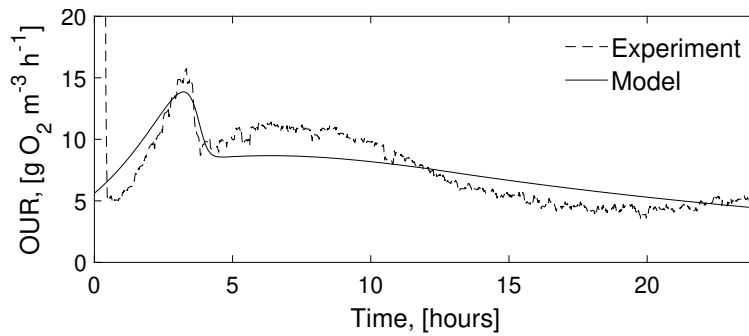
Figure 5.1: Data from OUR experiments with Hjørring wastewater sample taken at 2020-01-20 13:00

Furthermore, it is assumed, that throughout the pressure main anaerobic conditions are dominant. OUR experiment illustrates that, since initial X_{Hw} quantity is on a lower end. If pressure main would receive oxygen throughout the pressure main, concentration of aerobic biomass, X_{Hw}, most likely would be higher, since wastewater from Vrå is rich in easily biodegradable matter. It is well illustrated in Figure 5.1. Oxygen uptake rate increases rapidly with start of oxygen injection, which indicates rapid growth of aerobic biomass.

IC is the second part of laboratory methods used to quantify wastewater quality parameters. In this case acetate, which is closely related to the formation of sulfide, is determined. Concentration of acetate is calculated from Figure 4.8 by calculating area of acetate peak. Average area of acetate peak from three IC runs is 0.507 μS min^{-1}. Inserting this value into the calibration equation presented in Figure 4.7 delivers concentration of acetate in the wastewater sample, which is 18.9 g m^{-3}. Sample was collected at wastewater temperature of 10°C (Figure 3.7). Acetate concentration derived from IC corresponds well with S_S value from OUR experiment, since S_S is composed from fermentable substrate and fermentation products (such as VFA - acetate). While 18.9 g m^{-3} of acetate is a rather high concentration, it is to be expected with a presence of sulfide formation.

5.2   Odor logger

Ambient hydrogen sulfide concentrations, recorded by OdaLog in the inlet structure of Hjørring WWTP for continuous seven days period, are presented in Figure 5.2. Additionally, ambient temperature in the inlet structure was recorded. As seen in the figures, measured concentrations varies from 0–18 ppm. It has to be stressed, that detection resolution of logger is 1 ppm, thus exact measurements close to 0 are not available. May 8–10th was a long weekend and only small amounts of sulfide concentrations were detected. Even though they were above odor threshold. At May 13th highest value of 18 ppm is present. By comparing ambient temperature with H_2S concentrations, it can be seen, that hydrogen

sulfide formation is not directly correlated with ambient air temperature. This is reasonable, due to high water heat capacity.
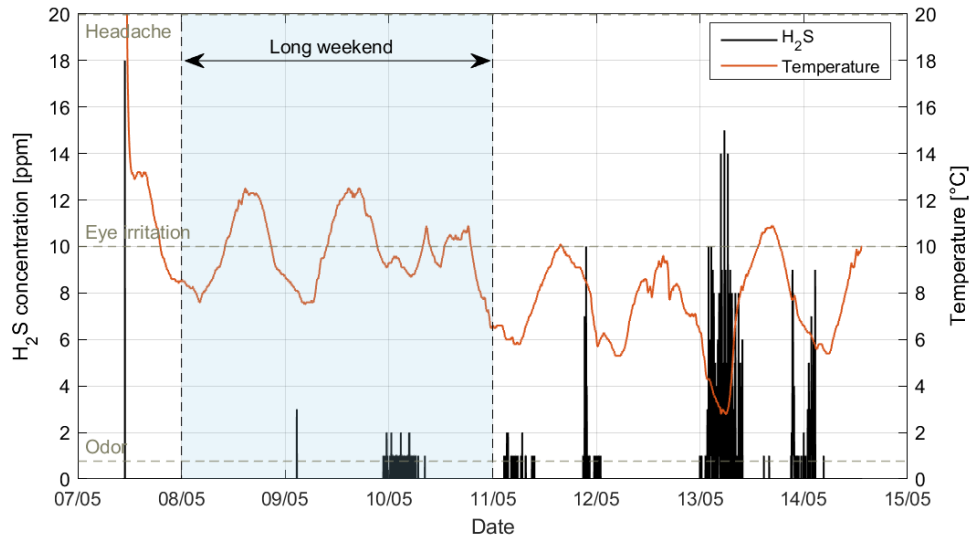
Figure 5.2: H₂S concentrations and surrounding air-temperature in inlet structure, May 7–14, 2020, including threshold values

To investigate aforementioned hypothesis, diurnal variation of sulfide concentration is plotted together with flow data, Figure 5.3. Is has to be mentioned that available hourly flow data is from 2017. From hourly inflow data, medians are calculated. H₂S formation at 22:00–08:00 is explained by pumping cycles. During day time, dilution occurs, as proved by high flow data. Data is recorded in May and, as figure above shows, air temperature is low, between 6 and 13°C. In the summer season at higher temperatures more sulfide will form. Formation of sulfide in summer time is also intensified by prevailing
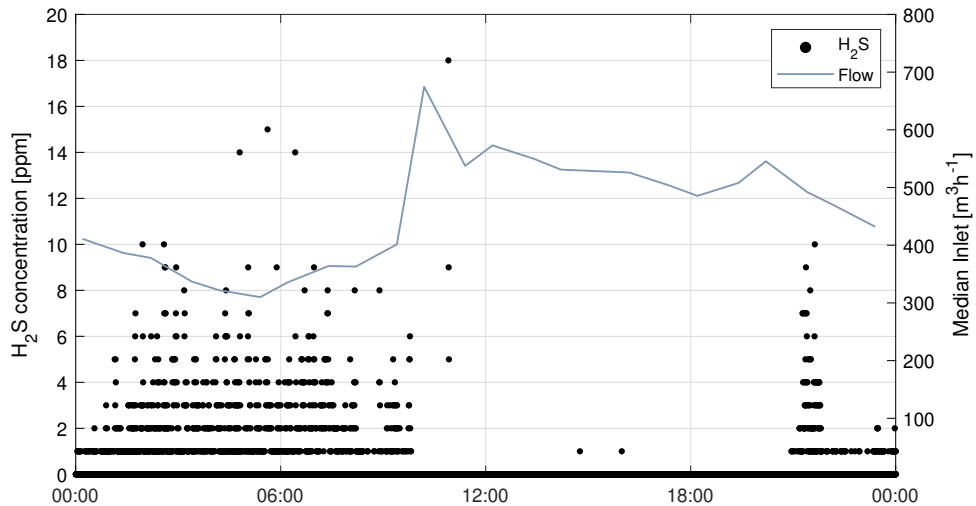
Figure 5.3: Diurnal variations in H₂S concentration in inlet structure (May 7–14, 2020) and median flow values at the inlet structure of Hjørring WWTP, from 2017

dry flow conditions, which increases hydraulic retention time in the pressure main as well as increases

concentrations of wastewater components. Furthermore, due to the placement of OdaLog and the design of the inlet structure, measured concentrations of sulfide are very likely diluted compared to the overall sulfide released from the pressure main. In order to evaluate full extent of sulfide production in the pressure main, data logging has to be carried out during the summer for prolonged periods of time. Even though recorded intervals of sulfide formation (1–18 ppm) might not seem substantial, it is proved that such amounts already causes corrosion problems in the sewer infrastructure, Appendix Table 11.1, not to mention overall health hazards, Table 3.3.

## 5.3   Results of sulfide formation model. Monte Carlo simulations

Wastewater is complex and it is well established that its composition and quality can change rapidly. Laboratory experiments, such as OUR evaluation or IC for VFAs, provide comprehensive analysis of wastewater quality. However, single wastewater sample is only a "snapshot" of overall composition of wastewater and can not fully account for transformations developing in the sewer system. Since extensive measurement campaigns over prolonged period of time are not always viable, which is the case in this thesis, statistical treatment of the data to estimate uncertainties have to be applied. For this purpose it is chosen to carry out Monte Carlo simulations on hydrogen sulfide formation model. One thousand model runs for each scenario (wet and dry flow conditions) are completed. Wastewater parameter intervals (min – max values) as well as, where it is possible, data distributions, averages and standard deviations are acquired from literature sources. In cases where average value and standard distribution are not available, parameter average is calculated as arithmetic mean, while standard deviation value is selected to represent complete interval of parameter in question. Most of parameters (except readily biodegradable substrate) are assumed to be normally distributed or constant value is selected. Assumption is based on (Vollertsen *et al.*, 2005), where wastewater parameter distribution is evaluated on 109 samples. In some cases a constant parameter value is selected either because a value is well documented (for example, temperature coefficients) or values presented in literature were not conclusive enough. In such case parameter values from Hvitved-Jacobsen *et al.*, 2013 or Hvitved-Jacobsen *et al.*, 2000 are used. For readily biodegradable substrate, it is decided to assume uniform distribution. Vollertsen *et al.*, 2005 finds out that data of readily biodegradable substrate is not normally distributed. Furthermore, it is documented that in case of the pressure main form Vrå to Hjørring, wastewater rich in readily biodegradable substrate is discharged into the sewer system. Also it is assumed, that high readily biodegradable substrate discharge is not constant (industry generally does not operate

in constant manner) and periods of wastewater discharge with low or medium readily biodegradable substrate concentrations are as likely. Parameters are presented in the appendix, Table 11.3.

After all the parameters are selected, one thousand values for each parameter are randomly generated according to its distribution and, if not uniformly distributed, standard deviation. Parameters are assumed to be independent of each other. Model is run with each data set and results are illustrated in Figure 5.4 as well as in appendix Figure 11.14. Plots illustrate data up to four distinct percentile values and a median. Median is used instead of the average because not all the parameters are assumed to be normally distributed.

(a) Dry flow conditions, pH=7   (b) Wet flow conditions, pH=7
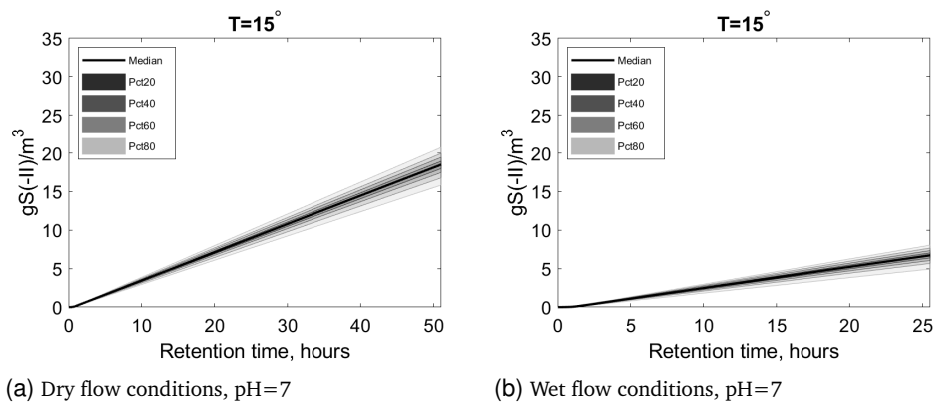
Figure 5.4: Sulfide production in the pressure main. Data is generated with Monte Carlo simulations from 1000 data sets for each scenario. 20th–80th percentiles are presented. Hydraulic retention times are described in Table 6.1

Possible sulfide production range from 5 g S m^{-3} – 9 g S m^{-3} under wet flow condition to 13 g S m^{-3} – 24 g S m^{-3} under dry flow conditions (Figure 5.4 and Appendix Figure 11.14). Upper value for wet flow has to be considered as an overestimation, since wet flow is not a 'summer time' condition (Figure 3.7, Figure 3.8) and 20 °C temperature of wastewater is highly unlikely to occur. Therefore, more realistic estimation of sulfide concentration in the pressure main should not be higher than about 6 g S m^{-3} (data from scenarios with 15 °C and 20 °C should probably be negated). Similar situation follows dry flow scenario as well. However, even though and 20 °C of wastewater is rare, it is by no means impossible. Furthermore, when discussing sulfide formation availability of sulfate in water must be taken into account. Sulfate content in potable water in Vrå is investigated (Appendix Table 11.2) and the average concentration of sulfate is 55.5 g m^{-3}. Therefore, on average, maximum of around 18.5 g S m^{-3} of sulfide can form in wastewater. Additionally, in CSR report (dan.: CSR Redegoerelse) from Vrå Dampvaskeri, 2015 it is stated that sulfuric acid is used to neutralise high pH wastewater from the laundry. Naturally, use of sulfuric acid increases sulfate concentration in wastewater to some extent. Overall, it is clear that high value of sulfide formed in the pressure main, 24 g S m^{-3}, is not implausible and with a relatively high standard deviation of sulfate in wastewater in Vrå, it is not a limiting factor in

sulfide production. With everything taken into account, it is apparent that model illustrates medium to high sulfide production in the pressure main from Vrå to Hjørring. Even if sulfide production in the pressure main is expected to be substantial, its dilution in the inlet structure of WWTP should not be overlooked. Inflow from the pressure main makes up only around 4% of total inflow to WWTP. Main part of sewage comes from Hjørring through gravity sewers, therefore sulfate reduction is limited to the pressure main from Vrå to Hjørring. It is expected that most intensive effects of sulfide are visible right at the outlet of the pressure main whereas further into the treatment plant its effects are diminished.

Sulfide abatement in the pressure main

In this chapter strategies of alleviating hydrogen sulfide in the pressure main are evaluated. Evaluation heavily relies on section 5, where result from the comprehensive analysis of hydrogen sulfide formation in pressure main from Vrå to Hjørring WWTP are presented. This study focuses on chemical and biological processes that prevent or decrease hydrogen sulfide formation in the sewer system. In this chapter, three sulfide abatement strategies are discussed: injection of oxygen in order to prevent anaerobic conditions and to initiate oxidation of sulfide, injection of nitrate to establish anoxic conditions and, possibly, oxidize sulfide and finally use of iron salts to precipitate sulfide. Several more abatement strategies exist but were not taken into further consideration, Figure 6.1.
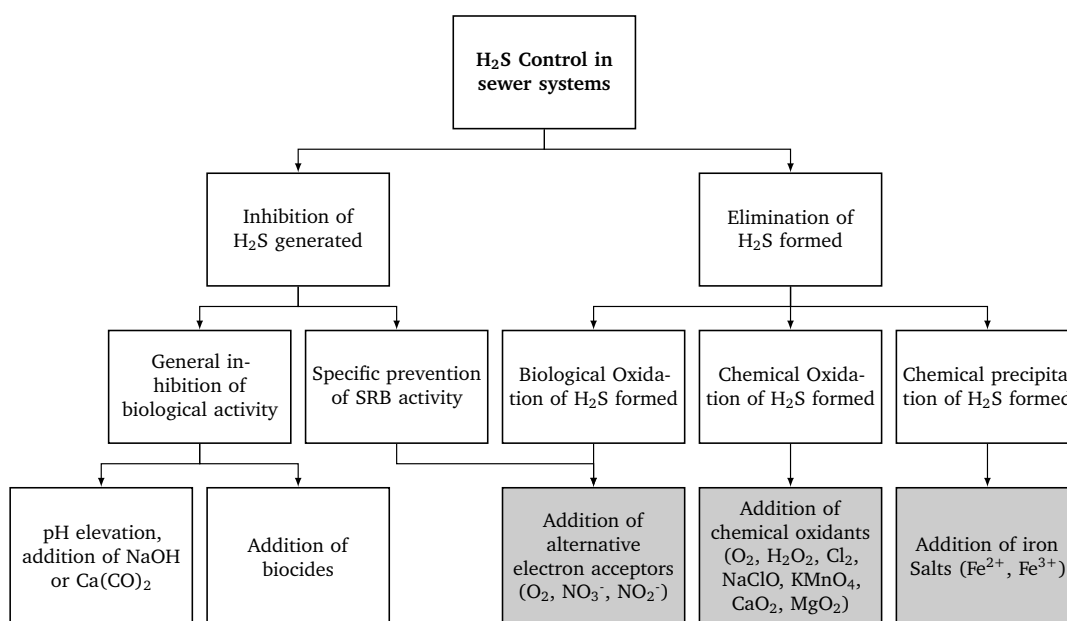
Figure 6.1: Chemical and biological technologies for H_2S emission control in sewer systems (from Zhang *et al.*, 2008). SRB: sulfate-reducing bacteria, grey: used methods

There are three viable places for addition of substances throughout the pressure main, Figure 6.2. Two are immediately accessible: the pumping station in Vrå and the inlet at Hjørring WWTP. Third potential place for substance addition is the pumping station at Hjørring. Currently pressure main bypasses this

pumping station, however, it is very likely that injection point to the pressure main could be installed here as well without huge economic repercussions.
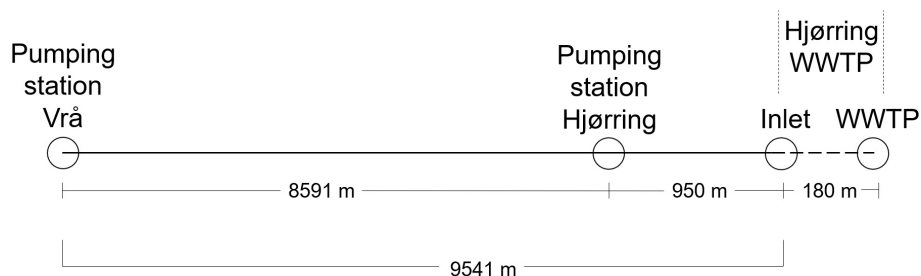
Figure 6.2: Sketch of force main. ◯ indicate access point for substance additions

The pumping station in Vrå and the inlet at Hjørring WWTP might seem as the most convenient injection points, because they are available to use without further ado. However, since pressure main from Vrå is a long structure, it is likely that some additional minor branches of pipe structures are connected to it. Such plug-flow system prevent mixing of wastewater from minor branches with wastewater from Vrå (Kiilerich *et al.*, 2018), which would in turn limit sulfide abatement. Injection point at inlet of Hjørring WWTP also has some negative consequences: very short retention time, due to limited distance from inlet to the main part of WWTP, mixing and dilution of wastewater from Vrå with wastewater from Hjørring and depressurisation of wastewater from Vrå, which releases a fraction of sulfides into the atmosphere.

Table 6.1 illustrates residence time of wastewater in the pressure main and how it depends from flow velocity in the pipe under 'normal' and dry/summer conditions. Columns named '0.1·Retention time' shows the required time for wastewater to reach Hjørring WWTP from Hjørring pumping station.

Table 6.1: Flow times from Vrå to Hjørring and from Hjørring pumping station to Hjørring WWTP inlet. Normal and dry (summer time) flow conditions.

Velocity	Time	0.1·Retention time	0.1·Retention time
m s^{-1}	h	h	s
0.10	26.5	2.65	9 541
0.05	51.0	5.10	19 082

6.1   Sulfide control with oxygen injection

Sulfate reduction reaction - production of hydrogen sulfide is strictly anaerobic, therefore changing anaerobic conditions into aerobic, by injection of oxygen to the pressure main, is a way of preventing sulfate reduction processes in wastewater. Furthermore, addition of oxygen enables a process of sulfide oxidation. Sulfide oxidation happens in water phase as well as in sewer biofilm and can be chemical as well as biological. Sulfide can be oxidised to four different products (Hvitved-Jacobsen *et al.*, 2013):

$$2HS^- + O_2 \longrightarrow 2S^0 + 2HO^- \tag{6.1}$$

$$2HS^- + 2O_2 \longrightarrow S_2O_3^{2-} + H_2O \tag{6.2}$$

$$2HS^- + 3O_2 \longrightarrow 2SO_3^{2-} + 2H^+ \tag{6.3}$$

$$2HS^- + 4O_2 \longrightarrow 2SO_4^{2-} + 2H^+ \tag{6.4}$$

As it is seen in Equation 6.1 - Equation 6.4, stoichiometry of sulfide oxidation due to the variety of reactions is quite diverse. Furthermore, as biological and chemical reactions in wastewater can happen in parallel, evaluation of reaction stoichiometry becomes even more complicated. In Hvitved-Jacobsen *et al.*, 2013 it is stated that under chemical oxidation of sulfide, reaction stoichiometric coefficient is 0.8–0.9 mol S (mol O_2)$^{-1}$ $\approx$ 0.8–0.9 g S (g O_2)$^{-1}$. Reaction scheme of chemical sulfide oxidation correspond to all the equations, from Equation 6.1–Equation 6.4. Under biological sulfide oxidation, the usual product in sewer environment is elemental sulfur, while further oxidation paths can be disregarded. Therefore stoichiometric ratio from Equation 6.1 is applicable, 2 mol S (mol O_2)$^{-1}$ $\approx$ 2 g S (g O_2)$^{-1}$. Nielsen *et al.*, 2006 determined reaction stoichiometric coefficient for chemical sulfide oxidation to be 0.87 g S (g O_2)$^{-1}$, which corresponds to previously mentioned data. And as far as biological sulfide oxidation, in most cases reaction stoichiometric coefficient corresponds to Equation 6.1, 2 g S (g O_2)$^{-1}$, however in some cases coefficient was determined to be lower, 1.7 g S (g O_2)$^{-1}$.

Hvitved-Jacobsen *et al.*, 2013 provides a general equation for sulfide oxidation reaction kinetics, Equation 6.5.

$$i = k_{S(-II)} S_{S(-II)}{}^m S_O{}^n \tag{6.5}$$

Where:

i	sulfide oxidation rate	[g S m^{-3} day^{-1}]
$k_{S(-II)}$	Rate constant for chemical oxidation of H2S	[(g S m^{-3})$^{1-mc}$(g O$_2$ m^{-3})$^{-nc}$ day^{-1}]
m and n	Reaction order, $m = 1$, $n = 0.1$ (Nielsen *et al.*, 2006)	[-]

This rate equation illustrates - with reaction order values - that in sulfide oxidation concentration of sulfide is way more influential (by factor 10), compared to oxygen concentration. Hvitved-Jacobsen *et al.*, 2013 also states, that $m >> n$ for chemical as well as biological sulfide oxidation. Sulfide oxidation is also depended on pH as well as temperature, which is evident form Nielsen *et al.*, 2006 research with formulated equations: Equation 6.6 and Equation 6.7, where optimal pH ≈ 8 and sulfide oxidation rate is proportional to temperature. Similar effects are observed for chemical as well as biological sulfide oxidation, with an exception that rate of biological oxidation is far more sensitive to low pH values.

$$i_c = \frac{k_{H_2Sc} + k_{HS^-c} \cdot K_{a1}/(1/10)^{pH}}{1 + K_{a1}/(1/10)^{pH}} S_{S(-II)}{}^m S_O{}^n \alpha_{S(-II)c}{}^{T-20} \qquad (6.6)$$

$$i_b = k_{S(-II)b} \frac{\omega_{S(-II)b}}{\omega_{S(-II)b} + 10^{|opt.pH-pH|} - 1} S_S(-II)^m S_O{}^n \alpha_{S(-II)b}{}^{T-20} \qquad (6.7)$$

Where:

i_c	Chemical sulfide oxidation rate	[g S m^{-3} day^{-1}]
i_b	Biological sulfide oxidation rate	[g S m^{-3} day^{-1}]
k_{H_2Sc}	Rate constant for chemical oxidation of H2S	[(g S m^{-3})$^{1-m}$(g O$_2$ m^{-3})$^{-n}$ day^{-1}]
k_{HS^-c}	Rate constant for chemical oxidation of HS-	[(g S m^{-3})$^{1-m}$(g O$_2$ m^{-3})$^{-n}$ day^{-1}]
$k_{S(-II)b}$	Rate constant for biological sulfide oxidation	[(g S m^{-3})$^{1-m}$(g O$_2$ m^{-3})$^{-n}$ day^{-1}]
K_{a1}	First dissociation constant for sulfide	[-]
$\omega_{S(-II)b}$	Width of optimum pH range for heterotrophic processes	[-]

Equation 6.6 and Equation 6.7 from Nielsen *et al.*, 2006 are used to construct a part of a matrix Table 6.2, which servers as an addition to previously described hydrogen sulfide production matrix (in Chapter 4). Estimation of stoichiometric rates are presented on a previous page as g S (g O$_2$)$^{-1}$, while in a matrix values illustrate in g O (g S2)$^{-1}$.

Applying the matrix from Table 4.3 together with the matrix from Table 6.2 allows to simulate production and oxidation of hydrogen sulfide in the pressure main. Modelling of sulfide oxidation is done with the assumption, that oxygen/compressed air is injected to Hjørring pumping station and oxygen

Table 6.2: Extension of matrix formulation of aerobic/anaerobic sulfide formation in sewers, (Hvitved-Jacobsen *et al.*, 2000), with aerobic sulfide oxidation. Reaction rates are from Nielsen *et al.*, 2006

	S_F	S_A	X_{S1}	X_{S2}	X_{HW}	S_{H2S}	$-S_O$	Rate
S aerobic oxidation, chemical						-1	100/87	Equation 6.6
S aerobic oxidation, biological						-1	1/2	Equation 6.7

concentration at that point reaches 6 g O_2 m^{-3}. Due to pressurised flow and at lower wastewater temperatures, it is possible to reach higher oxygen concentrations, especially since even at normal pressures, at 20°C, oxygen saturation in water is approximately 8 g O_2 m^{-3} (as illustrated in Appendix Figure 11.5). However, effect of higher dissolved oxygen concentration would not be significant due to its rapid consumption by biomass, if oxygen is injected via compressed air. Also, process of saturating water with oxygen is not rapid and temperature remains main factor controlling concentration of dissolved oxygen compared to pressure (Hvitved-Jacobsen *et al.*, 2013). Therefore conservative approach of 6 g O_2 m^{-3} injection is chosen. pH = 7 is assumed throughout modelling scenarios for wet and dry flow conditions, Figure 6.3.
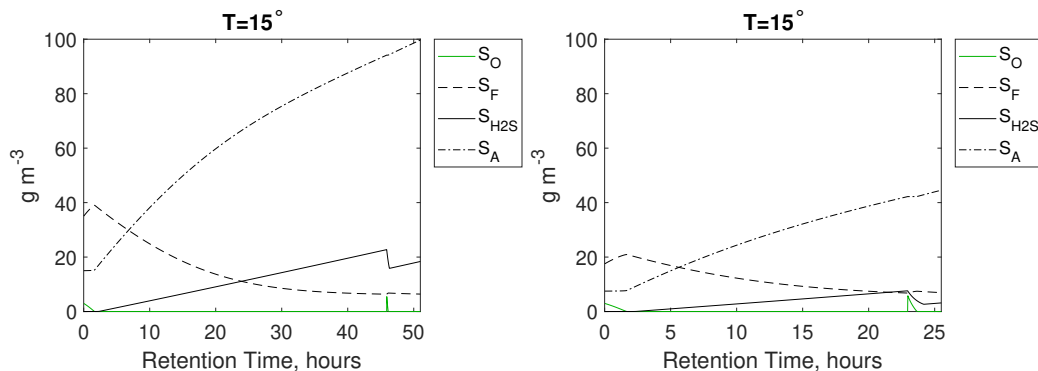
Figure 6.3: Sulfide formation and abatement with oxygen injection at Hjørring pumping station, dry (51.0 h retention time) and wet (26.5 h retention time) conditions. pH = 7

Key finding from the figure above is, that a single oxygen injection point is not enough to neither establish aerobic conditions to prevent sulfide formation, nor to oxidize existing sulfide. It is especially well visible in the left graph illustrating dry flow conditions, where retention time is longer and concentrations of COD parts are higher. Even though under wet conditions, where wastewater is more diluted and retention time is twice as short, single oxygen injection point is not enough. Total sulfide concentration is reduced to low–medium sulfide levels, which is not considered acceptable.

6.2 Sulfide control with addition of Nitrate

Throughout this thesis an emphasis is put on aerobic and anaerobic sewer conditions, mainly because anoxic conditions are not typically established in the sewer due to a low availability of nitrate or its products (Hvitved-Jacobsen *et al.*, 2013). However, artificial addition of nitrate in order to establish anoxic conditions in the sewer is possible and is used for hydrogen sulfide mitigation. Addition of nitrates to the system raises redox potential which encourages anoxic activity instead of anaerobic, with a condition that the DO concentration in wastewater is extremely low (Firer *et al.*, 2008). Anoxic metabolic processes have a higher energy balance then anaerobic ones. With the addition of nitrate, anaerobic creation of H_2S is suppressed due to the establishment of anoxic conditions. During heterotrophic anoxic processes, denitrification of NO^-_3 to N_2 occurs, Equation 6.8. Also already formed H_2S is reduced under autotrophic anoxic sulfide oxidation, Equation 6.9, where sulfide acts as electron donor and inorganic carbon as the carbon source while nitrate is electron acceptor (Hvitved-Jacobsen *et al.*, 2013).

$$NO^-_3 + C_{org} + H^+ \rightarrow CO_2 + N_2 + H_2O \tag{6.8}$$

$$H_2S + 2H_2O + 2NO^-_3 \rightarrow H_2SO_4 + N_2 + 4(OH)^- \tag{6.9}$$
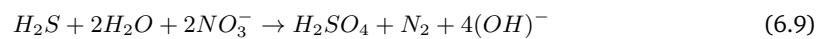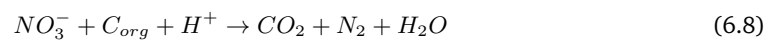
Equation 6.8 portrays generalised picture of heterotrophic anoxic processes with nitrogen acting as electron acceptor. However, Abdul-Talib *et al.*, 2002 states, that anoxic processes with addition of nitrate in wastewater happens in several steps, with most likely steps illustrated in Equation 6.10:

$$NO^-_3 \rightarrow NO^-_2 \rightarrow NO \rightarrow N_2O \rightarrow N_2 \tag{6.10}$$
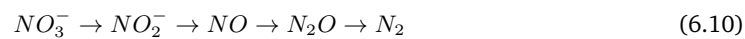
While all forms of nitrate presented in equation above can be present in wastewater, Abdul-Talib *et al.*, 2002 establishes, that while nitrous oxide, NO, may accumulate in wastewater under anoxic conditions, concentration of it is as low as 0.01 % of total nitrogen in the processes, thus for modeling purposes nitrogen transformation chain is assumed to be as illustrated in Equation 6.11. In aforementioned article it is also discussed, that nitrate consumption under anoxic conditions happens in two distinct steps. First one is illustrated in Equation 6.11. Throughout this step nitrite tends to accumulate. It is observed, that amount of nitrite reaches 40–60 % of initial amount of nitrate, and after nitrate is depleted, nitrite is rapidly utilised (Abdul-Talib *et al.*, 2002). Heterotrophic anoxic growth only on accumulated nitrite is the second step of nitrate consumption and is illustrated in Equation 6.12.

$$NO^-_3 \rightarrow NO^-_2 \rightarrow N_2 \tag{6.11}$$

$$NO^-_2 \rightarrow N_2 \tag{6.12}$$

Hvitved-Jacobsen $et\,al.$, 2013 mentions, that in nitrate nitrogen concentrations below 2–5 g m^{-3}, nitrate is a limiting factor in anoxic heterotrophic processes, and consequentially 5.0 g NO$_3$-N m^{-3} is deemed to be enough to create nitrate excess conditions in sewer system. Furthermore, nitrate initial utilisation rate by anoxic heterotrophic processes in general is found to be 0.8 – 2.0 g NO$_3$-N m^{-3} h^{-1} in wastewater alone (Abdul-Talib $et\,al.$, 2002). However, biomass related to anoxic heterotrophic processes is not sole consumer of nitrate.

Equation 6.9 describes complete autotrophic anoxic sulfide oxidation. Yang $et\,al.$, 2005 stated, that anoxic sulfide oxidation process in sewers is strictly biological, whereas chemical sulfide oxidation is either non-existent or happening at very low rates. Furthermore, Hvitved-Jacobsen $et\,al.$, 2013 discusses that in sewer conditions, sulfide is oxidised to elemental sulfur, which is rather stable and formation of it considered as a governing factor in rate of sulphide removal. Therefore, sulfide oxidation processes can be rewritten to Equation 6.13 and Equation 6.14, which enhances an understanding of stoichiometry of these processes.

$$H_2S + NO_3^- \rightarrow S^0 + NO_2^- + H_2O \tag{6.13}$$

$$3H_2S + 2NO_2^- + 2H^+ \rightarrow 3S^0 + N_2 + 4H_2O \tag{6.14}$$
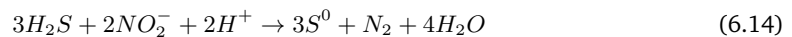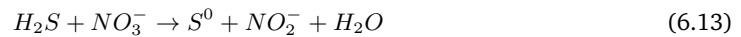
Yang $et\,al.$, 2005 investigated the stoichiometry of anoxic sulfide oxidation and its relation to total nitrate consumption: even though nitrate required for sulfide oxidation according to stoichiometric equations is 0.18 – 0.44 g NO$_3$-N (g S)$^{-1}$, total nitrate consumption is found to be 1.4 – 4.6 g NO$_3$-N (g S)$^{-1}$. This illustrates, that heterotrophic anoxic processes consumes 90 % of total nitrate in the system. Likely occurring sulfide transformations under anoxic oxidation are presented by Hvitved-Jacobsen $et\,al.$, 2013, Equation 6.13 and Equation 6.14. These formulas are used to estimate stoichiometric ratios for autotrophic anaerobic sulfide oxidation for nitrate and nitrite, which are as follows: 0.44 g NO$_3$-N (g S)$^{-1}$ and 0.29 g NO$_2$-N (g S)$^{-1}$. These values are only theoretical estimations from likely occurring process formulations, although it fits values provided by Yang $et\,al.$, 2005 rather well. It is important to mention that stoichiometric ratios do not take processes in biofilm into account, since kinetics of sulfide oxidising bacteria (SOB) in sewer biofilm are not fully investigated, even though SOB in biofilm have to contribute to sulfide oxidation. The sulfide oxidation rate under anoxic conditions is 0.48 and 0.62 g S m^{-3} h^{-1} at pH 7.0 respectively 8.5 (Yang $et\,al.$, 2005). Sulfide oxidation rates decrease with increase in anaerobic storage time of wastewater; Yang $et\,al.$, 2005 found, that after six days of anaerobic wastewater storage, sulfide oxidation rate was only 10 % of values in fresh wastewater. It is discussed in aforementioned article that this phenomena most likely occurs due to reduced activity of SOB in wastewater due to decay under prolonged residence time in anaerobic conditions.

Stoichiometric ratios as well as various parameters for anoxic wastewater transformations in sewer are coupled together and used to establish one model which could be used for anoxic sulfide abatement investigations. Matrix, which works as an extension to matrix presented (Table 4.3), includes heterotrophic anoxic processes and autotrophic anoxic sulfide oxidation. The matrix is build based on Yang *et al.*, 2004. In the article, S_S is not divided into S_F and S_A, however, in this thesis division is important part of the processes description. It is assumed that one unit of S_S is equal to 0.5 of S_F plus 0.5 of S_A, therefore overall mass balance in wastewater transformations remains unchanged. Throughout the modelling S_F and S_A does not drop to negative values. If that would be the case, ratio between S_F and S_A should be changed according to its concentrations present in wastewater. Furthermore, in wastewater, fermentable substrate is being replenished by hydrolysis from hydrolysable substrate.

Additional change in the matrix is an anoxic switch for sulfide production, Table 6.3 Equation g. Switch is applied as Monod kinetics and turns off sulfide production when nitrate and/or nitrite is present. Fraction of nitrate reducing biomass, f_n, is estimated via model fitting while trying to achieve peak concentrations of nitrite to be 40–60 % of added nitrate. Heterotrophic active biomass under anoxic conditions, X_{HWN} is assumed to make up 0.7 of total biomass in water phase. Equation o_n originates from Yang *et al.*, 2005 with addition of switches for nitrate and nitrite as well as oxygen. Switches for nitrate and nitrite ensures that autotrophic anoxic sulfide oxidation occurs only when nitrate and/or nitrite is presented. An oxygen switch activates the equation only when oxygen is depleted.

With above-mentioned factors taken into account, a model with heterotrophic anoxic processes and autotrophic anoxic sulfide oxidation in wastewater is build and result are presented in Figure 6.4. The figure illustrates wet and dry flow conditions at 15 °C. Four distinct situation are illustrated. Graphs (a) and (b) illustrate nitrate injection at Vrå pumping station. It is clear that under dry conditions (a) 30 g m^{-3} of nitrate is not enough to establish anoxic conditions throughout all the pressure main, while under wet conditions (b) its too much. A simple correction of nitrate concentration added would solve that issues. Graphs (c) and (d) illustrate nitrate injection at Hjørring pumping station.

Even with maximum sulfide oxidation rate from Yang *et al.*, 2005, 0.62 g S m^{-3} h^{-1}, assumed and with retention time of wastewater from Hjørring pumping station to the WWTP of 5.1 h at dry weather conditions, concentration of sulfide oxidised is 3.2 g S m^{-3}. It is not enough to abate sulfide completely even at low wastewater temperatures, Appendix Figure 11.14. Corresponding situation is illustrated in graphs (c) and (d): while sulfide oxidation is quite noticeable, rate is not high enough to abate sulfide to acceptable low levels, less than 0.5 g S m^{-3}. In theory, it is possible to argue for mixing both approaches: injecting nitrogen at Vrå as well as Hjørring pumping stations. However, this approach is not really valid: if enough nitrogen is delivered at Vrå, there is no need for additional injection at Hjørring.

Table 6.3: Extension of matrix formulation of aerobic/anaerobic sulfide formation in sewers with anoxic transformations, based on Yang *et al.*, 2004. Hydrolysable substrate is not visible in this matrix extension, because anoxic conditions has no significant influence on hydrolysis in model concept. However, overall, hydrolysis is still active, as seen in Table 4.3

	S_F	S_A	X_{HW}	S_{H2S}	$-S_{NO3}$	$-S_{NO2}$	$-S_O$	Rate
Anoxic growth, NO$_3$	$-0.5/Y_{NO3}$	$-0.5/Y_{NO3}$	1		$(1-Y_{NO3})/Y_{NO3}$	$(Y_{NO3}-1)/Y_{NO3}$		Eq. k
Anoxic growth, NO$_2$	$-0.5/Y_{HW}$	$-0.5/Y_{HW}$	1			$(1-Y_{NO2})/Y_{NO2}$		Eq. l
Anoxic maintenance, NO$_3$	-0.5	-0.5	-1^*		1			Eq. m
Anoxic maintenance, NO$_2$	-0.5	-0.5	-1^*			1		Eq. n
Anoxic oxidation, NO$_3$				-1	0.44			Eq. o$_n$
Anoxic oxidation, NO$_2$				-1		0.29		Eq. o$_n$

* *Biomass is consumed during anoxic maintenance, when there is no more S_F nor S_A*

Equation k: $\mu_{H,NO_3} \cdot \frac{S_{NO_3}}{(K_{S,NO_3}+S_{NO_3})} \frac{S_F+S_A}{K_{SW}+(S_F+S_A)} \cdot \frac{K_O}{(K_O+S_O)} \cdot f_n \cdot X_{HWN} \cdot \alpha_W^{(T-20)}$

Equation l: $\mu_{H,NO_2} \cdot \frac{S_{NO_2}}{(K_{S,NO_2}+S_{NO_2})} \frac{S_F+S_A}{K_{SW}+(S_F+S_A)} \cdot \frac{K_O}{(K_O+S_O)} \cdot (1-f_n) \cdot X_{HWN} \cdot \alpha_W^{(T-20)}$

Equation m: $q_{m,NO_3} \cdot \frac{S_{NO_3}}{(K_{S,NO_3}+S_{NO_3})} \cdot f_n \cdot X_{HWN} \cdot \alpha_W^{(T-20)}$

Equation n: $q_{m,NO_2} \cdot \frac{S_{NO_2}}{(K_{S,NO_2}+S_{NO_2})} \cdot (1-f_n) \cdot X_{HWN} \cdot \alpha_W^{(T-20)}$

Equation o$_n$: $k_{anoxic} \cdot 24 \cdot \frac{S_{H_2S}}{(S_{H_2S}+K_{sanoxic})} \cdot \frac{S_{NO_n}}{(K_{S,NO_n}+S_{NO_n})} \cdot \frac{K_O}{(K_O+S_O)} \cdot \alpha_W^{(T-20)}$

Equation g, updated: $k_{H2S} \cdot 24 \cdot 10^{-3} \cdot (S_F + S_A + X_{S1})^{0.5} \cdot a_S^{(T-20)} \cdot \frac{K_O}{(S_O+K_O)} \cdot A/V \cdot \frac{(K_{S,NO_3})}{(K_{NO_3}+S_{NO_3})} \frac{(K_{S,NO_2})}{(K_{NO_2}+S_{NO_2})}$

Table 6.4: Values used in hydrogen sulfide abatement in the sewers under anoxic conditions. Values of $\mu_{H,NO_n}, Y_{NO_n}, K_{S,NO_n}$ are from Yang *et al.*, 2004, f_n is from Hvitved-Jacobsen *et al.*, 2013

Symbol	Description	Value	Unit
μ_{H,NO_3}	Maximum specific growth rate	4.00	d^{-1}
Y_{NO_3}	Yield constant for heterotrophic biomass	0.24	mol e-eq (mol e-eq)$^{-1}$
K_{S,NO_3}	Saturation constant for readily biodegradable substrate	2.90	g NO$_3$-N m^{-3}
μ_{H,NO_2}	Maximum specific growth rate	4.50	d^{-1}
Y_{NO_2}	Yield constant for heterotrophic biomass	0.22	mol e-eq (mol e-eq)$^{-1}$
K_{S,NO_2}	Saturation constant for readily biodegradable substrate	3.80	g NO$_3$-N m^{-3}
f_n	Fraction of nitrate reducing biomass	0.70	-
X_{HVN}	Heterotrophic biomass under anoxic conditions	-	g COD m^{-3}
k_{anoxic}	Maximum sulfide anoxic oxidation rate	0.4	g S m^{-3} h^{-1}
$K_{s,anoxic}$	Half-saturation constant for anoxic sulfide oxidation	0.4	g S m^{-3}

Advanced sulfide logger suitable for continuous sulfide measurements in wastewater could be installed before Hjørring pumping station to estimate at what point in time nitrogen injection at Vrå is insufficient to abate sulfide production. With such data, model with feedback control could estimate how much nitrate to inject at Hjørring pumping station. However, it is very unlikely that the autotrophic anoxic sulfide oxidation rate would be high enough to reduce sulfide concentrations to acceptable levels if injected at Hjørring pumping station. Since autotrophic anoxic sulfide oxidation is not crucial in sulfide abatement in this particular case, it is not investigated further in the thesis.
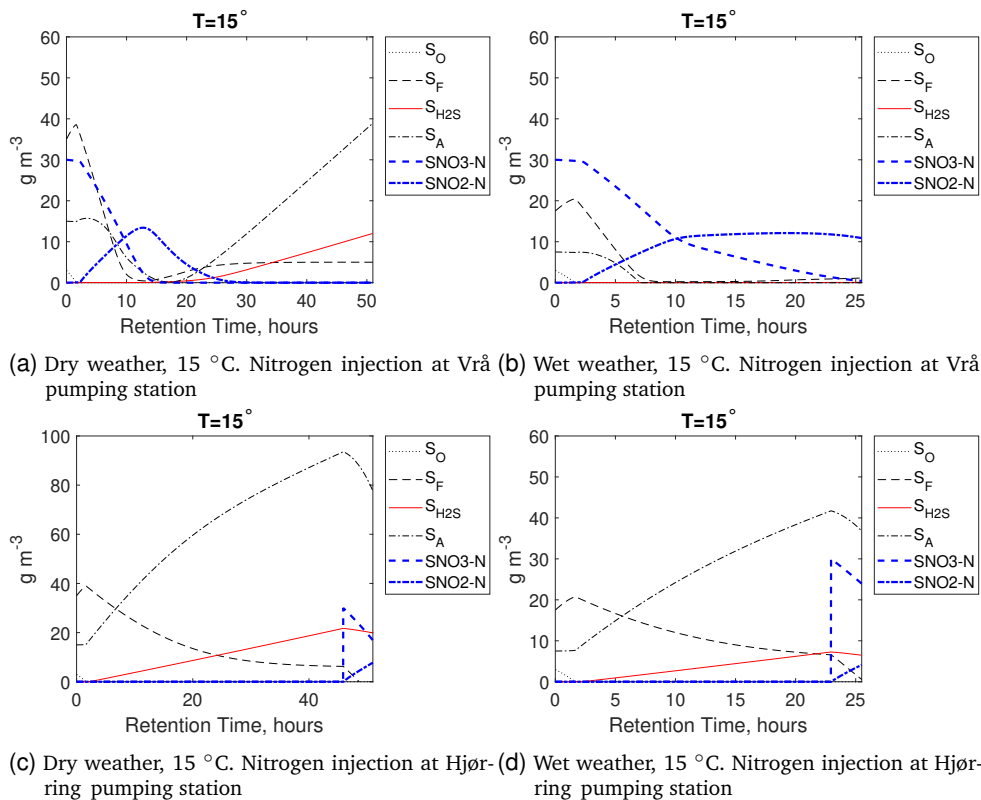
(a) Dry weather, 15 °C. Nitrogen injection at Vrå pumping station

(b) Wet weather, 15 °C. Nitrogen injection at Vrå pumping station

(c) Dry weather, 15 °C. Nitrogen injection at Hjørring pumping station

(d) Wet weather, 15 °C. Nitrogen injection at Hjørring pumping station

Figure 6.4: Sulfide formation and abatement with nitrate injection at Vråpumping station or Hjørring-pumping station. Dry (51.0 h) and wet (26.5 h) conditions. pH = 7

6.3   Sulfide control with addition of Fe(II) and Fe(III)

In the previous sections it was established that oxygen and nitrate mainly works as a preventative measures in H_2S control, which enforces aerobic and anoxic conditions in wastewater accordingly. However, since maintaining aerobic conditions all thorough the pressure main is problematic, and oxidising sulfide aerobically and, especially, anoxically requires relatively high retention time of wastewater, other possibilities of H_2S control are investigated. In this section, sulfide control with addition of Fe(II) and Fe(III) salts as an alternative to oxygen and nitrogen injection are looked into.

Addition of iron salts into wastewater is well established and a widely used method for H_2S abatement (Hvitved-Jacobsen *et al.*, 2013; Firer *et al.*, 2008). Iron salts are specific to H_2S in odor control, reaction between them are rapid, but not instantaneous, and the price is relatively low (Firer *et al.*, 2008; Kiilerich *et al.*, 2018). Theoretically, iron and sulfide reactions and stoichiometry can be described with Equation 6.15 and Equation 6.16. Ferrous iron (FeII) directly precipitates as FeS, while ferric iron (FeIII) has to undergo reduction to ferrous iron first. Sulfide reduction can be biological or chemical: sulfide

could be used by specific bacteria or reaction may occur from oxidation of bisulfide to elemental sulfur Kiilerich *et al.*, 2018.

$$Fe^{2+} + HS^- \longleftrightarrow FeS + H^+ \qquad (6.15)$$

$$2Fe^{3+} + HS^- \longleftrightarrow 2Fe^{2+} + S^0 + H^+ \qquad (6.16)$$
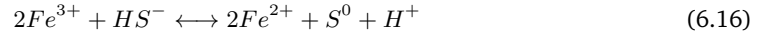
For accurate selection of iron to sulfide ratio, understanding of stoichiometrics of Equation 6.15 and Equation 6.16 is crucial. It is usually assumed that sulfide precipitation with ferrous iron is faster compared to ferric iron, since ferric iron has to go through an additional chemical reaction step. But recent research of iron precipitation kinetics in wastewater by Kiilerich *et al.*, 2018 shows otherwise: under anaerobic conditions with sulphide already present in wastewater, ferric iron is faster to precipitate sulfide compared to ferrous iron. Study carries on further, and it is demonstrated that for both, ferrous and ferric, iron salt precipitation increases with increase in pH. However, only ferrous iron exhibits effect on precipitation with increased iron to sulfide ratio. Effectiveness of sulfide precipitation with ferrous and ferric iron can be evaluated with half-life of sulfide in wastewater, which is described by Equation 6.17 (Kiilerich *et al.*, 2018). Half-life provides a good way to estimate time required to precipitate sulfide to a certain concentration.

$$t_{1/2} = \frac{([S(-II)_{t=0}] - [S(-II)_{end}])^{(1-\alpha_{obs})} - (\frac{[S(-II)_{t=0}]}{2} - [S(-II)_{end}])^{(1-\alpha_{obs})}}{k_{obs,20}(1-\alpha_{obs})}, for\ \alpha_{obs} > 1 \qquad (6.17)$$

Where:

$[S(-II)_{t=0}]$	Concentration of total dissolved sulfide at t=0	[μM S]
$[S(-II)_{end}]$	Sulfide concentration at equilibrium	[μM S]
α_{obs}	Observed reaction order; $\alpha_{obs}(e(II) = 2.1, \alpha_{obs}(e(III) = 1.9$	[-]
$k_{obs,20}$	Observed rate constant	[(μM S)$^{(1-\alpha_{obs})}$ s^{-1}]

This equation takes into account $[S(-II)_{end}]$, which is sulfide concentration at equilibrium in wastewater. To elaborate on this: salt which precipitates during reaction described by Equation 6.15 is FeS, which, even if poorly soluble, still is in equilibrium with dissolved sulfide. $[S(-II)_{end}]$ depicts this dissolved sulfide concentration. It means that under certain conditions it is not possible to precipitate all the sulfide, since a part of it always remains soluble in equilibrium. Complete process of deriving equations for calculating sulfide concentration at equilibrium (Equation 6.18 and Equation 6.20), observed reaction

orders and observed rate constants (Equation 6.19 and Equation 6.21) are described in Kiilerich *et al.*, 2018.

$$k_{obs,20,Fe(II)} = e^{(-12.64+0.23pH-8.75Ratio_{initial}+1.35pH\cdot Ratio_{initial})} \tag{6.18}$$

$$S(-II)_{end,Fe(II)} = e^{(7.78-0.42pH-1.05Ratio_i nitial)} - 10 \tag{6.19}$$

$$k_{obs,20,Fe(III)} = e^{(-25.98+2.59pH-4.03Ratio_{initial}-0.53pH\cdot Ratio_{initial})} \tag{6.20}$$

$$S(-II)_{end,Fe(III)} = e^{(5.22-0.42pH+0.05Ratio_i nitial)} - 10 \tag{6.21}$$

Using Equation 6.17 to Equation 6.21, half-life for sulfide under different pH and ratios of iron and sulfide are estimated. Initial concentration of sulfide is chosen as 304 [S(-II) μM] (9.7 g m^{-3}), which corresponds to highest average (wet and dry conditions) concentration of sulfide in pressure main in 10 °C, presented in Chapter 5. Calculated data is presented in Figure 6.5 while full range of rate constant dependency on pH and sulfide concentration in wastewater, in equilibrium is presented in the appendix, Figure 11.12. Temperature coefficient for these reactions is kept constant, for it does not exhibit significant variations under normal wastewater temperatures (Kiilerich *et al.*, 2018). Figure 6.5
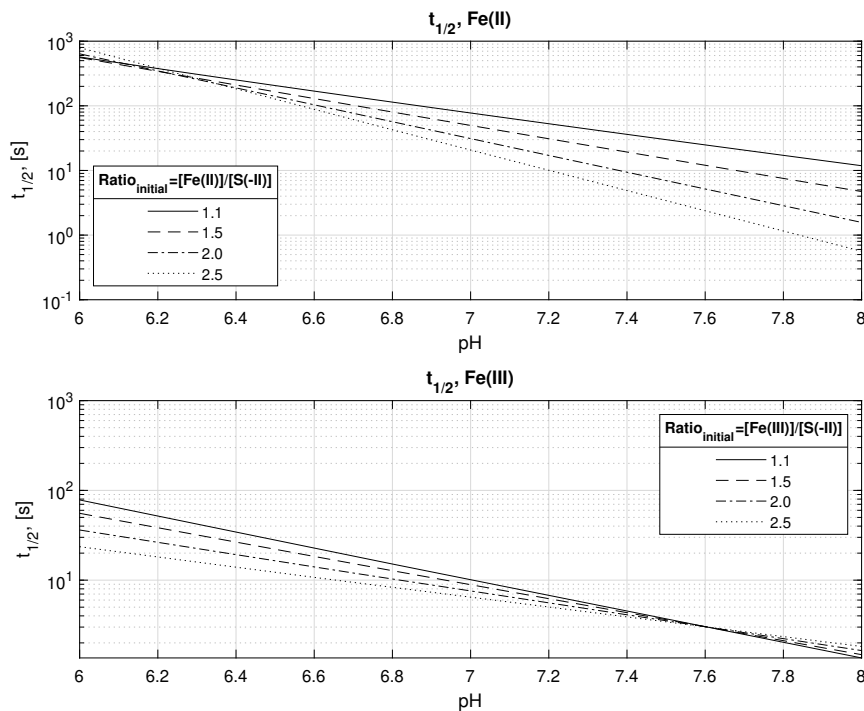

Figure 6.5: Variations in $t_{1/2}$ of sulfide precipitation with ferrous and ferric iron under variations of pH and initial ratio of iron to sulfide. Initial S(-II) concentration 304 μM (9.7 g/m3)

shows that ferrous iron is around factor 10 slower in precipitating sulfide than ferric iron. Furthermore, it is visible, that while pH has a significant impact on sulfide precipitation for both ferrous and ferric

iron, increase in initial ratio of iron to sulfide considerably increases precipitation only with ferrous iron. Therefore, when ferric iron is concerned, iron to sulfide ratio has to be kept close to stoichiometric ratio (Kiilerich *et al.*, 2018).

Figure 6.5 illustrates effect of pH as well as initial ratio of iron to sulphide effect on sulphide precipitation under single value of sulphide concentration. In order to make data more applicable in determining suitable methods for sulphide precipitation with iron salts in pressure main from Vrå to Hjørring , Figure 6.6 is presented. The figure illustrates decrease in sulfide concentration per time under precipitation with ferrous and ferric iron. Figures display scenarios with different pH values and different initial ratios of iron to sulfide. Figures depicts a decrease in sulfide concentration in wastewater from 1000 μM S to 100 μM S, which is considered as a higher boundary for low sulphide concentration in wastewater. It is crucial to stress, that Figure 6.6 illustrates half-lifes under decreasing initial concentration of sulphide, not overall reaction times. In order to estimate total time which is required to reach low sulfide
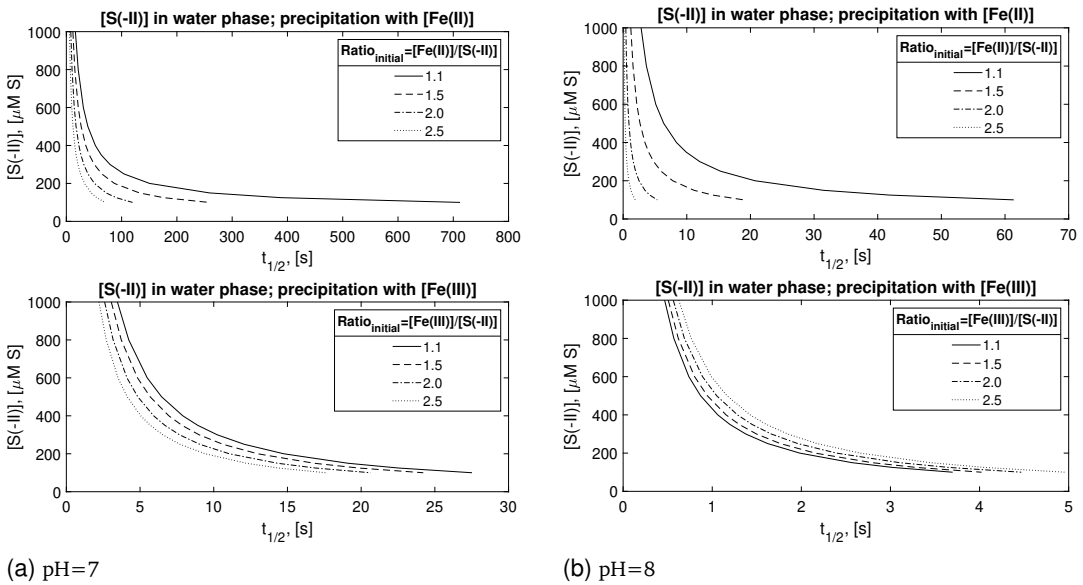

(a) pH=7 (b) pH=8

Figure 6.6: Half-life dependency of sulfide concentration in water phase during precipitation with ferrous or ferric iron; figures on the left illustrates process under pH=7, figures on the right - process under pH=8.

concentration, simple sum equation could be devised, such as Equation 6.22. This equation should deliver satisfactory results in estimation of time needed to precipitate sulfide to desired concentration.

$$Total\ time = t_{1/2,([S(-II)]=800\mu M)} + t_{1/2,[S(-II)]=400\mu M)} + ... + t_{1/2,[S(-II)]=n\cdot\mu M)} \tag{6.22}$$

For further estimation of sulfide precipitation with Equation 6.22, data from Figure 6.6 is used. pH values in aforementioned figure are selected according to Figure 3.7, where pH = 7 could be considered lower average approximated pH value and pH = 8 an ideal scenario value, as in value of pH with pH control in pressure main. In the table below, Table 6.5, time required to precipitate sulfide to required

amount is presented. To take a conservative approach and to simplify calculations, sulfide concentration selected for estimations is 800 μM (25.6 g m^{-3}), which is on a higher spectrum of sulfide concentrations in the pressure main even at 20 ° C. However, this higher concentration will have no notable effect on overall time required for satisfactory sulfide precipitation, since, as it is illustrated in Figure 6.6, half-life of sulfide in wastewater in high sulfide concentrations is very short. Here sulfide is considered precipitated to satisfactory level when sulfide concentration in wastewater reaches 50 μM (1.6 g m^{-3}). 50 μM is selected to illustrate equal basis for comparison - sulfide at 1.1 ratio can not be precipitated to higher extent with ferrous iron, due to part of sulfide remaining in the equilibrium. Ideally, 15 μM (0.5 g m^{-3}) is considered as a boundary below which sulfide has no effect on sewer infrastructure.

Table 6.5: Total time [s] required to reduce sulfide concentration in wastewater with ferrous and ferric iron from 800 μM to 50 μM under different pH and iron to sulfide initial ratios

	Ratio$_{initial}$=[Fe]/[S(-II)]			
pH	1.1	1.5	2.0	2.5
7, Fe(II)	937	396	204	126
8, Fe(II)	94	31	10	3
7, Fe(III)	54	48	41	35
8, Fe(III)	7	8	9	10

Table 6.5 is only an estimation of total time required to precipitate sulfide. It it possible to model the behavior of sulfide precipitation via expanding hydrogen sulfide production matrix from Chapter 4 with matrix from Table 6.6. This matrix extension works in the same ways as an original matrix. When it comes to the rate formulations, Equation 6.19 through Equation 6.21 and Equation 6.23 are used to estimate sulfide precipitation with ferrous or ferric iron. It is important to notice, that in aforementioned rate equation sulfide concentrations are molar, μM, while matrix deals in mass concentration. Consequently appropriate unit transformations are carried out. In Equation 6.23 k_{obs} (observed rate constant), is estimated with Equation 6.19 or Equation 6.21 in accordance to iron salt selected for precipitation: ferrous or ferric.

Table 6.6: Extension of matrix formulation of aerobic/anaerobic sulfide formation in sewers, (Hvitved-Jacobsen *et al.*, 2000), with iron precipitation. Reaction rate is from Kiilerich *et al.*, 2018

	$\mathbf{S}_F$	$\mathbf{S}_A$	$\mathbf{X}_{S1}$	$\mathbf{X}_{S2}$	$\mathbf{X}_{HW}$	$\mathbf{S}_{H2S}$	-$\mathbf{S}_O$	Rate
S precipitation						-1		Equation 6.23

$$j = (k_{obs} \cdot ([S(-II)] \cdot \frac{1000}{32}) - [S(-II)_{end}])^{\alpha_{obs}} \cdot \frac{32}{1000} \qquad (6.23)$$

Model results are presented in Figure 6.7. Since sulfide precipitation with iron, ferrous as well as ferric, is rapid, compared to hydraulic retention time, Figure 6.7 mainly illustrates an effect of pH and ratio of iron to sulfide variations on sulfide concentration which remains in equilibrium in water phase, even with addition of iron. With increasing pH and ratio, equilibrium is shifted towards higher precipitation of sulfide. Modelling has an evident advantage when compared to estimation total time needed to precipitate sulfides via sulfide half-life equations, since it clearly illustrates that pH and iron/sulfide ratio is a more important factor considering sulfide precipitation than reaction time.

(a) pH=6, ferrous iron/sulfide ratio=1.1

(b) pH=7, ferrous iron/sulfide ratio=2

(c) pH=6, ferrous iron/sulfide ratio=1.1

(d) pH=7, ferrous iron/sulfide ratio=2

(e) pH=6, ferric iron/sulfide ratio=1.1
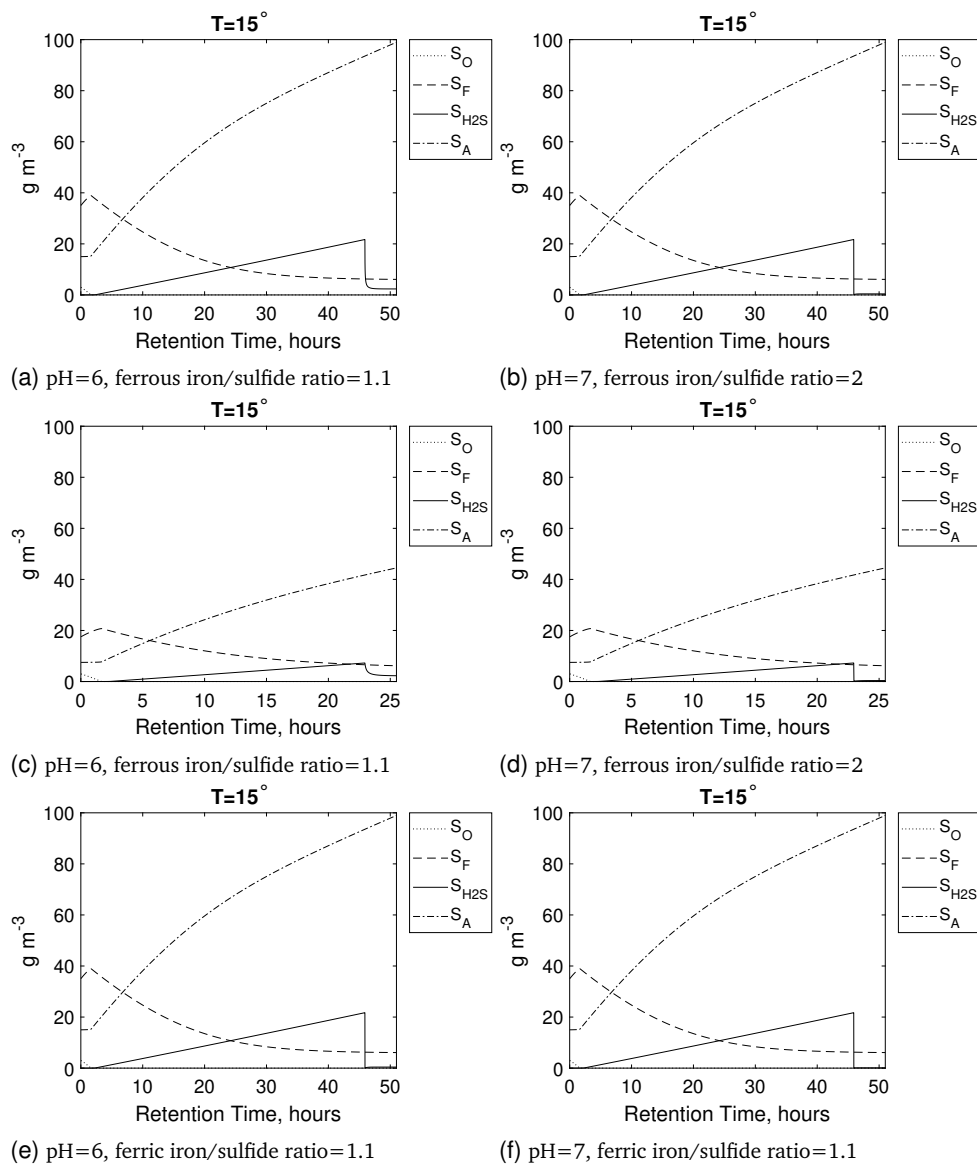
(f) pH=7, ferric iron/sulfide ratio=1.1

Figure 6.7: Modeling results of sulfide production and precipitation with ferrous iron under different pH and iron/sulfide ratios and varying (wet or dry) flow conditions.

If data from Table 6.5, Figure 6.7 is analysed in accordance with data from Table 6.1 illustrating flow conditions and retention time, viability of sulfide precipitation method can be established. In Table 6.5 instantaneous complete mixing of wastewater with iron salts is assumed. Furthermore, injection of

iron salts into Vrå pumping station is not investigated. Even if precipitation rates at low sulfide concentrations are low, reaction times are short compared to total hydraulic retention time in the pressure main, illustrated in Figure 6.6 and Table 6.5. If there are no minor branches throughout the pressure main, iron salts could be dosed without paying attention to time needed to precipitate sulfide. However, iron, especially ferric iron, acts as an inhibitor of biofilm activity. Ferric iron affects sewer biofilm on a biochemical and physical level by not only reducing activity of biofilm, but also by reducing diffusivity of biofilm surface (Kiilerich, 2018). While, in general terms, inhibition of sulfide production is a positive phenomena, in case of Vrå pressure main that would mean inhibition of VFA production, which could have negative implications on a WWTP processes. Ideal injection place is Hjørring pumping station: there are no minor branches connecting to the pressure main between pumping station and WWTP, while retention time of wastewater is still sufficient. Ferrous iron dosing should commence under higher than stoichiometric ratio of iron to sulfide due to sulfide left in equilibrium in the water phase. For ferric iron, initial ratio should be close to stoichiometric ratio.

6.4　New abatement methods and outlook

All previously presented measures in section 6 are widely used and extensively studied (Matsché *et al.*, 2005; Hydrogen Sulphide Corrosion in Sewerage Works (Australia), 1989). New approaches promises good suppression of H_2S at lower costs, even if only some are tested in real life situations Figure 6.8. A general overview over these methods is given here to reveal future research and implementation possibilities.
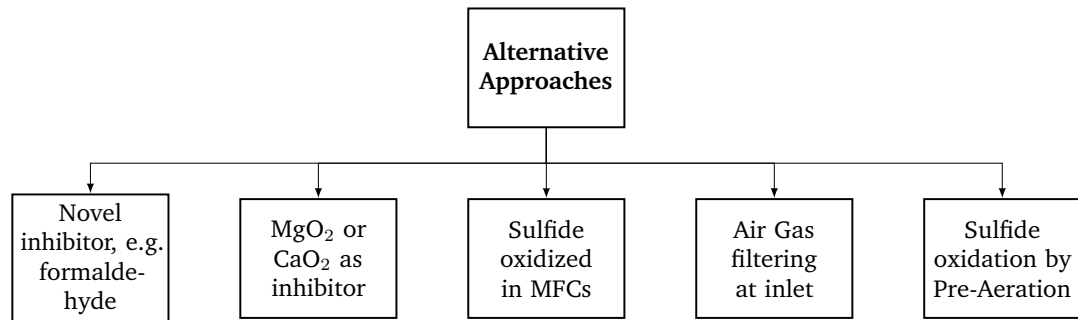

Figure 6.8: Alternative approaches for hydrogen sulfide emission control in sewer. MFCs: microbial fuel cells; SRB: sulfate-reducing bacteria. Figure adapted from Zhang *et al.*, 2008

Inhibition of H_2S can be achieved by dosing formaldehyde into sewage. There it serves as an inhibitor. Formaldehyde is used regularly in food producing processes (e.g. disinfectant, antimicrobial agent). Research articles show promising results (Zhang *et al.*, 2009). The dosage concentration is directly linked to the detected decrease of H_2S. Because formaldehyde can have negative impact on the receiving waters, formaldehyde dosing should be only applied to corroded, high risk spots. When sewage enters the WWTP, formaldehyde is biodegraded and of no further harm. No negative impact on COD removal and nitrification rates were observed (Kaszycki *et al.*, 2001).

Another option is the application of slow release solid-phase oxygen. A solid compound with the potential to release oxygen when it comes in contact with water is used (e.g. MgO_2, CaO_2). Initially this method was developed for the oil industry, where H_2S emission can be a major threat. It was never tested for sewer control, but lab scale batch experiments showed, that the addition of solid phase oxygen - here magnesium peroxide (MgO_2) was used - inhibits H_2S formation for more than 40 days and inhibition of SRB growth is observed (Chang *et al.*, 2007). The added chemicals react with water and slowly release oxygen to prevent hydrogen sulfide formation. For practical application, the challenge is to let the chemical not to flush out too fast. With characteristics of long persistence, harmlessness to humans and environment as well as H_2S suppression, the application of slow release substances seems promising.

Also quite promising is the idea of using Microbial fuel cells (MFCs), Figure 6.9. MFCs are used to convert carbon-based substrates to electricity. The electrons generated during metabolism of organic

matter are transferred to an electrode by electrochemical active bacteria, which work as a biocatalyst and thus enable electricity to be generated (Logan, 2008). Here they work on complex wastewater substrates. Sulfide can be used as fuel for this cells and is converted to elemental sulfur. Sulfide oxidation in MFcs result in electricity generation with power outputs up to 101 mW L^{-1} (Rabaey *et al.*, 2006).
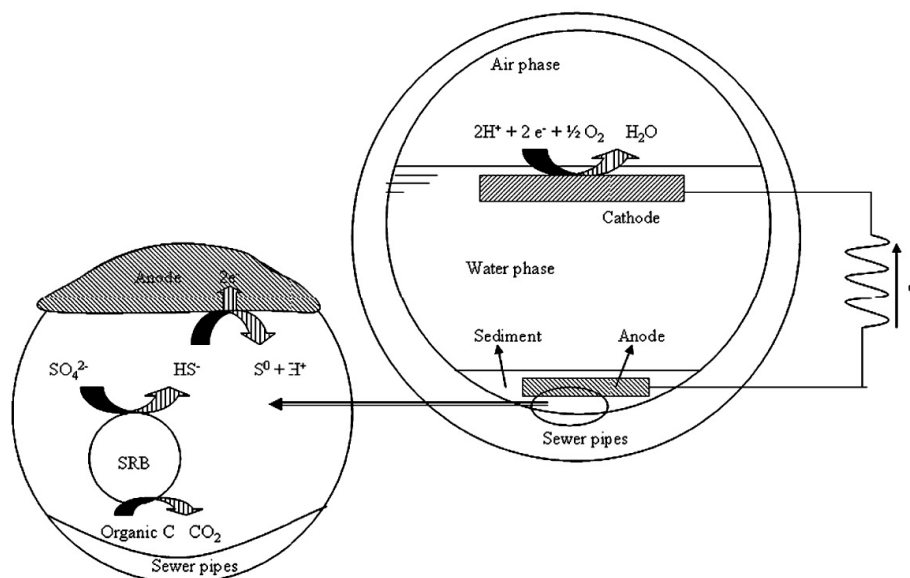

Figure 6.9: Schematic of a microbial fuel cell in a sewer system converting the sulfide to sulfur, from Zhang *et al.*, 2008

More practical and simpler, from the technical point of view, group of approaches regarding end-of-pipe treatments is filtration of sewer gases. The potential of filtering H$_2$S-contaminated air was examined and processes have been developed to remove H$_2$S (Abraham *et al.*, 2015; Choo *et al.*, 2013). At atmosphere conditions, occurring turbulence from mixing, releases H$_2$S from the water phase. It is converted to elemental sulphur, which further leads to SO$_4^{2-}$. Biofilters containing a fixed bed are a simple solution, Figure 6.10. Bed material consists of widely available and cheap material, such as wood chips, lava rock, coconut fiber, compost or synthetic media such as discarded tire material (Kennes and Veiga, 2013; Park *et al.*, 2011), as long as they provide high porosity, large specific surface area and high water retention capacity capacity (Andersson-Chan, 2006).

An application of an air filter at the inlet structure is also plausible. Inlet structure should be covered with a funnel. Air with all occurring malodorous compounds from the inlet structure would be collected through a funnel and filtered to allow pollution control at low operating costs. This also ensures future air treatment, if wastewater load increases or changes in its composition. Filtering might seem as labor intensive process, since filters require high maintenance as a result of filter-saturation or ageing. By using improved materials, such as f K$_2$CO$_3$ impregnated activated carbon (which is chemically improved activated carbon with enhanced adsorption properties), the negative aspects of frequent filter material
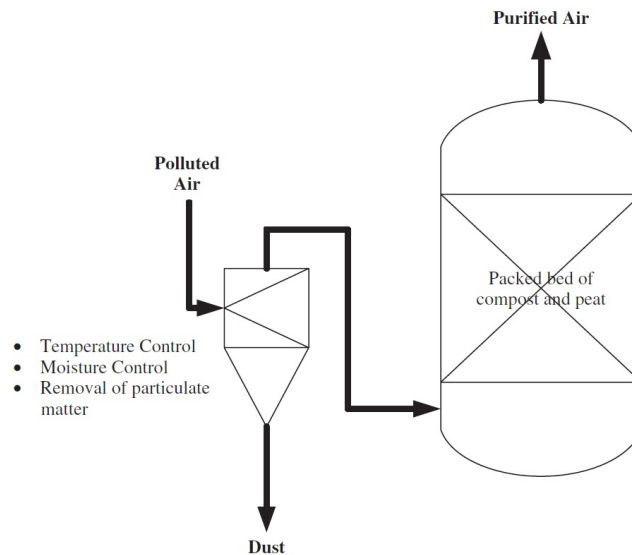
Purified Air

**Polluted
Air**

Packed bed of
compost and peat

- Temperature Control
- Moisture Control
- Removal of particulate
  matter

Dust

Figure 6.10: Schematics of a biofilter, from Kennes and Veiga, 2013

replacement can be negated by higher adsorption capacities of a filter, hence longer filter lifetime Appendix Figure 11.35.

Another, rather straightforward, sulfide control method applicable for Hjørring WWTP is an end-of-pipe sulfide oxidation. Since total daily flow from Vrå is not very high, sulfide could be allowed to form freely in the pressure main. Wastewater from it would be collected and stored in a storage tank, with a volume equal to pumping stations volume. By aerating the wastewater in a storage tank, sulfide would be oxidised and hydrogen sulfide would not cause corrosion in the inlet structure nor possible complications in further WWTP processes.

Results of sulfide abatement modelling

Results from previously discussed three commonly used sulfide abatement methods are presented in this chapter as well as appendix. Monte Carlo simulations are done for each method presented, each individual scenario is composed of one thousand model runs with randomly generated data according to value distribution. Parameter description is provided in Appendix, Table 11.3, where additional parameter values required for modeling of aerobic sulfide oxidation are created from values provided by Hvitved-Jacobsen *et al.*, 2013 and Nielsen *et al.*, 2006 and parameter values used simulating wastewater transformation under anoxic conditions are made from data from Abdul-Talib *et al.*, 2002 and Yang *et al.*, 2004. Simulations of sulfide precipitation with iron does not introduce additional parameters, since rate equations used for precipitation are empirical and are derivatives of already established wastewater conditions.

7.1 Results of sulfide control with oxygen injection

Oxygen injection directly into the pressure main is presented as the first abatement method, for oxygen is readily available, despite the fact that its oxidising effects are local due to the low oxygen solubility (Figure 11.5) and its rapid consumption by sulfide oxidation, as well as aerobic heterotrophic growth of biomass. Oxygen injection point is Hjørring pumping station, since it is the only location where aerobic oxidation might be effective and can be modeled reasonably well. For modeling, it is assumed that oxygen injection is instantaneous and wastewater reaches a concentration of 6 g O_2 m^{-3} instantly. Results of the simulations are presented bellow, Figure 7.1, and in the appendix, Figure 11.19 – Figure 11.20.

Figure 7.1 and figures in the appendix reveals that single oxygen injection point throughout the pressure main is not enough to sufficiently reduce sulfide concentration. Decrease in sulfide concentration is substantial and quick. However, after oxygen is depleted, sulfide production continues. Overall, during dry flow conditions, decrease of approximately 5 g S m^{-3} sulfide concentration is detected and under wet flow it is even lower. Increase in oxygen concentration injected (higher amount of oxygen), does
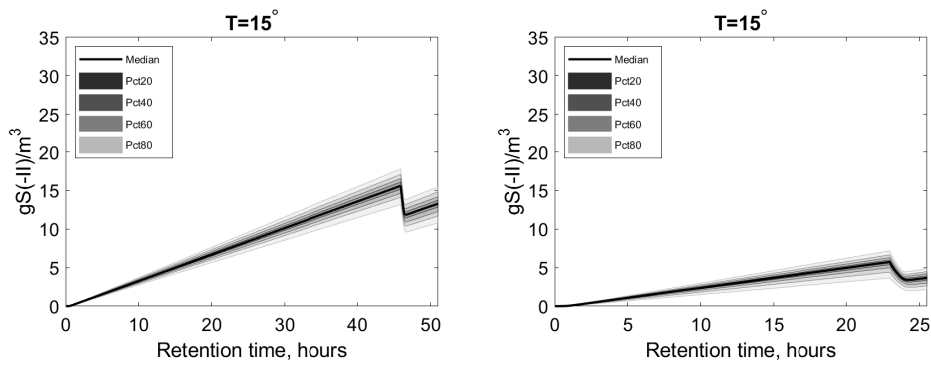
Figure 7.1: Results of sulfide production in the pressure main with aerobic sulfide oxidation. Oxygen injection point - Hjørring pumping station. pH = 7. Data generated with Monte Carlo simulations from 1000 data sets for each scenario. 20_{th} to 80_{th} percentiles are presented

not effectively change the situation: sulfide oxidation rate is mainly governed by sulfide concentration, while oxygen is rapidly used for heterotrophic processes. However, under wet flow conditions and lower temperatures (up to $10°$ C, appendix Figure 11.20), sulfide concentrations reduced to the levels that is considered as medium sulfide concentration in the sewer (0.5 g S m^{-3} – 3 g S m^{-3}). this illustrates how effective aerobic sulfide oxidation can be if the limitations of this particular sulfide abatement method - local effect which requires multiple oxygen injection points throughout the pressure main - are taken into account. Possibilities of adapting sulfide control via establishment of aerobic conditions in the pressure main are investigated further in the thesis.

7.2   Results of sulfide control with addition of nitrate

A single oxygen injection point proved to be insufficient for sulfide abatement in the pressure main from Vrå to Hjørring. In this case establishment of anoxic conditions is a logical next step towards the solution. Nitrate is used to establish anoxic conditions in the sewer. Unlike oxygen, nitrate is highly soluble, therefore it is plausible to inject it at the beginning of the pressure main and expect anoxic conditions to be maintained for a prolonged period of time. Initial oxygen concentration at the Vrå pumping station is assumed to be 3 g O$_2$ m^{-3} (Hvitved-Jacobsen *et al.*, 2013). At the same point nitrate injection is assumed. Two initial nitrate concentrations are investigated: 30 g NO$_3$-N m^{-3} and 80 g NO$_3$-N m^{-3}. These concentrations are selected to illustrate group of scenarios with insufficient nitrogen for complete sulfide abatement and scenarios where nitrogen concentration selected is satisfactory. Results of model simulations are presented in Figure 7.2 and in appendix: Figure 11.21 - Figure 11.26

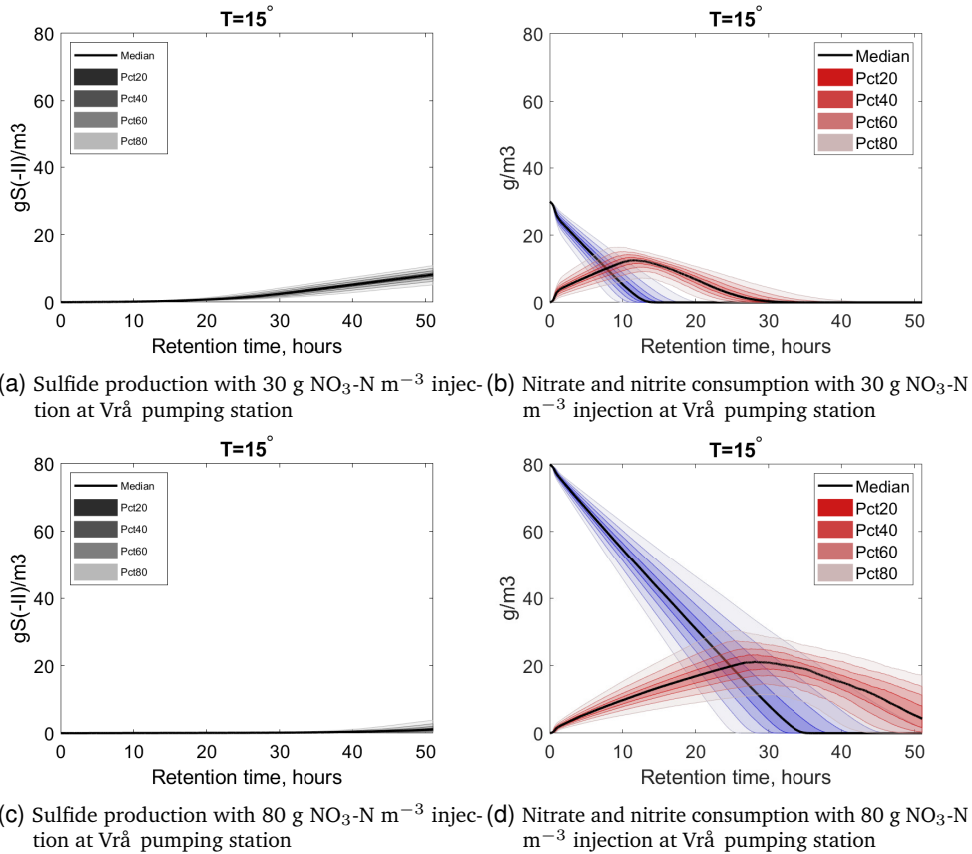(a) Sulfide production with 30 g NO_3-N m^{-3} injection at Vrå pumping station

(b) Nitrate and nitrite consumption with 30 g NO_3-N m^{-3} injection at Vrå pumping station

(c) Sulfide production with 80 g NO_3-N m^{-3} injection at Vrå pumping station

(d) Nitrate and nitrite consumption with 80 g NO_3-N m^{-3} injection at Vrå pumping station

Figure 7.2: Sulfide production and control via establishment of anoxic conditions with nitrate. Graphs a and c illustrate sulfide production while b and d illustrates change in nitrate (blue) and nitrite (red) concentrations. pH=7, dry flow conditions. Data is generated with Monte Carlo simulations from 1000 data sets for each scenario. 20th to 80th percentiles are presented

Modelled data in the figure above as well as in the appendix illustrates three main situations: dry flow with 30 g NO_3-N m^{-3}, wet flow with 30 g NO_3-N m^{-3} and dry flow with 80 g NO_3-N m^{-3}. For each scenario four distinct temperatures are investigated. Visual analysis of the results reveals that establishment of anoxic conditions is an effective sulfide production mitigation technique.

As graphs (a) and (b) in Figure 7.2 illustrate, proper dosing of nitrate is crucial. While nitrate and nitrite are highly soluble and its consumption by wastewater biomass is not rapid (compared to oxygen consumption under aerobic processes), it is being used constantly, and immediately after nitrite is depleted, sulfide production initiates. Graphs (c) and (d) in the same figure illustrate more appropriate dosing of nitrate, 80 g NO_3-N m^{-3}, where anoxic conditions lasts throughout the pressure main and no sulfide is produced with the simulations in 20th percentile.

A similar situation is illustrated in appendix, Figure 11.24, where wet flow conditions are assumed and 30 g NO_3-N m^{-3} is injected at Vrå pumping station. However, it illustrates one of the shortcomings of this method. If nitrate (and nitrite) is not consumed in the pressure main (as illustrated in the appendix, wet flow with 30 g NO_3-N m^{-3} dosing and dry flow with 80 g NO_3-N m^{-3} up to 15°C, Figure 11.24 and

Figure 11.26 accordingly) for heterotrophic anoxic processes, it reaches the WWTP, which constitutes as an additional load of nitrates and has to be dealt with. Additionally, denitrification processes consume much needed VFAs and readily biodegradable substrate in general. This process is mirrored in sewer as well. Estimating from the in-sewer process models, up to 1.3–5.0 g m^{-3}h^{-1} of readily biodegradable substrate is consumed in denitrification processes in sewers. This particular outcome is discussed further in the thesis.

Finally, the role of wastewater temperature can not be neglected, when describing anoxic processes: with an increase in temperature, rates of anoxic processes are increasing substantially. For example, if graphs in the appendix Figure 11.22, nitrate and nitrite consumption under 15°C and 20°C, are analysed, it is evident that anoxic processes in wastewater under 20°C are approximately 1.5 times faster than under 15°C, therefore anoxic conditions lasts shorter. Furthermore, by examining the same figure, amount nitrate injected in the scenario of 5°C is almost optimal (depending on the simulation run), while with a temperature of 15°C or 20°C its far from enough which results in extensive sulfide production under these higher wastewater temperatures.

Overall, the establishment of anoxic conditions in the sewer with nitrate dosing might seem straightforward, but temperature fluctuations and change in wastewater flow conditions introduce a massive uncertainty. A broad array of scenarios have to be considered in order to provide optimal abatement. Aforementioned uncertainties and methods of dealing with it are discussed further in the thesis, after all modeled results are introduced.

7.3 Results of sulfide control with addition of Fe(II) and Fe(III)

Injection of iron salts into the pressure main, as a sulfide abatement method, differs from methods based on oxygen and nitrate by the control mechanism itself. Introduction of oxygen or nitrate prevents anaerobic conditions from taking place in the sewer system and ideally sulfide does not form in a first place, whereas iron works as a precipitant. Main advantage of use of iron as a sulfide abatement method is that reactions are rapid due to their chemical nature. Where aerobic or anoxic oxidation deemed to be insufficient due to the low reaction rates or excessive consumption of the substances by biomass, injection of iron salts overcomes both of these problems. Iron works selectively, reactions are quick and, according to recent research (Kiilerich *et al.*, 2018), it can be dosed in low quantities, sometimes even close to the stoichiometric ratios.

Monte Carlo simulations are done for abatement scenarios with ferrous and ferric iron, under different pH values (pH = 6 and pH = 7) and with different flow conditions assumed. Iron to sulfide ratios are selected as lowest realistic values according to section 6.3. Instant mixing of iron with wastewater is assumed. Results of these simulations are presented in Figure 7.3 and in appendix, Figure 11.27–Figure 11.34.
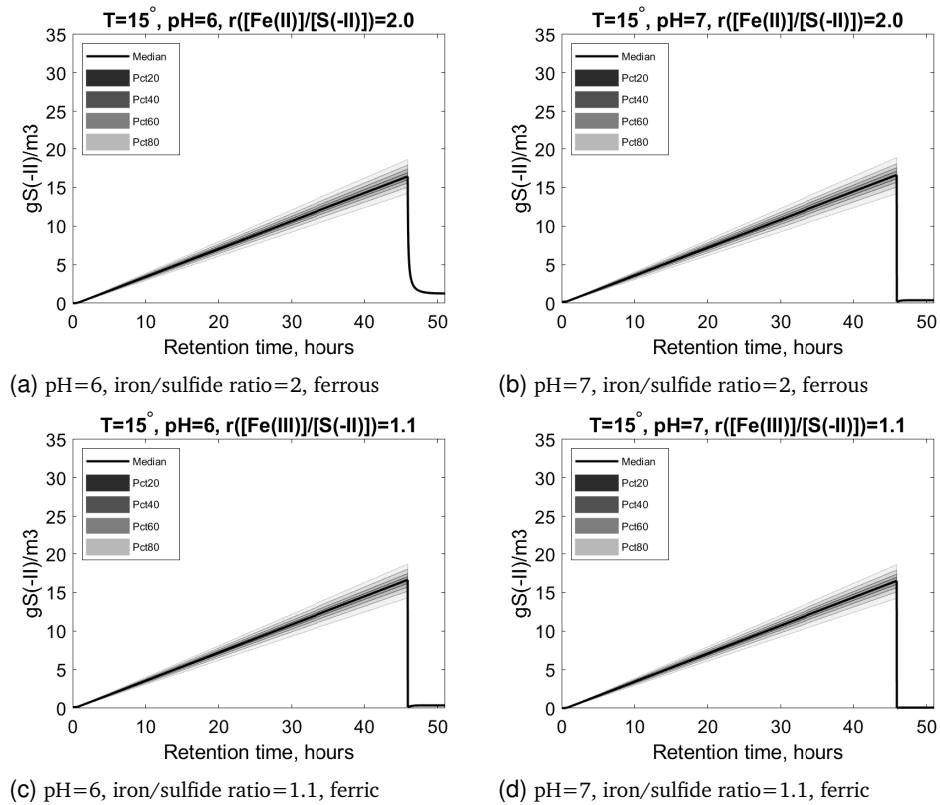

(a) pH=6, iron/sulfide ratio=2, ferrous

(b) pH=7, iron/sulfide ratio=2, ferrous

(c) pH=6, iron/sulfide ratio=1.1, ferric

(d) pH=7, iron/sulfide ratio=1.1, ferric

Figure 7.3: Sulfide production and control via iron precipitation at 15°C for dry and wet flow. Data is generated with Monte Carlo simulations from 1000 data sets for each scenario. 20th to 80th percentiles are presented

Since all scenarios are modeled with iron/sulfide ratio and not the distinct concentration of iron, it is implied that iron is not a limiting factor throughout modeling process. Therefore two distinct situations are illustrated in the graphs depicting modeled data: either dissolved sulfide concentration left in wastewater in equilibrium is relatively high, as in, for example, graph (a) in Figure 7.3, or it is minuscule, same figure, graphs (b), (c) or (d). It is related to low pH values of wastewater, where with decrease in pH, concentration of sulfide left in wastewater increases. Ferrous iron is especially effected by this phenomena. Also it is important to mention, that precipitation of sulfide is not instantaneous, even though it is rapid compared to hydraulic retention time. Since pH is one of the governing factors in sulfide precipitation, wastewater buffering capacity has to be looked into. Wastewater consist mainly of potable water, therefore pH and bicarbonate values of water can be applied for evaluation of wastewater. Potable water in Vrå has an average values of pH of 7.6 and bicarbonate concentration of 192 g m^{-3}

(3.1·10^{-3} mol L^{-1}) (data from https://geus.dk). Since 1 mole of sulfide precipitated produces 1 mole of H$^+$ (Equation 6.15 and Equation 6.16) and maximum sulfide concentration produced is around 24 g m^{-3} (7.3·10^{-4} mol L^{-1}), wastewater has enough buffering capacity to maintain the pH at the acceptable level. Even if drop in buffering capacity is quite noticeable, wastewater from the pressure main mixes with wastewater from Hjørring at the WWTP inlet structure with a ratio of around 1:24. Effects of decrease in buffering capacity are diminished and it should not cause any problems in further wastewater treatment at the WWTP.

Besides ferrous irons tendency to not precipitate sulfide completely under lower pH (pH < 7), the method of controlling sulfide concentration in wastewater with ferrous or ferric iron is extremely efficient. This method, however, is not without complications: ferric iron also precipitates with phosphates, so it has to be taken into account, when estimating required ratio of iron to sulfide. Furthermore, depending on the used iron salt, unwanted anions might appear in wastewater. Model was run with pH values as low as pH = 6. Even though results of simulations illustrated in the aforementioned plots demonstrates sufficient sulfide precipitation at low ferric iron to sulfide ratios at low pH values (Figure 7.3 plot (c)), literature data suggest, that effects of sulfide precipitation with iron is highly diminished with pH<6.5 (Boon, 1995). On the other hand, during the reduction of ferric iron to ferrous iron, elemental sulfur forms, which initiates precipitation of pyrite. Pyrite, being less soluble than other sulfide compounds, shifts the equilibrium and consequently low sulfide concentration in wastewater in equilibrium could be achieved (Rickard and Luther, 2007; Kiilerich *et al.*, 2018). In any case, pH<6.5 values in the WWTP and in the pressure main are considered to be very rare (Figure 3.7). With substantial buffering capacity of potable water in Vrå, low pH in pressure main should not become a problem for sulfide precipitation with iron. Complications and possible variations of this abatement method are discussed further in the following chapter.

Discussion

<div style="text-align: right; font-size: large;">8</div>

Throughout the thesis an evaluation of sulfide production in the pressure main from Vrå to Hjørring is carried out. This evaluation is based on a number of intertwined approaches: literature analysis, laboratory experiments, in-situ measurements and modelling. The literature analysis, which is carried out all throughout the thesis, is self evident. It conceptually proves high risk of sulfide formation in the pressure main, which creates a precedent for further investigation. Laboratory, in-situ measurement and modelling data, however, requires additional evaluation, which is conducted throughout this chapter. However, before that, short evaluation of flow conditions and parameters has to be concluded. Hydraulic retention time (HRT) in the pressure main is assumed to be 26.5 h for wet flow and 51 h for dry flow conditions, following average flow velocities in the pressure main. Average velocities are used, because of the flow cycles of the pump station and long pressure main, where wastewater in the pipe is not moving most of the time. It is assumed that flow velocities ultimately regresses to the mean, where wastewater transformations are concerned. Long HRT promotes more substantial transformations - more hydrogen sulfide is produced. Sun *et al.*, 2015 proves that increased HRT is not only a direct cause of increased sulfate reduction, but also increases methane production. The influence of temperature and retention time in the force main was determined qualitatively and quantitatively by combining comprehensive literature analysis with modelling and in-situ measurement data as well as laboratory experiments. Nonetheless, investigations on the three main industries regarding wastewater flow patterns, qualities and composition would be beneficial to better evaluate wastewater transformations including sulfate reduction.

OUR experiments, IC and in-situ data logging were used to investigate wastewater properties and transformations. Data from OUR and IC experiments is used to describe wastewater properties in regard to composition, matter and undergoing processes. Results are presented and described in detail throughout Chapter 5. Wastewater parameters gathered from OUR experiment with modeling deviates slightly from values presented in the literature. For example, result of readily biodegradable substrate, S_S, is 50 g COD m^{-3}, which is 10 g COD m^{-3} larger than the maximum value proposed by Hvitved-Jacobsen *et al.*, 2000. While heterotrophic biomass (19 g COD m^{-3}) is on a lower side of range proposed in literature (20–100 g m^{-3}, Hvitved-Jacobsen *et al.*, 2000). However, deviations are to be expected due to

the nature of wastewater and unique composition of wastewater from Vrå. Furthermore, high amount of readily biodegradable substrate together with low concentration of heterotrophic biomass just might be an indication of anaerobic conditions and formation of sulfide within the pressure main. Tanaka and Hvitved-Jacobsen, 2001 demonstrates, that under anaerobic conditions in a pilot pressure main, net generation of S_S is observed: while S_S is consumed for sulfide production, hydrolysis rate is higher than formation of sulfide. Therefore, concentrations of S_S at the end of pilot pressure main was as high as 100 g COD m^{-3}. Sharma *et al.*, 2008 illustrates, that concentration of VFA in the 778 m of the pressure main increases from 1.6 to 7.5 times, depending on the sampling time, and reaches concentration of 4–60 g COD m^{-3}. Pressure main from Vrå to Hjørring is 12 times longer, so S_S concentrations the end of pressure should be significantly higher, however it is 50 g COD m^{-3}, which can be explained by the low wastewater temperature in Denmark, compared to Australia. Result is comparable to Sharma *et al.*, 2008 findings with low sulfide production (low VFA concentration) and, as shown further in the discussion, such value is expected due to the sampling time. Overall, data from OUR model serves as the initial basis - parameter wise - for further investigation of wastewater, sulfide formation models and sulfide abatement methods.

Data from IC measurements is used to quantify VFAs from the outlet of the pressure main. Acetate concentration of 18.9 g m^{-3} was found. Value itself is comparable to S_A in sulfide formation models, for example Figure 6.3 (40–100 g m^{-3}). Value is several times lower. However, wastewater sample for IC was taken at 13:00, when sulfide concentrations at the inlet are expected to be low (Figure 5.3).

Finally, OdaLog was set up at the inlet to the WWTP to measure sulfides in the gas phase in-situ. Up to 18 ppm of of sulfide was measured throughout the measurement campaign, Figure 5.3. Furthermore, sulfide production appears to be semi-regular, with sulfide discharge peaking at 22:00 – 08:00. Such atmospheric concentrations are enough to cause corrosion problems as well as to be considered as a nuisance and a health hazard. Due to construction of the inlet structure and immediate mixing of wastewater from Vrå with wastewater from Hjørring, measured concentration of sulfide can be considered as a gross underestimation, if related to possible localised effects. Based on both Tanaka and Hvitved-Jacobsen, 2001 and Sharma *et al.*, 2008 as well as data from IC and OdaLog, Figure 5.3, it is obvious that sample taken at Hjørring WWTP at 13:00 provides data which delivers parameters related to low rate of sulfide production. If wastewater samples were takes from 22:00 to 08:00, VFA, including acetate, concentrations would likely be several times higher.

In this thesis, a limited number of experiments and measurements were carried out. Ideally, much more in-depth laboratory work, measurements and in-situ data logging should be concluded, especially since high wastewater temperatures during the summer amplifies sulfide formation processes significantly and makes sulfide more volatile. However, gathered data still serves its purpose. All three different

methods are analysed together with the literature study and it confirms sulfide production in the pressure main from Vrå to Hjørring. It lies the foundation for further investigation of the phenomena based on modeling of sulfide formation in the sewer as well as evaluation of plausible sulfide abatement methods.

Sulfide formation model is used to simulate sulfide formation in the pressure main from Vrå to Hjørring. Results of the simulations are provided in appendix Figure 11.14. Depending on the conditions, 5 g S m^{-3} – 24 g S m^{-3} sulfide forms in the pressure main according to the simulated scenarios. It is illustrated throughout the thesis, that number of simulations and conditions tested with a model is virtually unlimited and, if enough data (wastewater parameters, temperature, pH, etc.) is gathered prior to simulation, model run can be very precises and with low uncertainty. However, it is not usually the case. Due to limited amount of laboratory experiments and, more importantly, stochastic nature of wastewater and related environmental conditions Monte Carlo simulations are used to take uncertainties into account. Here, the reason behind use of uniform distribution for generation of readily biodegradable substrate (S_A and S_F) has to be addressed. It is known, that when the inflow from Vrå started, Hjørring WWTP stopped adding additional substrate to the wastewater treatment processes. This, together with the knowledge of type of industries housed in Vrå (hatchery, marmalade factory, laundry) illustrates, that wastewater in-flowing via pressure main has an increased concentration of readily biodegradable matter (compared to wastewater flowing from Hjørring). Since industries do not produce wastewater constantly and with constant parameters, it is safe to assume that high concentrations of readily biodegradable matter are as likely as low or medium concentrations.

It is worthwhile to mention total COD value assumed throughout the simulations. It is decided to keep single total COD value throughout the thesis, 600 g COD m^{-3} (la Cour Jansen *et al.*, 2019). Sole purpose of total COD exist in modeling process. It is used to calculate $X_{S,slow}$ (as illustrated in Table 11.3) and $X_{S,slow}$ itself does not undergo substantial transformations, within the relevant time frame, according to the model matrix, nor in real life scenario. While changes in total COD might have significant effect on WWTP itself, it is not a governing factor in simulations of wastewater transformations in the pressure main. Furthermore, estimation of total COD in the pumping station in Vrå is quite complicated, since there is no information on when and what industries discharge, therefore a literature value is a better choice.

Another source of uncertainties and reason why precise pin-point simulation of sulfide formation is not valid solution and Monte Carlo simulation has to be carried out regardless to the amount of data available is uncertainties in flow parameters. Firstly, assumptions of dry - wet flow conditions are rough. In real life situation neither of these are completely accurate, but these assumed scenarios are useful to illustrate complete opposites and average true flow velocities and retention times lies in between of

presented intervals. Furthermore, its is unknown how many (if any) additional sewage system branches are connected to the pressure main. Throughout the simulation zero branches are assumed. Assumption is deemed correct, since additional branches would be almost insignificant in flow and therefore - in dissolved oxygen content, which would be consumed immediately without any substantial effect to sulfide formation. Main complication related to lateral branches is the possibility of plug flow which could create gaps of sulfide formation unaffected of implemented abatement methods.

Sulfide release at the WWTP inlet structure is estimated based on sulfide emission rate equation from Yongsiri *et al.*, 2003, where hydrogen sulfide emission rate is integrated with WATS model. However, it is not implemented to the model in the course of this thesis, because sulfide release rate is highly dependant on flow velocity at the outlet on the pressure main. Since sulfide formation simulations are carried out with average flow velocities, modeled sulfide emissions at the WWTP inlet structure would be highly underestimated. Governing factors in the equation are mass-transfer coefficient of hydrogen sulfide ($K_L\alpha_{H_2S}$) and concentration of hydrogen sulfide in the wastewater (S_{H_2S}). $K_L\alpha_{H_2S}$ depends on pH, temperature and flow conditions, such as velocity and geometry of the sewer. While average flow velocity in the pressure main fluctuates due to the number of pumping cycles, real discharged velocity is not influenced by dry/wet conditions. Sulfide emissions in-situ were measured at the beginning of May. Figure 3.7 illustrates that average wastewater temperature in may is around 13 °C, and pH is 7.5. Wastewater temperature peaks in July with 20 °C with pH value of 7.3. Increasing temperature and decreasing pH value increases emissions of hydrogen sulfide. Increase in temperature also highly increases sulfide production in the pressure main. If in this time period, from May to July, estimated hydrogen sulfide production rises from 5 g S m^{-3} to 24 g S m^{-3} (estimation from Figure 11.14) with wastewater properties described above, $K_L\alpha_{H_2S}$ increases 50 % while hydrogen sulfide emissions increase 750 %. Huge increase in sulfide emission is mainly due to the increase in sulfide produced in the pressure main. It can be estimated that maximum measured sulfide concentration of 18 ppm in May, would potentially become 152 ppm in July, with changes in wastewater levels in the WWTP inlet structure not taken into account. WWTP in July has the lowest inflow of wastewater (Figure 3.6). Which means that hydrogen sulfide emission from the pressure main could potentially be amplified by the pre-existing low wastewater level at the inlet structure: low dilution, more turbulent mixing.

Sulfide release can be roughly estimated. Concentrations in the inlet structure above 300 ppm can be expected, from deriving occurring concentrations in Appendix Table 11.1. Here findings in Austria with similar wastewater temperature of 15°C yields concentrations up to 367 ppm (Grengg *et al.*, 2015) in sealed manholes. While atmospheric hydrogen sulfide in the inlet is more difficult to measure and is released to a larger volume compared to a manhole, localized effects here will be substantial. The given value should be considered as a careful estimation, due to even higher volatility of H$_2$S in summer.

Resulting sulfide formation in the pressure main according to the simulations is a rather large interval and while it might not be precise, it is accurate: simulations are clearly in agreement with a hypothesis based on literature, that sulfide indeed forms in the pressure main. Furthermore, laboratory experiments also are in agreement with claims made. Finally, measurement congaing with OdaLog proved significant hydrogen sulfide formation in the pressure main. Overall, literature, experimental values, in-situ measurements and modelling show the same result - sulfide in the pressure main forms, therefore it is worthwhile to investigate sulfide abatement methods.

It is already established, that sulfate reduction gives net production of S_S via a substantial increase in S_A (VFAs) (Tanaka and Hvitved-Jacobsen, 2001, Sharma *et al.*, 2008). Model is used to simulate the increase in total S_S due to increase in S_A (VFAs). Simulations are in agreement with literature, as illustrated in Appendix Table 11.4. The figure clearly illustrates that net S_S increase is substantial. On average, net 6.5–17.1 Mg COD year $^{-1}$ of substrate is generated, from which most of is VFAs. Total readily biodegradable substrate inflow to the WWTP from Vrå pressure main is 13.9–24.5 Mg COD year $^{-1}$. It is a substantial addition to the WWTP. Readily biodegradable substrate is necessary for advanced wastewater treatment in the WWTP, mainly for aerobic heterotrophic growth of biomass, denitrification and biological phosphorus removal. Before Hjørring WWTP started to receive wastewater from Vrå, readily biodegradable substrate has to be added manually. This illustrates, that substrate inflowing via pressure main is crucial for WWTPs functions.

Sulfide abatement methods are implemented as an extension of sulfide formation model, therefore limitations of sulfide formation model are all valid in abatement simulations as well. Additionally, uncertainties related to abatement methods itself are introduced with sulfide abatement simulations. Uncertainties due to introduction of new parameters and parameter intervals are self explanatory and are not discussed further. However, uncertainties as well as complications related to abatement method implementation into simulations should be examined in more detail. General goal throughout the simulations is the use of existing infrastructure for sulfide abatement (pumping stations).

Oxygen injection as a method of sulfide abatement is considered. It works in establishing aerobic conditions and oxidising existing sulfide in the water phase. In modeled simulations injection point is Hjørring pumping station. Possibility to oxidise sulfide formed in pressure main is investigated. Simulation results are unambiguous: single oxygen injection point via pressurised air is not enough to oxidise sulfide to desired low levels. Similar results are demonstrated by Gutierrez *et al.*, 2008, where around 65 % of total sulfide was oxidized via single injection point. Furthermore, results of simulations (Figure 11.19 and Figure 11.20 (excluding 5°C wet flow scenarios)) reveal that if oxygen is depleted before wastewater is discharged to the WWTP, sulfate reduction initiates immediately and sulfide content

in the pressure mains rises rapidly, since oxygen does not exhibit toxicity towards sulfate reducing bacteria, as discussed by Gutierrez *et al.*, 2008. Identical phenomena of immediate re-establishment of sulfide production is demonstrated by Nielsen *et al.*, 2006 in a laboratory setting. Underlying problems with sulfide abatement with oxygen injection are low solubility of oxygen and single injection point. Only latter can be controlled in economically viable way. With an increasing number of oxygen injection points between Hjørring pumping station and WWTP, sulfide oxidation time would be prolonged up until the discharge point. By extrapolating from data presented in aforementioned figures, substantial decrease of sulfide concentration could be expected. Establishment of aerobic conditions throughout the pressure main is also a viable strategy in preventing sulfide formation. However, since aerobic heterotrophic biomass consumes oxygen rapidly, very high number of injection points throughout the pressure main would be required. Heterotrophic aerobic biomass would also consume readily biodegradable substrate, which is required for advanced nutrient removal in the WWTP. In regards to reasoning from economical point of view, installation of new sewer infrastructure for oxygen injections diminishes the attractiveness of this particular abatement method. Where oxygen is readily available, additional infrastructure is not, and building it would increase operational expenses of this method substantially. To achieve constantly sufficient sulfide control with one injection point at Hjørring pumping stations, more than 40 g O_2 m^{-3} should be injected into wastewater. Such concentrations are possible only at high pressure or by supersaturating wastewater by extracting it, mixing it with liquid oxygen under high pressure and reintroducing supersaturated wastewater into the main wastewater stream (illustrated by Horne *et al.*, 2019, McMillen *et al.*, 2008). While this technology exist, it is relatively new, it requires installation of new infrastructure and generation of liquid oxygen and therefore - it is expensive.

Nitrate addition to the wastewater in order to establish anoxic conditions is, at its basis, very similar method to sulfide abatement with oxygen injection. In both methods aim is to prevent anaerobic conditions and to oxidise sulfide. However, due to highly soluble nature of nitrate, approach is different. Results illustrate, that anoxic conditions can be successfully maintained throughout the pressure main, if adequate initial nitrate concentration is injected at Vrå pumping station Appendix Figure 11.19–Figure 11.26. However, this method has one main disadvantage: if too much nitrate is dosed and it is not consumed in the pressure main, it reaches WWTP as an additional nitrate load, which has to be denitrified whilst increasing consumption of much needed readily available substrate.

Sophisticated nitrate dosing control would ensure adequate sulfide production control. Sulfide production model with integrated real-time data acquisition, with a feedback system, relying on sulfide sensors installed along the pressure main, would allow to pinpoint time and location of sulfide production re-initiation. Such model would allow to dose nitrate very accurately. However, for it to work efficiently, additional injection points are required in order to avoid sulfide buildup. Additional injection point

at Hjørring pumping station might not be enough. While it would stop sulfide production, anoxic autotrophic sulfide oxidation rates might not be sufficient to oxidise already present sulfide. Furthermore, this process is inefficient in terms of nitrate consumption, since autotrophic anoxic sulfide oxidation accounts for 10 % of total nitrate consumed, while the rest is used for anoxic heterotrophic growth of biomass (Yang et al., 2005). On the other hand, knowing that wastewater from pressure main constitutes only approximately 4% of total wastewater at the inlet of WWTP, it might be plausible to purposely dose too much nitrate in order to avoid sulfide production and assume that it would not have a significant negative effect on the treatment processes. In addition, Jiang et al., 2010 demonstrates that when sewer system is exposed to nitrate for prolonged period of time (up to 24 days), nitrate induces inhibition of sulfide reduction, demonstrating that the higher concentration of nitrate is injected, the higher inhibition level is present. Still, such a bold approach has to be investigated for economical validity. Constant overdose of nitrates might add up in price, even if flow from Vrå is not high compared to the entire inflow to WWTP. Furthermore, denitrification process consumes much needed readily biodegradable substrate, which has to be artificially added, if wastewater is not enriched enough.

Sulfide precipitation with iron is modeled as end-of-pipe treatment of wastewater rich with sulfide. Ferrous and ferric iron is considered in the simulations. Main advantage of using iron compared to other sulfide abatement methods is fast reaction times. Rapid reactions, compared to hydraulic retention time, are visible in the simulation results, Appendix Figure 11.27–Figure 11.34. If iron is injected at Hjørring pumping station, this method has no grave major disadvantages: it is relatively inexpensive, even if beyond stoichiometric amounts of salts has to be dosed, efficient, quick, chemicals used are non toxic and, where odor compounds are concerned, specific to sulfide. Furthermore, if iron salts are used as a precipitant, it can be beneficial in reducing phosphates in the sewer as well as enhancing chemical phosphorus removal in the WWTP. Similar findings are demonstrated by Rebosura et al., 2018, Gutierrez et al., 2010. Also, phosphate concentration in the sewer has to be taken into account when estimating amount of ferric salts dosed. Gutierrez et al., 2010 demonstrates that in activated sludge under aerobic conditions iron sulfide is rapidly re-oxidised, resulting is precipitation of phosphate. In such cases short HRT of iron sulfide in the pressure main is crucial for effective phosphate removal, which is another reason why injection of iron salts at the Hjørring pumping station is a superior location.

Limitations of this method are mainly related to pH<6.5 and are already discussed in methodology and results sections. To summarise it: when pH drops bellow 7, ratio of iron to sulfide has to be increased. Phenomena is especially visible with ferrous iron, where iron has to be dosed at least 2 or 3 times above stoichiometric levels. But, with pH in WWTP rarely dropping below 7 and a sufficient buffering capacity of potable water from Vrå, it should not be regularly occurring problem. Firer et al., 2008 mentions, that addition of iron into sewers might cause unsolicited flocculation, but when pressured

flow is concerned, this should not become a prevailing complication. Fan *et al.*, 2017 discusses that overdose of iron salts has a negative effect on biological phosphorus removal in the WWTP. With an iron overdose, metabolic capacity for phosphorus is reduced. Also release of phosphorus from precipitated iron phosphate during anaerobic - aerobic transition in WWTP processes, and, consequentially, increase in phosphate concentration in the effluent, is noticed. On the other hand, Rebosura *et al.*, 2018 states that no key biological processes in WWTP are influenced by sulfide control in the sewer system by precipitation with iron. While further investigation on iron influence to biological processes of WWTP is required, it is generally desirable to keep iron to sulfide ratios as low as possible in order not to waste chemical compounds and not to add unnecessary anions to the wastewater.

In order to dose iron with an appropriate concentration, several approaches can be taken. The model presented in this thesis could be used to account for uncertainties and to select appropriate iron to sulfide ratio as well as appropriate dosing concentration according to the highest sulfide quantity produced for the particular temperature and flow conditions. Since iron salts are in general, if not grossly overdosed, beneficial to the functions of wastewater treatment, slight overdosing would not be problematic. However, time of dosing is also crucial. As mentioned above, sulfide discharges semi-regular from the pressure main. Feedback system, with continuous measurements of sulfide concentrations in the sewer would be especially beneficial in such scenario. Since single injection point for iron is enough, only a couple of sensors installed right before the Hjørring pumping station would ensure overwhelmingly accurate time of dosing. Currently available sensors are limited to the measurement interval of 0 g m^{-3}–5 g m^{-3} sulfide in wastewater (according to Unisense, 2020), therefore overdosing of iron salts could not be avoided at higher sulfide concentrations. Nonetheless, when wet flow conditions are prevalent and sulfide concentration is reduced, logger would also provide data towards accurate dosing of iron salts in quantitative form.

New abatement strategies are promising. However, they are not investigated further, due to the limited availability; most of the methods mentioned are only tested at laboratory scale and not yet developed for sewer application. Contrary, end-of-pipe treatment with air-filtering are widely used and serves as a reliable option against hydrogen sulfide induced corrosion. Nevertheless, it would serve only as a control of symptoms but additionally alleviate all occurring malodors. Installation of an air filter system above the inlet structure is straightforward and building cost can be kept at a minimum by using funnels for covering the inlet structure. Additional costs can be saved by running air filters only during the night and morning hours. The biggest advantage compared to aforementioned in-situ treatments is that there is no need of sensors and logging of occurring sulfide .

Pre-treatment of wastewater from Vrå pressure main with aeration is another potential option, especially considering rather low flow from Vrå. A small covered basin or tank with aeration equipment is required.

Treated wastewater would consequently be H_2S free. It would neither cause corrosion nor malodor at main inlet, and any possible interruptions to WWTP process would be avoided. Additionally, part of COD would be removed here.

Outlook and preliminary price evaluation of methods with possible application for sulfide abatement is carried out. Since sulfide forms in the pressure main from Vrå to Hjørring with a prospect of formation rate increase during the summer, this phenomena should be addressed, because untreated sulfide leads to accumulating problems mainly related to the corrosion of the sewer infrastructure. Throughout the course of the thesis it is established that from three investigated methods only two are viable in case of Hjørring WWTP: establishment of anoxic conditions throughout the pressure main with injection of nitrate and precipitation of sulfide with iron salts. If it is assumed that for complete abatement of sulfide 80 g NO_3-N m^{-3} is required, it would result in 577 g KNO_3 m^{-3} or 469 g $Ca(NO_3)_2$ m^{-3} of salts to be injected at Vrå pumping station. On the other hand, precipitation of sulfide with iron requires lower quantities of substances: 191 g $FeCl_2$ m^{-3} and 102 g $FeCl_3$ m^{-3} (stoichiometric ratios of 2.0 and 1.1 accordingly, with concentration of phosphate in wastewater assumed to be 7 g m^{-3}.), if concentration of sulfide to be precipitated is 24 g S m^{-3}. It is apparent, that, quantity wise, it is required 2.5–5 times less iron salts compared to nitrate salts to abate sulfide in the pressure main. Available industrial chemical compounds are looked into to evaluate yearly requirements for chemical dosing. Dry flow conditions are assumed for the estimations (80 g NO_3-N m^{-3} and stoichiometric ratio of 1.1 for ferric iron). Two compounds are investigated: ferric iron based PIX-111 (active component, $FeCl_3$, makes up approximately 40% of the compound) and nitrate based Nutriox Nx 45(active component, $Ca(NO_3)_2\cdot4$ H_2O, makes up 50–65% of the compound). For complete abatement of sulfide with nitrate based injection 243 Mg year^{-1} of Nutriox is required. To precipitate sulfide with ferric iron, it requires 53 Mg year^{-1} of PIX-111. It is apparent, that sulfide precipitation with iron salts is a more accessible abatement method due to the significantly lower amount of chemical compounds required. Furthermore, iron use at Hjørring pumping station does not increase the nitrate load nor increase readily biodegradable substrate consumption. That being said, more innovative sulfide abatement methods should not be overlooked. While implementation of experimental methods on a full scale pressure main might be too audacious, implementing sewer sulfide collection in the gas phase and filtering it at the inlet or pre-aeration of wastewater before releasing it to the inlet structure of WWTP might be very plausible sulfide abatement methods, which would not require unreasonable investments.

Conclusion

<div style="text-align: right">

9

</div>

Throughout this thesis wastewater transformations under increased readily biodegradable substrate load in the pressure main and its effects on the WWTP are investigated. Main objective is to confirm the hypothesis of sulfide formation in the pressure main from Vrå to Hjørring, quantify forming sulfides and investigate possible sulfide abatement methods. Key findings are summarised in following conclusions:

- Comprehensive literature analysis establishes basis for further investigation of wastewater transformations in the pressure main from Vrå to Hjørring, with an strong emphasis on sulfide formation. All key sulfate formation factors are present: long pressure main, high concentration of readily biodegradable substrate, relatively high wastewater temperature, especially during the summer.

- Laboratory OUR experiments and IC reveals wastewater from the pressure main properties are related to the formation of sulfide. Wastewater from the outlet of the pressure main contains increased levels of acetate (18.9 g m^{-3} or 20.2 g COD m^{-3}) as well as low concentration of aerobic heterotrophic biomass (19 g COD m^{-3}), even if it was sampled at 13:00, when sulfide discharge is low.

- Measurements with OdaLog shows sulfide concentration in the gas phase at the inlet of WWTP to be considerable with maximum concentration of 18 ppm. High sulfide discharge is measured between 22:00–08:00. It poses a risk of corrosion of the sewer infrastructure, even if the inlet structure is not favorable for precise sulfide originating from the pressure main measurements due to its construction. Furthermore, sulfide formation in the summer will increase significantly due to rising wastewater temperature (2–3 % sulfide formation rate increase per 1°C) and lower flow. Sulfide emissions during the summer likely becomes critical with possible $K_L\alpha_{H_2S}$ increase of 50 % and hydrogen sulfide emissions increase of 750 %. Based on literature values, gas phase hydrogen sulfide concentrations up to 300 ppm can be expected.

- To counterbalance limited amount of laboratory experiments, wastewater aerobic/anaerobic transformations model is constructed to simulate sulfide formation in the pressure main. Uncertainties are taken into account by utilizing Monte Carlo simulations. Depending on the conditions, 5–24 g S m^{-3} sulfide forms in the pressure main according to the model runs. Simulations reveal,

that, on average, 13.9–24.5 Mg COD year $^{-1}$ of readily biodegradable substrate is discharged from the pressure main to the WWTP.

- Sulfide abatement methods are investigated. Sulfide oxidation with injected air proves to be insufficient due to the limited amount of injection points. Nitrate salt addition shows satisfactory reduction in comparison. However, uncertainties in increase of nitrate load to WWTP and consumption of much needed VFAs due to nitrification should be investigated further. Iron salts addition in Hjørring pumping station for sulfide precipitation shows good results and it proves to be an advantageous strategy. It also promotes chemical P-removal in WWTP.

- It is estimated that up to 243 Mg year^{-1} of Nutriox is required for complete sulfide abatement with nitrate. To precipitate sulfide with ferric iron, it requires 53 Mg year^{-1} of PIX-111 .

Since Hjørring WWTP started to receive wastewater from Vrå, efficiency of wastewater treatment process increased, due to the increase in inflowing readily biodegradable substrate. While this is advantageous, wastewater transformations in the pressure main - primarily sulfide formation - should not be overlooked. Untreated sulfide undoubtedly corrodes sewer infrastructure and damage accumulates over time. Furthermore, sulfides in the wastewater might interrupt wastewater treatment process further into the plant due to the disrupted flocculation.

Due to the increasing centralisation of wastewater treatment plants, situations where long pressure mains have to be used to convey wastewater will become more common. While this thesis deals with a case of Hjørring WWTP and even though more elaborate measurement campaign has to be carried out before any real-life implementations of sulfide abatement strategies are made, general future perspectives can be drawn from this thesis. While centralisation of wastewater treatment is beneficial on a large scope, possible local disadvantages should not be overlooked in order to ensure proper function of the entire wastewater treatment system.

Bibliography

10

Abdul-Talib, S., Hvitved-Jacobsen, T., Vollertsen, J., and Ujang, Z. (Feb. 2002). „Anoxic transformations of wastewater organic matter in sewers - process kinetics, model concept and wastewater treatment potential". In: *Water science and technology: a journal of the International Association on Water Pollution Research* 45, pp. 53–60.

Abraham, S., Joslyn, S., and Suffet, I. H. (2015). „Treatment of odor by a seashell biofilter at a wastewater treatment plant". In: *Journal of the Air & Waste Management Association* 65.10, pp. 1217–1228.

Andersson-Chan, A. (2006). „Biofiltration of odorous gas emissions". PhD thesis. Luleå tekniska universitet.

Barnett, K.L., Harringtion, B., and Harrington, T.W. Graul (2013). „Chapter 3 - Validation of Liquid Chromatographic Methods". In: *Liquid Chromatography - Applications*. Ed. by S. Fanali, P. R. Haddad, C Poole, P. Schoenmakers, and D. Lloyd. Second Edition. Elsevier, pp. 58–72.

Boon, A. G. (Apr. 1995). „Septicity in sewers: causes, consequences and containment". In: *Water Science and Technology* 31.7, pp. 237–253.

Boon, A. G. and Lister, A. R. (1975). „Formation of sulfide in rising main sewers and its prevention by injection of oxygen". In: *Prog. Water Technol.* 7.2, p. 289.

Bowlus, F. D. and Banta, A. P. (1932). „Control of anaerobic decomposition in sewage transportation". In: *Water Works Sewerage* 79.11, p. 369.

Chang, Y., Chang, Y., and Chen, H. (2007). „A method for controlling hydrogen sulfide in water by adding solid phase oxygen". In: *Bioresource Technology* 98.2, pp. 478–483.

Chmiel, H. (2011). *Bioprozesstechnik*. German. Springer Spektrum, p. 546.

Choo, H. S., Lau, L. C., Mohamed Abdul, R., and Lee, K. T. (2013). „Hydrogen sulfide adsorption by alkaline impregnated coconut shell activated carbon". In: *J. Eng. Sci. Technol* 8.6, pp. 741–753.

EPA, US Environmental Protection Agency US (1992). *Detection, Control, and Correction of Hydrogen Sulfide Corrosion in Existing Wastewater System*. Office of Wastewater Enforcement and Compliance.

Fan, J., Zhang, H., Ye, J., and Ji, B. (Dec. 2017). „Chemical stress from Fe salts dosing on biological phosphorus and potassium behavior". In: *Water Science and Technology* 77.5, pp. 1222–1229.

Firer, D., Friedler, E., and Lahav, O. (Apr. 2008). „Control of sulfide in sewer systems by dosage of iron salts: Comparison between theoretical and experimental results, and practical implications". In: *The Science of the total environment* 392, pp. 145–56.

Frey, M. (2008). „Untersuchungen zur Sulfidbildung und zur Effizienz der Geruchsminimierung durch Zugabe von Additiven in Abwasserkanalisationen". German. PhD thesis. Kassel university press GmbH, p. 436.

Grengg, c., Mittermayr, F., Baldermann, A., Böttcher, M. E., Leis, A., Koraimann, G., Grunert, P., and Dietzel, M. (2015). „Microbiologically induced concrete corrosion: A case study from a combined sewer network". In: *Cement and Concrete Research* 77, pp. 16–25.

Gutierrez, O., Mohanakrishnan, J., Sharma, K. R., Meyer, R. L., Keller, J., and Yuan, Z. (2008). „Evaluation of oxygen injection as a means of controlling sulfide production in a sewer system". In: *Water Research* 42.17, pp. 4549–4561.

Gutierrez, O., Park, D., Sharma, K. R., and Yuan, Z. (2010). „Iron salts dosage for sulfide control in sewers induces chemical phosphorus removal during wastewater treatment". In: *Water Research* 44.11, pp. 3467–3475.

Henze, M. (1997). „Trends in advanced wastewater treatment". In: *Water Science and Technology* 35.10. Advanced wastewater treatment: Nutrient removal and anaerobic processes, pp. 1–4.

Hjørring Kommunes Spildevandsplan (2020). *Dynamisk Spildevandskort*. Danish. URL: `https://hjorring.viewer.dkplan.niras.dk/plan/12#/13768` (visited on Apr. 21, 2020).

Hjørring Vandselskab A/S (2020). *Hjørring Renseanlæg*. Danish. URL: `http://www.hjvand.dk/sites/default/files/foldere/folder_hjoerring_ra_komprim.pdf` (visited on Apr. 10, 2020).

Horne, A. J., Jung, R., Lai, H., Faisst, B., and Beutel, M. (2019). „Hypolimnetic oxygenation 2: oxygen dynamics in a large reservoir with submerged down-flow contact oxygenation (Speece cone)“. In: *Lake and Reservoir Management* 35.3, pp. 323–337.

Hvitved-Jacobsen, T., Vollertsen, J., and H., Nielsen A. (2013). *Sewer Processes - Microbial and Chemical Process Engineering of Sewer Networks*, p. 399.

Hvitved-Jacobsen, T., Vollertsen, J., and Nielsen, A. H. (2005). „A Century with Hydrogen Sulfide in Sewer Networks: A Comprehensive Review of Models and New Approaches“. unpublished.

Hvitved-Jacobsen, T., Vollertsen, J., and Tanaka, N. (Mar. 2000). „An integrated aerobic/anaerobic approach for prediction of sulfide formation in sewers“. In: *Water Science and Technology* 41.6, pp. 107–115.

Hydrogen Sulphide Corrosion in Sewerage Works (Australia), Technological Standing Committee on (1989). *Hydrogen Sulphide Control Manual: Septicity, Corrosion and Odour Control in Sewerage Systems*. Melbourne Metropolitan Board of Works.

Jiang, G., Gutierrez, O., Sharma, K. R., and Yuan, Z. (2010). „Effects of nitrite concentration and exposure time on sulfide and methane production in sewer systems“. In: *Water Research* 44.14, pp. 4241–4251.

Jiang, G., Sun, X., Keller, J., and Bond, P. L. (2015). „Identification of controlling factors for the initiation of corrosion of fresh concrete sewers“. In: *Water Research* 80, pp. 30–40.

Kaszycki, P., Tyszka, M., Malec, P., and Kołoczek, H. (2001). „Formaldehyde and methanol biodegradation with the methylotrophic yeast Hansenula polymorpha . An application to real wastewater treatment“. eng. In: *Biodegradation* 12.3, pp. 169–177.

Kennes, C. and Veiga, M. C. (2013). *Air Pollution Prevention and Control: Bioreactors and Bioenergy*. John Wiley & Sons.

Kiilerich, B. (2018). „Ferrous and Ferric Iron Treatment of Sewer Force Main Biofilms: The Influence of Sulfide Abatement“. PhD thesis. Aalborg University.

Kiilerich, B., Nielsen, A. H., and Vollertsen, J. (Aug. 2018). „Kinetics of sulfide precipitation with ferrous and ferric iron in wastewater“. In: *Water Science and Technology* 78.

Kiilerich, B., Van de Ven, W., Nielsen, A. H., and Vollertsen, J. (2017). „Sulfide Precipitation in Wastewater at Short Timescales“. In: *Water* 9.9.

Kyeoung-Suk, C. and Mori, T. (Apr. 1995). „A newly isolated fungus participates in the corrosion of concrete sewer pipes“. In: *Water Science and Technology* 31.7, pp. 263–271.

la Cour Jansen, J., Arvin, E., Henze, M., and Harremoës, P. (2019). *Wastewater Treatment. Biological and Chemical Processes*, p. 371.

Lea, F. M. and Desch, C. H. (1936). *The chemistry of cement and concrete*. Edward Arnold, London.

Lewis, W. K. and Whitman, W. G. (1924). „Principles of Gas Absorption." In: *Industrial & Engineering Chemistry* 16.12, pp. 1215–1220.

Libralato, G., Ghirardini, A. V., and Avezzù, F. (2012). „To centralise or to decentralise: An overview of the most recent trends in wastewater treatment management". In: *Journal of Environmental Management* 94.1, pp. 61–68.

Logan, B. E. (2008). *Microbial fuel cells*. John Wiley & Sons.

Loosdrecht, M. C. M. van, Nielsen, P. H., Lopez-Vazquez, C. M., and Brdjanovic, D. (2016). *Experimental Methods in Wastewater Treatment*. Vol. 15. IWA Publishing, p. 362.

Matsché, N., Saracevic, E., Bertrán de Lis, F., and Brooks, L. (2005). „Korrosions - und Geruchsprobleme in Abwasserdruckleitungen". German. In: *Lebensministerium, Vienna: TU Wien*, p. 115.

May, P. M., Batka, D., Hefter, G., Königsberger, E., and Rowland, D. (2018). „Goodbye to S2- in aqueous solution". In: *Chem. Commun.* 54 (16), pp. 1980–1983.

McMillen, J., Jordan, B., Rackley, W., Tatum, B., and Woolsey, M. (Jan. 2008). „Large-Scale Oxygen Injection for Odor Control at Primary Clarifiers at the Trinity River Authority of Texas". In: *Proceedings of the Water Environment Federation* 2008, pp. 826–841.

Michalski, R. (2018). „Ion Chromatography Applications in Wastewater Analysis". In: *Separations* 5.1.

Nielsen, A. H., Vollertsen, J., and Hvitved-Jacobsen, T. (Apr. 2006). „Kinetics and Stoichiometry of Aerobic Sulfide Oxidation in Wastewater from Sewers—Effects of pH and Temperature". In: *Water environment research : a research publication of the Water Environment Federation* 78, pp. 275–83.

Nielsen, P. H. and Keiding, K. (1998). „Disintegration of activated sludge flocs in presence of sulfide". In: *Water Research* 32.2, pp. 313–320.

Nielsen, P. H., Raunkjær, K., and Hvitved-Jacobsen, T. (1998). „Sulfide production and wastewater quality in pressure mains". In: *Water Science and Technology* 37.1. The Sewer as a Physical, Chemical and Biological Reactor II, pp. 97–104.

Niero, M., Pizzol, M., Bruun, H. G., and Thomsen, M. (2014). „Comparative life cycle assessment of wastewater treatment in Denmark including sensitivity and uncertainty analysis". In: *Journal of Cleaner Production* 68, pp. 25–35.

O'connell, M., Mcnally, C., and Richardson, M. G. (2010). „Biochemical attack on concrete in wastewater applications: A state of the art review". eng. In: *Cement and Concrete Composites* 32.7, pp. 479–485.

Olmstead, F. H. and Hamlin, H. (1900). „Converting portions of the Los Angeles outfall sewer into a septic tank". In: *Engineering news* 44.19, pp. 317–318.

Park, J., Evans, E., and Ellis, T. (2011). „Development of a Biofilter with Tire-Derived Rubber Particle Media for Hydrogen Sulfide Odor Removal". In: *Water, Air & Soil Pollution* 215.1, pp. 145–153.

Parker, C. D. (1945). „The corrosion of concrete: 1. The isolation of a species of bacerbium associated with the corrosion of concrete exposed to atmospheres containing hydrogen sulphide." In: *Australian Journal of Experimental Biology and Medical Science* 23.2, pp. 81–90.

Pomeroy, R. (1936). „The Determination of Sulphides in Sewage". In: *Sewage Works Journal* 8.4, pp. 572–591.

Pomeroy, R. D. and Parkhurst, J. D. (1978). „The forecasting of sulfide build-up rates in sewers". In: *Eighth International Conference on Water Pollution Research*. Elsevier, pp. 627–634.

Pomeroy, R. and Bowlus, F. D. (1946). „Progress Report on Sulfide Control Research". In: *Sewage Works Journal* 18.4, pp. 597–640.

Rabaey, K., Van de Sompel, K., Maignien, L., *et al.* (2006). „Microbial Fuel Cells for Sulfide Removal". In: *Environmental Science & Technology* 40.17, pp. 5218–5224.

Rebosura, M., Salehin, S., Pikaar, I., Sun, X., Keller, J., Sharma, K. R., and Yuan, Z. (2018). „A comprehensive laboratory assessment of the effects of sewer-dosed iron salts on wastewater treatment processes". In: *Water Research* 146, pp. 109–117.

Rickard, D. and Luther, G. W. (2007). „Chemistry of Iron Sulfides". In: *Chemical Reviews* 107.2, pp. 514–562.

Sharma, K. R., Yuan, Z., de Haas, D., Hamilton, G., Corrie, S., and Keller, J. (2008). „Dynamics and dynamic modelling of H2S production in sewer systems". In: *Water Research* 42.10, pp. 2527–2538.

Sharma, K., Derlon, N., Hu, S., and Yuan, Z. (2014). „Modeling the pH effect on sulfidogenesis in anaerobic sewer biofilm". In: *Water Research* 49, pp. 175–185.

Sudarjanto, G., Sharma, K. R., Gutierrez, O., and Yuan, Z. (2011). „A laboratory assessment of the impact of brewery wastewater discharge on sulfide and methane production in a sewer". In: 64, pp. 1614–1619.

Sun, J., Hu, S., Sharma, K. R., Bustamante, H., and Yuan, Z. (2015). „Impact of reduced water consumption on sulfide and methane production in rising main sewers". In: *Journal of Environmental Management* 154, pp. 307–315.

Tanaka, N and Hvitved-Jacobsen, T (2001). „Sulfide production and wastewater quality-investigations in a pilot plant pressure sewer". In: vol. 43. 5, pp. 129–136.

Thermo Fisher Scientific (Oct. 2012). *Dionex ICS-1100 Ion Chromatography System Operator's Manual*. 3rd ed. Thermo Fisher Scientific.

Thistlethwayte, D. K. B. (1972). *The Control of Sulphides in Sewerage Systems*. Ann Arbor Science.

U.S. Department of Labor (2020). *Hydrogen Sulfide*. URL: https://www.osha.gov/SLTC/ hydrogensulfide/hazards.html (visited on Feb. 6, 2020).

Unisense (2020). *SulfiLogger: Sensor by Unisense*. URL: https://sulfilogger.com/wp-content/uploads/2020/01/SulfiLogger-Wastewater-flyer-2020-01-3.00_www.pdf (visited on May 24, 2020).

Vollertsen, J. and Hvitved-Jacobsen, T. (1999). „Stoichiometric and kinetic model parameters for microbial transformations of suspended solids in combined sewer systems". In: *Water Research* 33.14, pp. 3127, 3141.

Vollertsen, J. and Hvitved-Jacobsen, T. (2002). „Biodegradability of wastewater–a method for COD-fractionation". In: *Water science and technology* 45.3, pp. 25–34.

Vollertsen, J., Hvitved-Jacobsen, T., and Nielsen, A. (July 2005). „Stochastic Modeling of Chemical Oxygen Demand Transformations in Gravity Sewers". In: *Water environment research* 77.4, pp. 331–339.

Vollertsen, J., Nielsen, A. H., Jensen, H. S., Wium-Andersen, T., and Hvitved-Jacobsen, T. (2008). „Corrosion of concrete sewers—The kinetics of hydrogen sulfide oxidation". In: *Science of The Total Environment* 394.1, pp. 162–170.

Vrå Dampvaskeri (2015). *Vrå Dampvaskeri CSR Redegoerelse*. Danish.

Weiss, J. (2004). *Handbook of ion chromatography*. 3., completely revised and updated ed. Weinheim: Wiley-VCH.

Wu, M., Wang, T., Wu, K., and Kan, L. (2020). „Microbiologically induced corrosion of concrete in sewer structures: A review of the mechanisms and phenomena“. In: *Construction and Building Materials* 239.

Yang, W., Vollertsen, J., and Hvitved-Jacobsen, T. (Aug. 2004). „Anoxic control of odour and corrosion from sewer networks“. In: vol. 50. 4, pp. 341–349.

Yang, W., Vollertsen, J., and Hvitved-Jacobsen, T. (Aug. 2005). „Anoxic sulfide oxidation in wastewater of sewer networks“. In: *Water science and technology: a journal of the International Association on Water Pollution Research* 52.3, pp. 191–199.

Yongsiri, C., Hvitved-Jacobsen, T., Vollertsen, J., and Tanaka, N. (2003). „Introducing the emission process of hydrogen sulfide to a sewer process model (WATS)“. In: 47, pp. 85–92.

Zhang, L., De Schryver, P., De Gusseme, B., De Muynck, W., Boon, N., and Verstraete, W. (2008). „Chemical and biological technologies for hydrogen sulfide emission control in sewer systems: a review“. In: *Water research* 42.1-2, pp. 1–12.

Zhang, L., Mendoza, L., Marzorati, M., and Verstraete, W. (2009). „Inhibition of sulfide generation by dosing formaldehyde and its derivates in sewage under anaerobic conditions“. In: *Water Science and Technology* 59.6, pp. 1247–1254.

Appendix

<div style="text-align: right; font-size: 2em;">11</div>

11.1 Corrosion rates based on full-scale experiments

Table 11.1: Concrete and Mortar corrosion rates based on real conditions or full-scale experiments simulating site conditions, Table adopted from Wu *et al.*, 2020, page 10.

$H_2S_{(g)}$ ppm	Exposed Material[1]	Corrosion rate mm/year	Country/Year
0.1-50	Concrete	2.5-10	US (1991)
5-400	Concrete	1.4 (crown) 4.5 (waterline)	Japan
25-300	Mortar	7.64[2]	Japan
N.A.	Concrete	1.1-1.8	Belgium (2002)
40-75	Concrete (OPC + Sil. Ag.)	>7.55[3]	South Africa (2011)
	Concrete (OPC + Cal. Ag.)	3.1[3]	
	Concrete (CAC + Sil. Ag.)	1.9[3]	
	Concrete (CAC + Cal. Ag.)	0.6[3]	
0-1000	Concrete	3.1[4]	Denmark (2008)
2	Concrete	1-2	Australia (2012)
80-420	Concrete	3.7-12.7	Australia (2014)
0.1-367	Concrete (OPC (C_3A-free)+FA)	1-10	Austria (2015)

[1] OPC - ordinary Portland cement; FA – fly ash; CAC – calcium aluminate cement; Sil. Ag. – siliceous aggregate; Cal. Ag. – calcareous aggregate; C_3A – cement notation for $3CaOAl_2O_3$

[2] Sample in pilot plant

[3] 14 years of exposure in sewer

[4] pilot scale reactor in Frejlev

11.2   Hjørring WWTP data
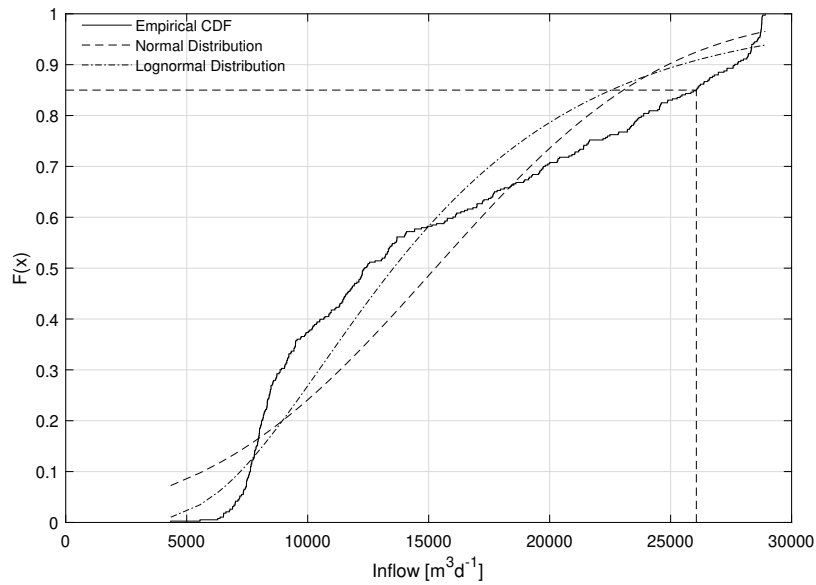
Figure 11.1: Cumulative probability function of inflow for 2019 $(-)$ and 85% percentile $(--)$

Figure 11.1 shows the empirical, normal and lognormal distribution for inlet data. 85% percentile is 26 063 $m^3 d^{-1}$. Lillifors test for normal distribution shows rejected null hypothesis (*test statistic k* = 0.15 > *critical value c* = 0.05). Therefore no normality is present in inlet data, which confirms the observed figure.
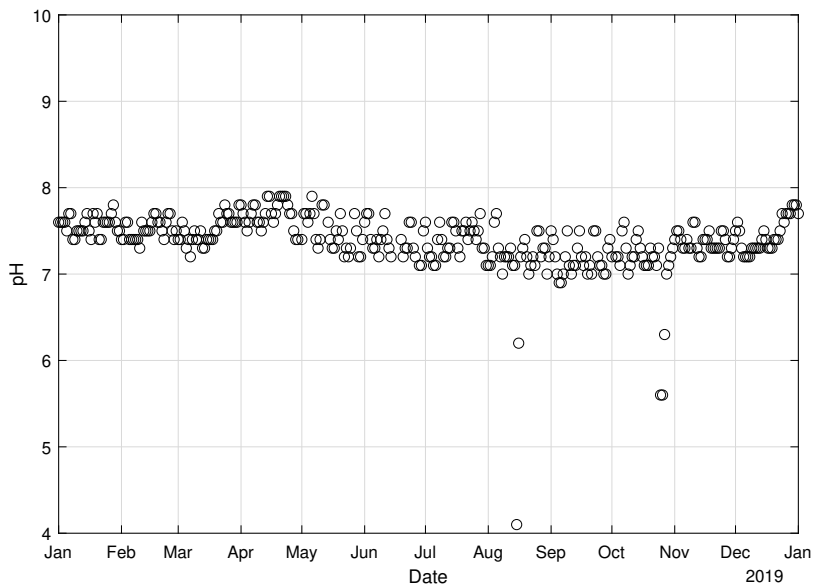
Figure 11.2: pH measurements for 2019 full data set
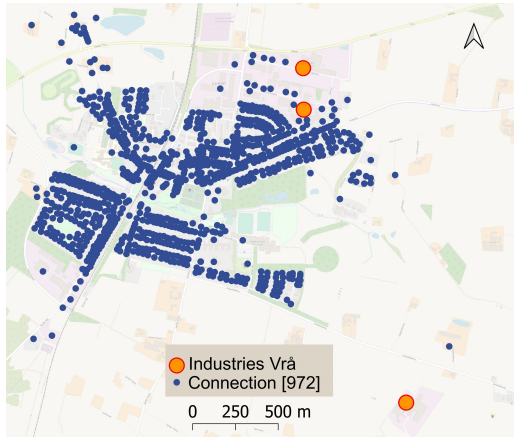
Figure 11.3: Detail map of Vrå with potable water connections and location of three main industries
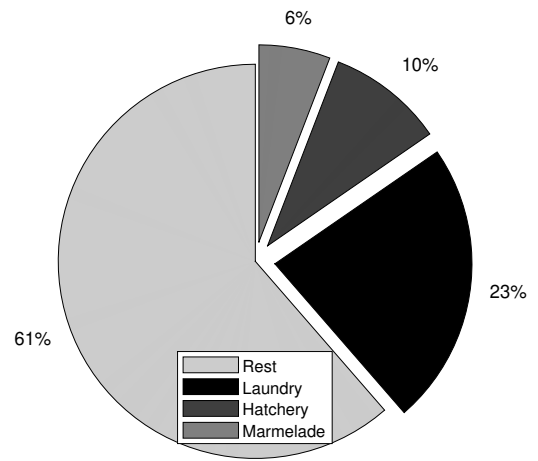
Figure 11.4: Potable water consumption in Vrå 2016 for three main industries and rest (e.g. households)

11.3 Additional data and figures for methods used for wastewater quality and parameter description
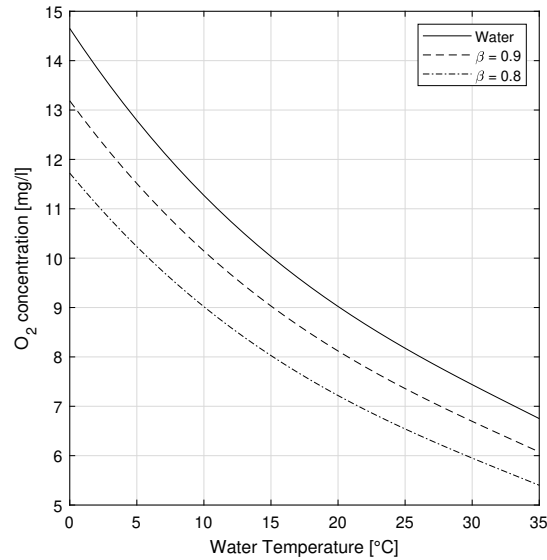
Figure 11.5: Temperature dependency for dissolved oxygen with correction factor β for wastewater, from Hvitved-Jacobsen *et al.*, 2013

Table 11.2: Sulfate concentration in potable water; frequency in Vrå. Data from https://geus.dk

Bin, g S m^{-3}	Frequency [-]	Cumulative %
20	1	8.3
40	2	25.0
60	4	58.3
80	3	83.3
100	2	100
>100	0	100
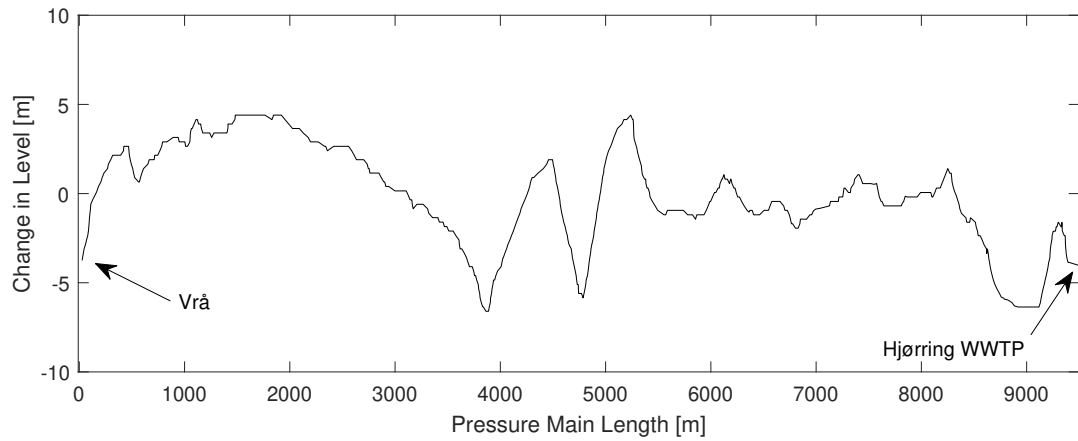
Figure 11.6: Cross section force main from Vrå to Hjørring WWTP, displayed is entire length. Note, that Scale is 1:500 and slope appears exaggerated.
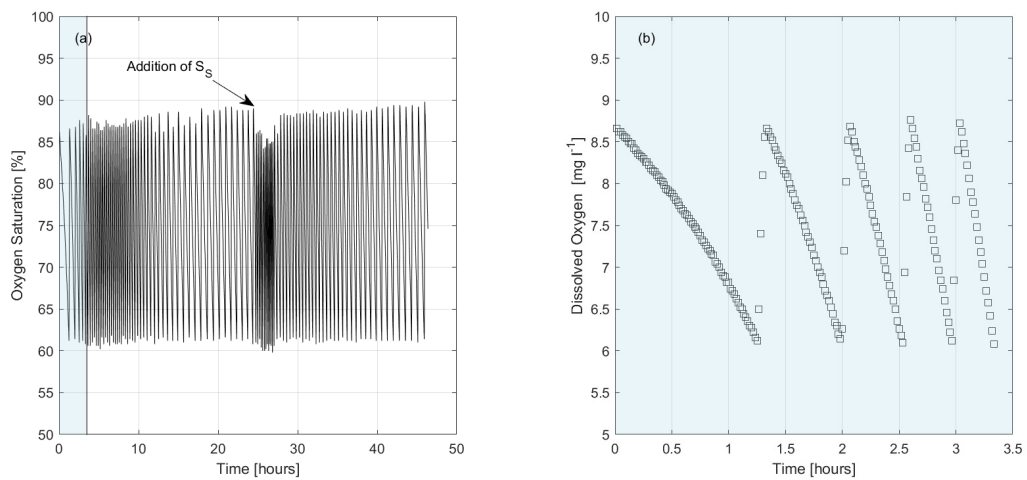
Figure 11.7: DO probe signal from Frejlev Test batch experiment 12.02.2019: addition of 60g COD m^{-3} (ethanol) after 24 h. (a) full experiment and (b) first 3.5h of the experiment.
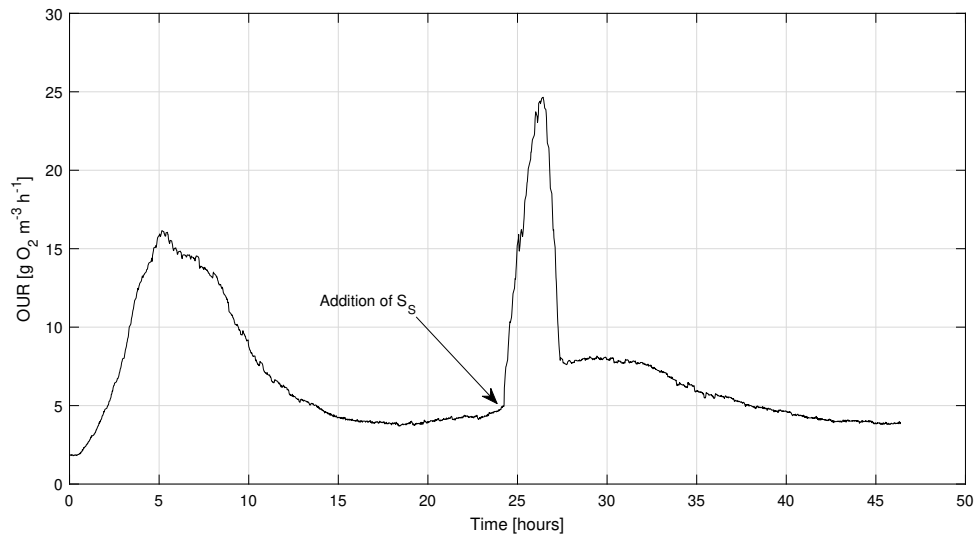
Figure 11.8: Resulting OUR measurement from upstream wastewater Frejlev with 60g COD m^{-3} addition (ethanol) after 24 h
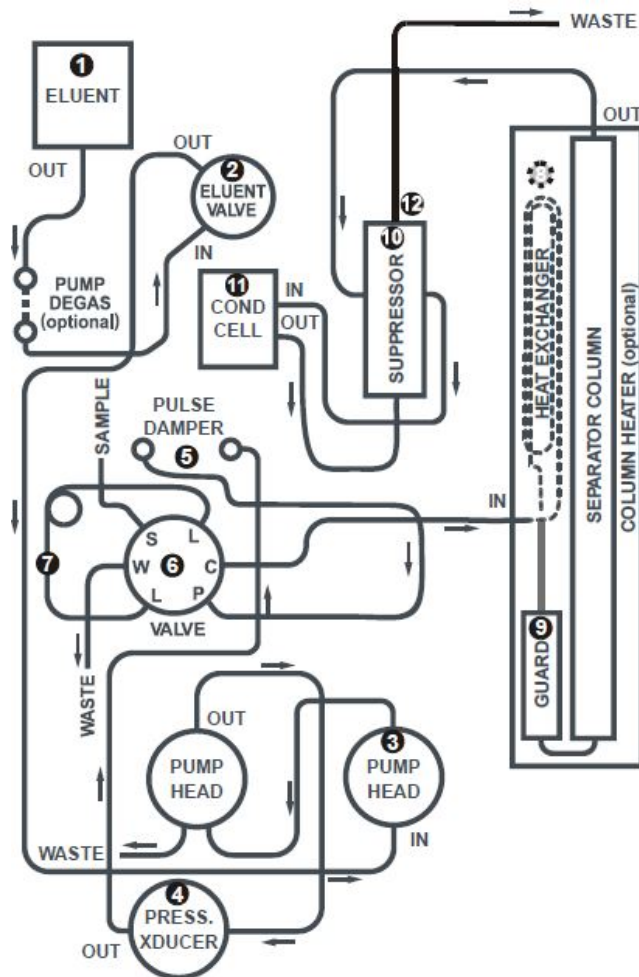
Figure 11.9: Flow Diagram for Ion Chromatograph Dionex ICS 1000, from Thermo Fisher Scientific, 2012

11.4 Transformations of wastewater with increased heterotrophic biomass
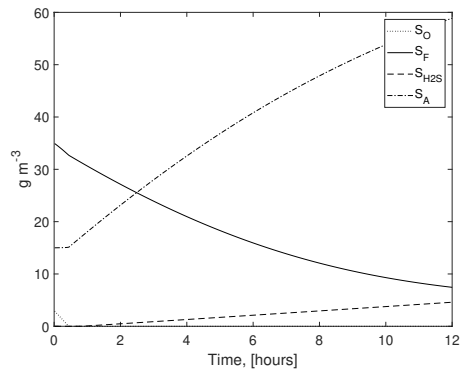
Figure 11.10: Wastewater composition during aerobic/anaerobic processes in pressure main, 10°C with increased X_{HW}; X_{HW}=35 g COD m^{-3}
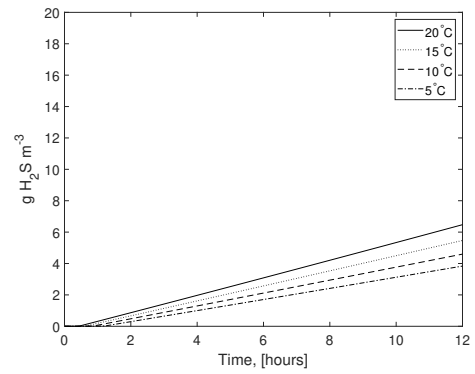
Figure 11.11: H_2S formation dependency on wastewater temperature and retention time

11.5 Rate constants and sulfide left in solution in equilibrium during precipitation of sulfide with ferrous or ferric iron
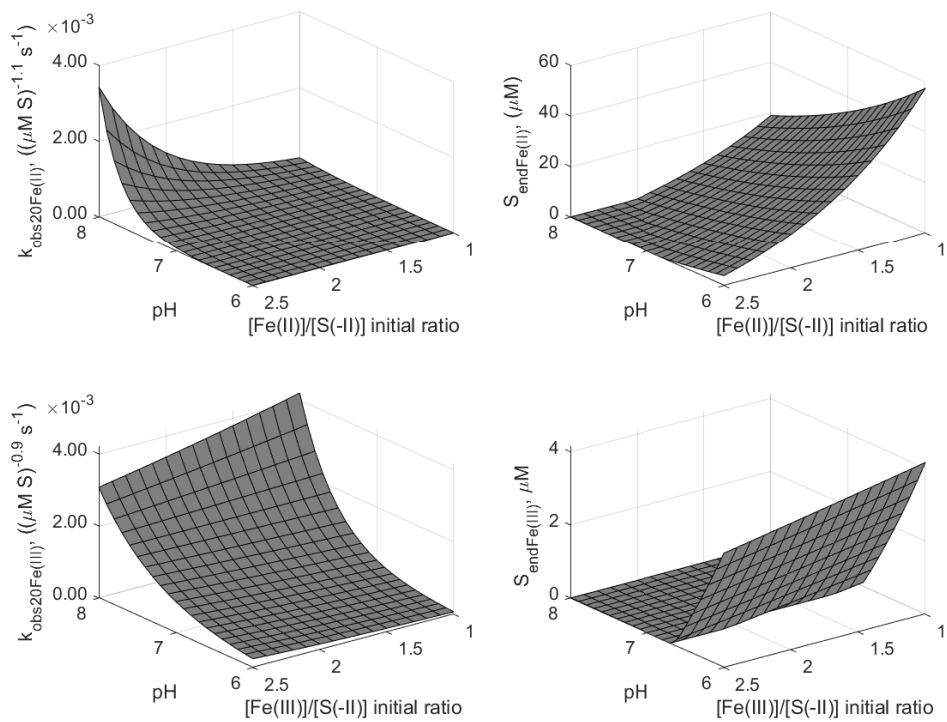
Figure 11.12: Plots describing rate constant of sulfide precipitation with addition of ferrous or ferric iron and sulfide concentration left in equilibrium after addition of iron. Made with empirical equations from Kiilerich *et al.*, 2018

11.6 Results of sulfide formation and abatement methods

In this part of the appendix results of sulfide production and abatement methods in the pressure main from Vrå to Hjørring are presented. Data is generated with Monte Carlo simulations from 1000 data sets for each individual scenario. Data sets are created according to the table bellow, Table 11.3. Results are presented graphically throughout this section of the appendix, plots illustrating 20th to 80th percentiles are presented.

Table 11.3: Parameter values used for Monte Carlo simulations of wastewater transformations under aerobic, anoxic and anaerobic conditions. Data is generated from values presented here, which are based on values from Hvitved-Jacobsen *et al.*, 2013, Abdul-Talib *et al.*, 2002, Yang *et al.*, 2004, Nielsen *et al.*, 2006

| Symbol	Description	Average; SD or constant value	Unit
S_a	Readily biodegradable substrate	5.0 - 40.0 (uniform dist.)	g COD m^{-3}
S_f	Readily biodegradable substrate	5.0 - 20.0 (uniform dist.)	g COD m^{-3}
$X_{S,fast}$	Hydrolysable substrate	95; 20	g COD m^{-3}
$X_{S,slow}$	Hydrolysable substrate	COD-S_a - S_f - $X_{S,fast}$ - X_{Hw}	g COD m^{-3}
X_{Hw}	Heterotrophic biomass	20.5; 5	g COD m^{-3}
μ_H	Maximum specific growth rate	6.0; 1.0	d^{-1}
Y_{HW}	Suspended biomass yield constant for heterotrophs	0.55; 0.05	g COD g COD^{-1}
K_S	Saturation constant for readily biodegradable substrate	1.25; 0.2	g COD m^{-3}
K_O	Saturation constant for dissolved oxygen	0.255; 0.05	g O$_2$m^{-3}
α_W	Temperature coefficient in water phase	1.07	-
q_m	maintenance energy requirement rate constant	1.0	d^{-1}
$k_{1/2}$	1/2 order rate constant	4.0	g O$_2^{0.5}$ m$^{-0.5}$ d^{-1}
Y_{HF}	Biofilms yield constant for heterotrophs	0.55; 0.05	g COD g COD^{-1}
K_{SF}	Saturation constant for readily biodegradable substrate	5.0	g COD m^{-3}
ϵ	Efficiency constant for biofilm biomass	0.15	-
α_F	Temperature coefficient in the biofilm	1.05	-
$k_{h,fast}$	Hydrolysis rate constant	7.29; 2.00	d^{-1}
$k_{h,slow}$	Hydrolysis rate constant	1.03; 0.25	d^{-1}
$K_{X,fast}$	Saturation constant for hydrolysis	1.5	g COD g COD^{-1}
$K_{X,slow}$	Saturation constant for hydrolysis	0.5	g COD g COD^{-1}
h_{fe}	Anaerobic hydrolysis reduction rate	0.14	-
q_{fe}	Maximum rate for fermentation	3.0	d^{-1}
K_{Fe}	Saturation constant for fermentation	20.0	g COD g COD^{-1}
k_{H2S}	H_2S production rate constant	2.5; 0.2	g S^{2-} m^{-2} h^{-1}
α_S	Temperature coefficient for hydrogen sulfide production	1.030	-
k_{H_2Sc}	Rate constant for aerobic chemical oxidation of H2S	0.27; 0.08	(g S m^{-3})$^{1-m}$(g O$_2$ m^{-3})$^{-n}$ day^{-1}
k_{HS^-c}	Rate constant for aerobic chemical oxidation of HS-	0.27; 0.08	(g S m^{-3})$^{1-m}$(g O$_2$ m^{-3})$^{-n}$ day^{-1}
$k_{S(-II)b}$	Rate constant for aerobic biological sulfide oxidation	0.671; 0.106	(g S m^{-3})$^{1-m}$(g O$_2$ m^{-3})$^{-n}$ day^{-1}
K_{a1}	First dissociation constant for sulfid	$8.913 \cdot 10^{-8}$	-
$\omega_{S(-II)b}$	Width (shape of the activity curve) of optimum pH range for sulfide oxidation	25	-
$\mu_{H,NO3}$	Maximum specific growth rate	3.9; 0.2	d^{-1}
Y_{NO3}	Yield constant for heterotrophic biomass	0.24	mol e-eq (mol e-eq)$^{-1}$
$K_{S,NO3}$	Saturation constant for readily biodegradable substrate	2.94; 0.25	g NO$_3$-N m^{-3}
$\mu_{H,NO2}$	Maximum specific growth rate	4.8; 0.4	d^{-1}
Y_{NO2}	Yield constant for heterotrophic biomass	0.22	mol e-eq (mol e-eq)$^{-1}$
$K_{S,NO2}$	Saturation constant for readily biodegradable substrate	3.76; 0.35	g NO$_3$-N m^{-3}
f_n	Fraction of nitrate reducing biomass	0.895; 0.03	-
X_{HVN}	Heterotrophic biomass under anoxic conditions	$0.7X_{HV}$	g COD m^{-3}
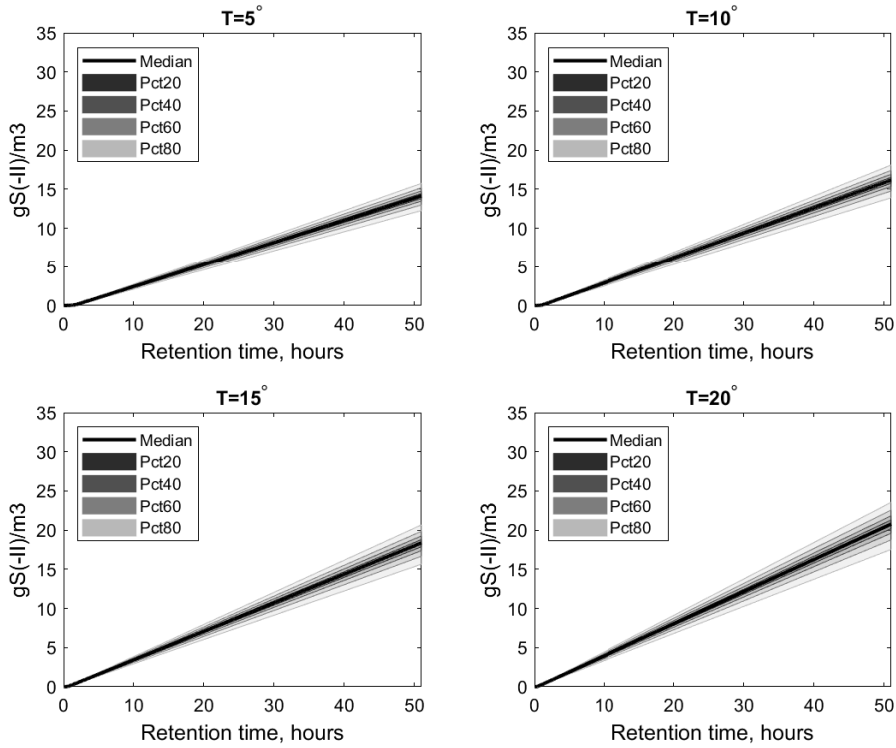
Figure 11.13: Sulfide production in the pressure main, pH=7 and DO at injection time = 6g/m3. Dry conditions. Plots illustrate 20th to 80th percentiles from Monte Carlo simulations
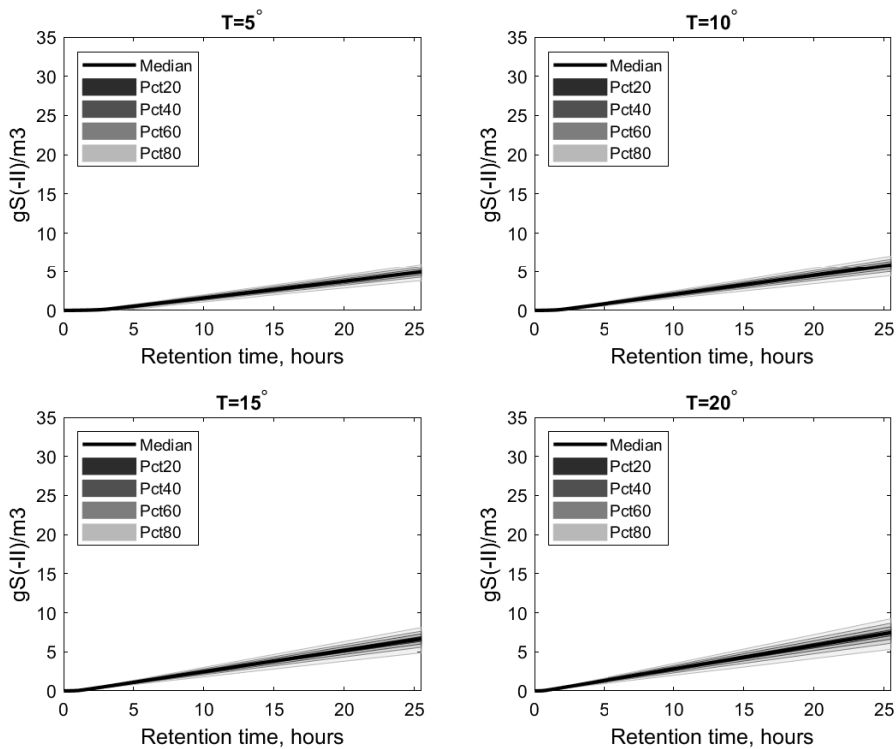

Figure 11.14: Sulfide production in the pressure main, pH=7 and DO at injection time = 6g/m3. Wet conditions. Plots illustrate 20th to 80th percentiles from Monte Carlo simulations
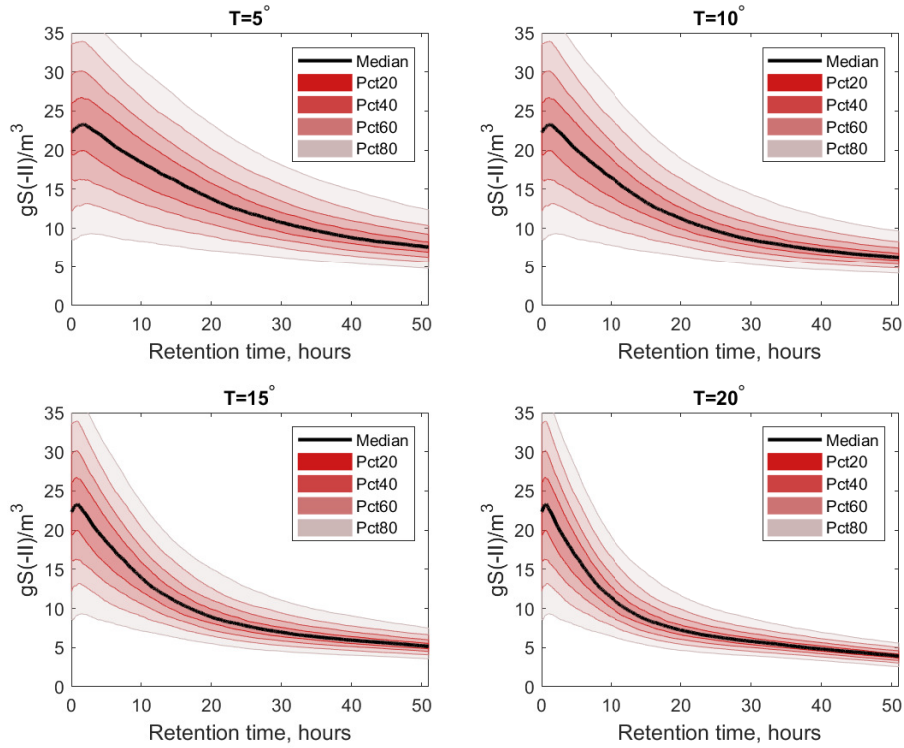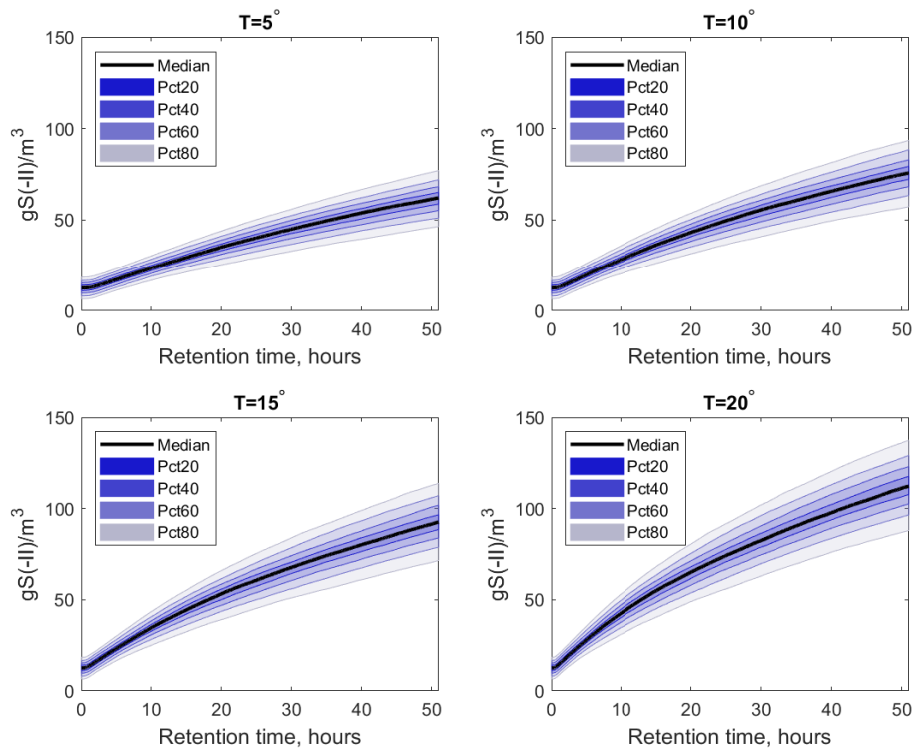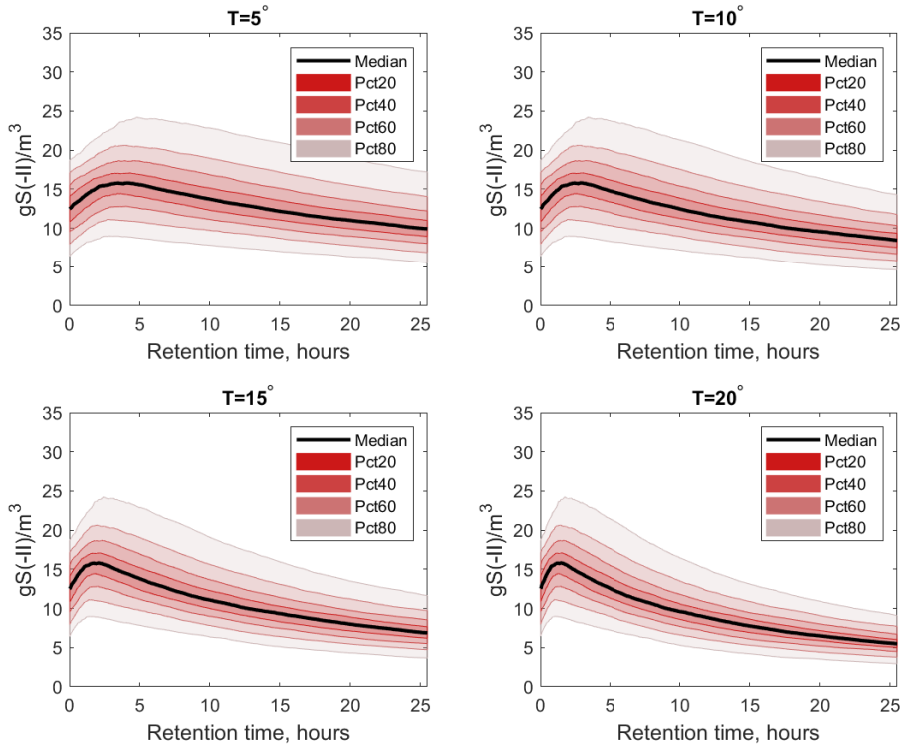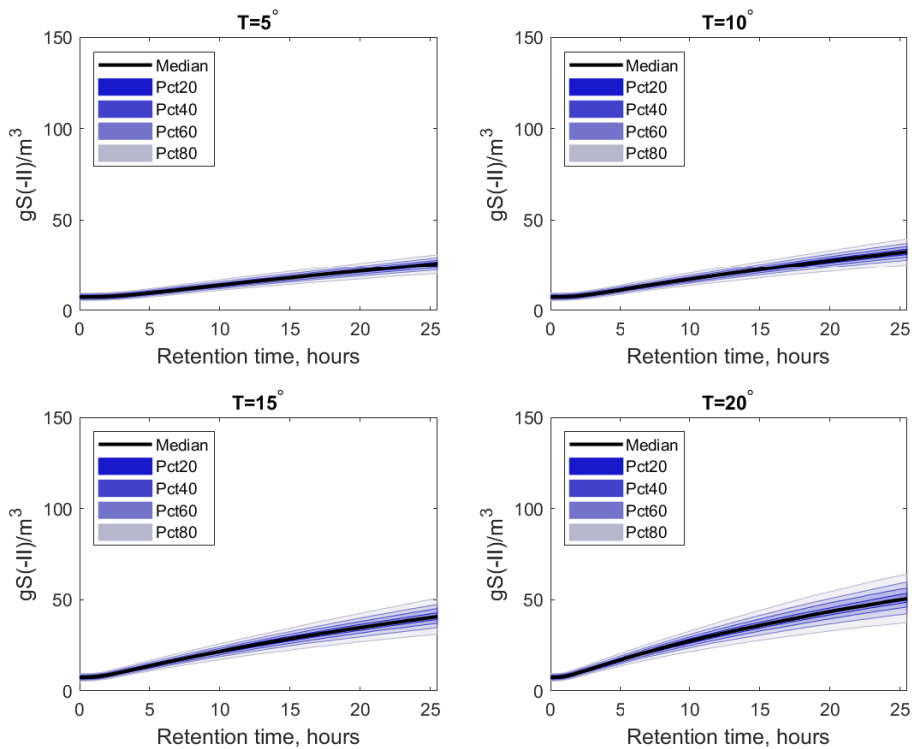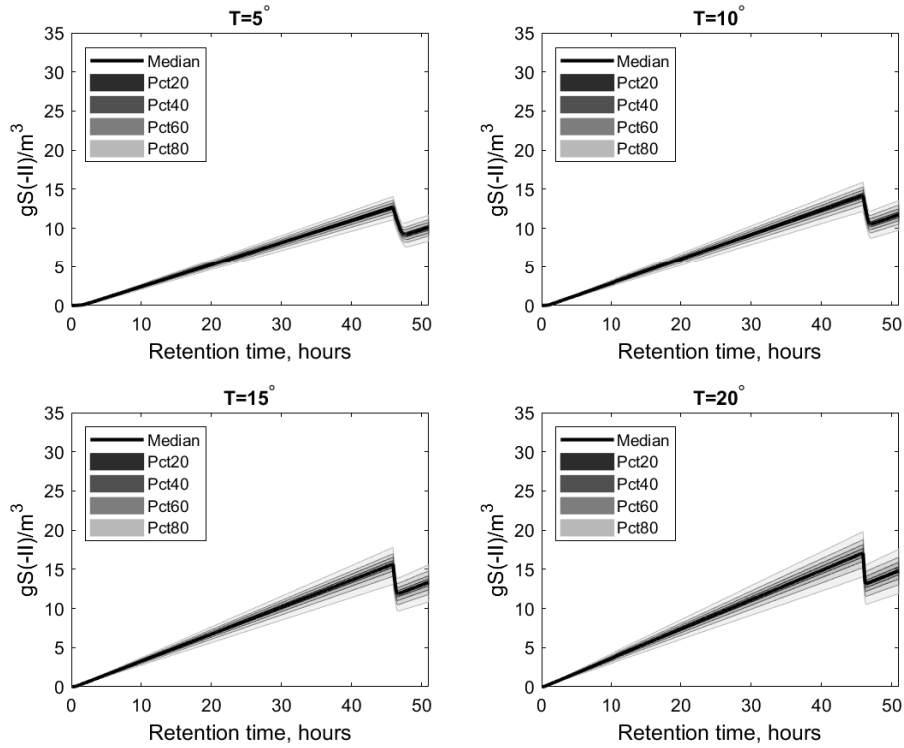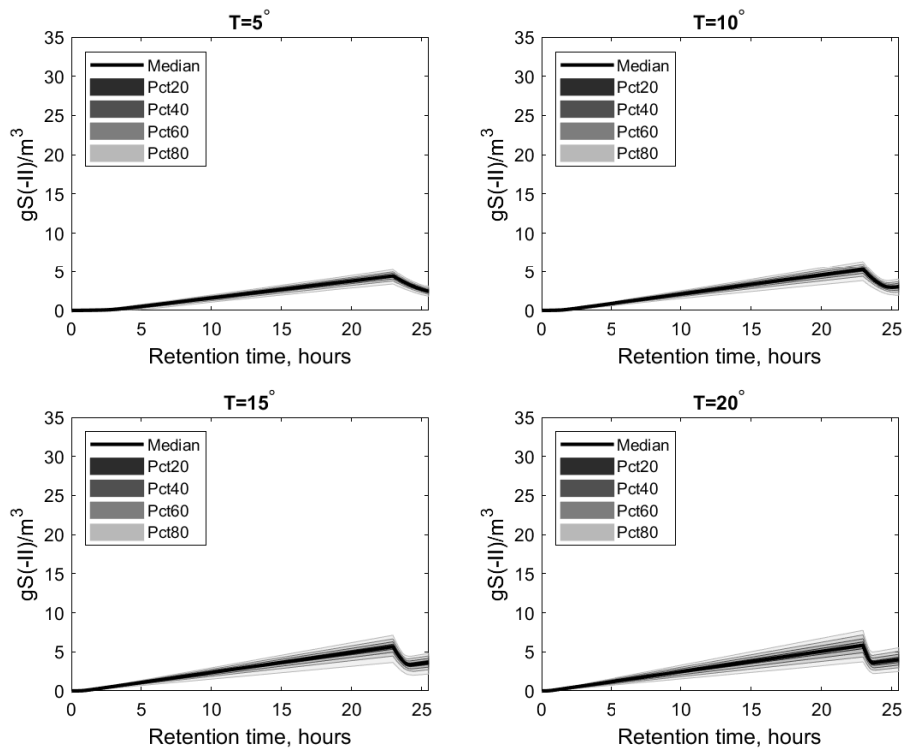
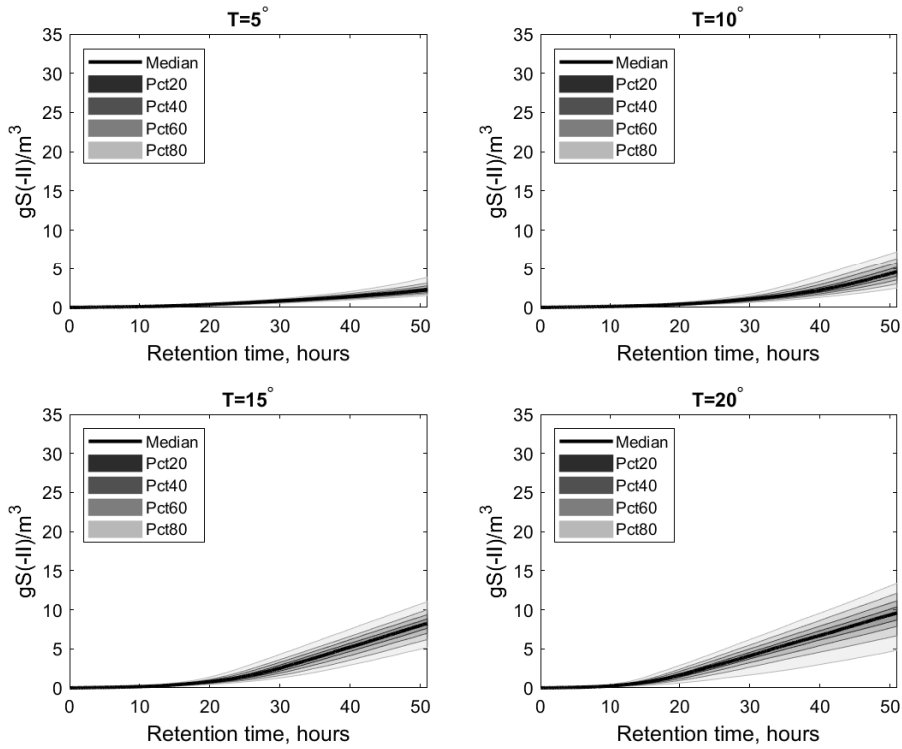Figure 11.15: S_F transformations in the pressure main, pH=7 and DO at injection time = 6g/m3. Dry conditions. Plots illustrate 20th to 80th percentiles from Monte Carlo simulations

Figure 11.16: S_A transformations in the pressure main, pH=7 and DO at injection time = 6g/m3. Dry conditions. Plots illustrate 20th to 80th percentiles from Monte Carlo simulations

Figure 11.17: S_F transformations in the pressure main, pH=7 and DO at injection time = 6g/m3. Wet conditions. Plots illustrate 20th to 80th percentiles from Monte Carlo simulations

Figure 11.18: S_A transformations in the pressure main, pH=7 and DO at injection time = 6g/m3. Wet conditions. Plots illustrate 20th to 80th percentiles from Monte Carlo simulations

Figure 11.19: Sulfide abatement, oxygen injection, pH=7 and DO at injection time = 6 g O_2/m3. Dry conditions. Plots illustrate 20th to 80th percentiles from Monte Carlo simulations

Figure 11.20: Sulfide abatement, oxygen injection, pH=7 and DO at injection time = 6 g O_2/m3. wet conditions. Plots illustrate 20th to 80th percentiles from Monte Carlo simulations

Figure 11.21: Sulfide concentration. Sulfide control, nitrate injection of 30 g NO_3-N/m3, pH=7, dry conditions. Plots illustrate 20th to 80th percentiles from Monte Carlo simulations
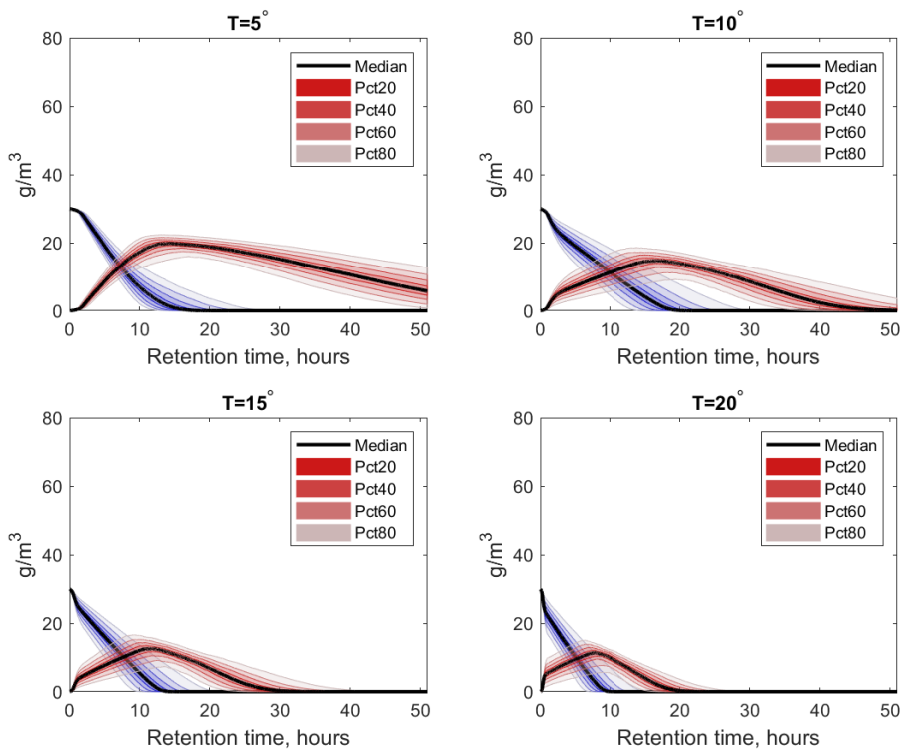

Figure 11.22: Nitrate nitrogen (blue) and nitrite nitrogen (red) concentrations. Sulfide control, nitrate injection of 30 g NO_3-N/m3, pH=7, dry conditions. Plots illustrate 20th to 80th percentiles from Monte Carlo simulations
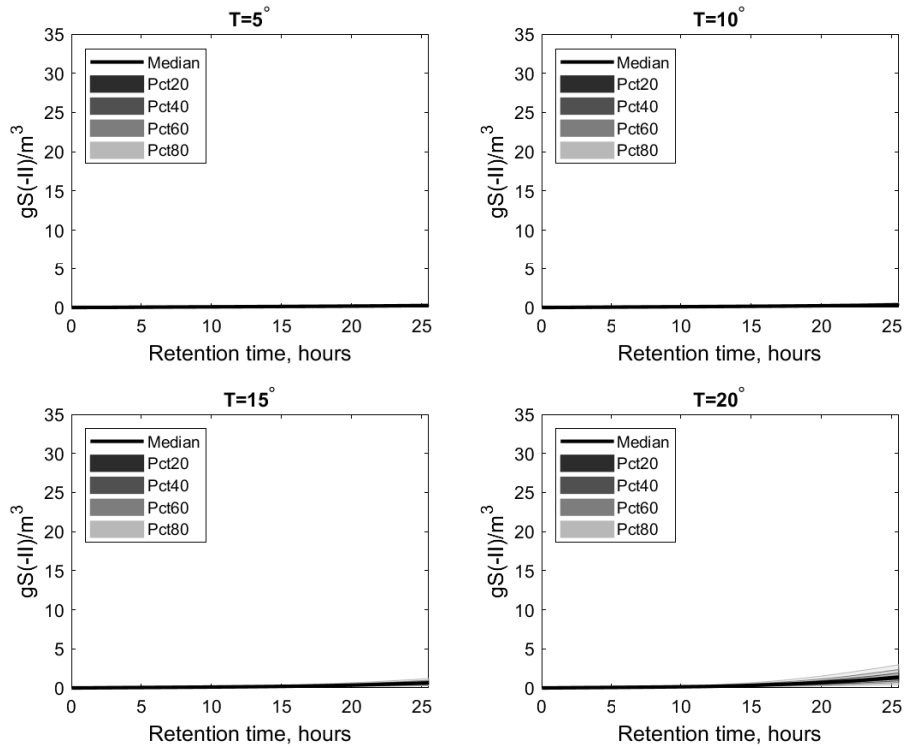
Figure 11.23: Sulfide concentration. Sulfide control, nitrate injection of 30 g NO$_3$-N/m3, pH=7, wet conditions. Plots illustrate 20th to 80th percentiles from Monte Carlo simulations
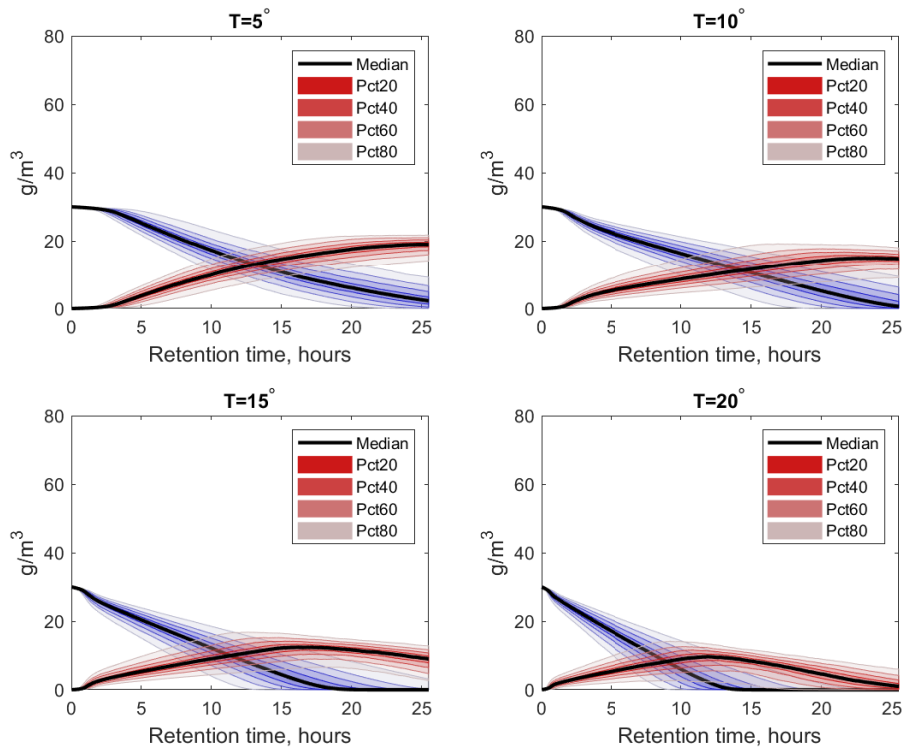
Figure 11.24: Nitrate nitrogen (blue) and nitrite nitrogen (red) concentrations. Sulfide control, nitrate injection of 30 g NO$_3$-N/m3, pH=7, wet conditions. Plots illustrate 20th to 80th percentiles from Monte Carlo simulations
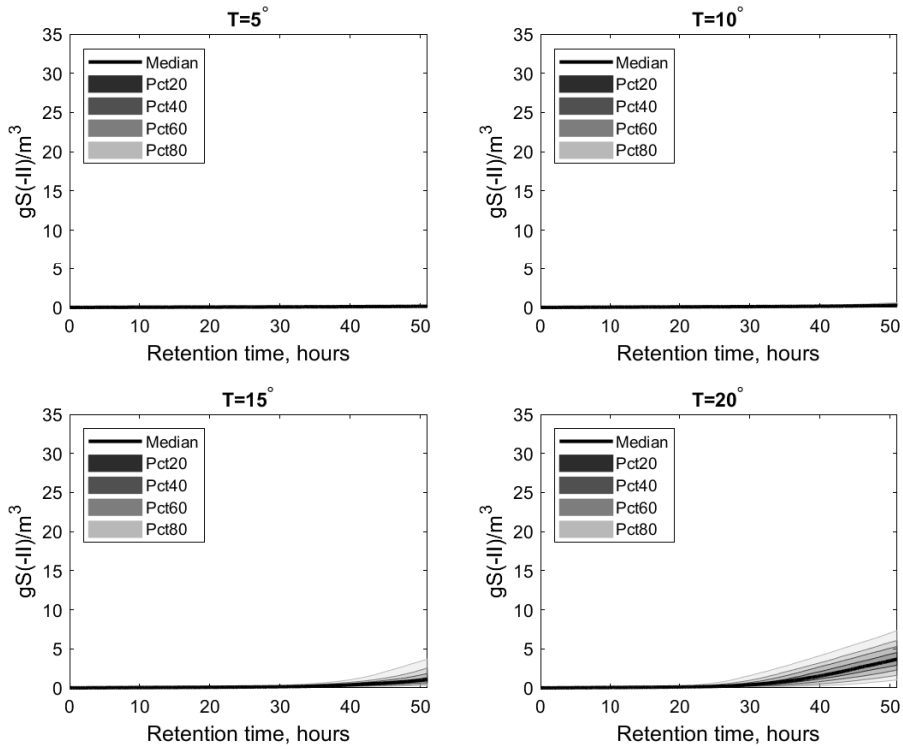
Figure 11.25: Sulfide concentration. Sulfide control, nitrate injection of 80 g NO_3-N/m3, pH=7, dry conditions. Plots illustrate 20th to 80th percentiles from Monte Carlo simulations
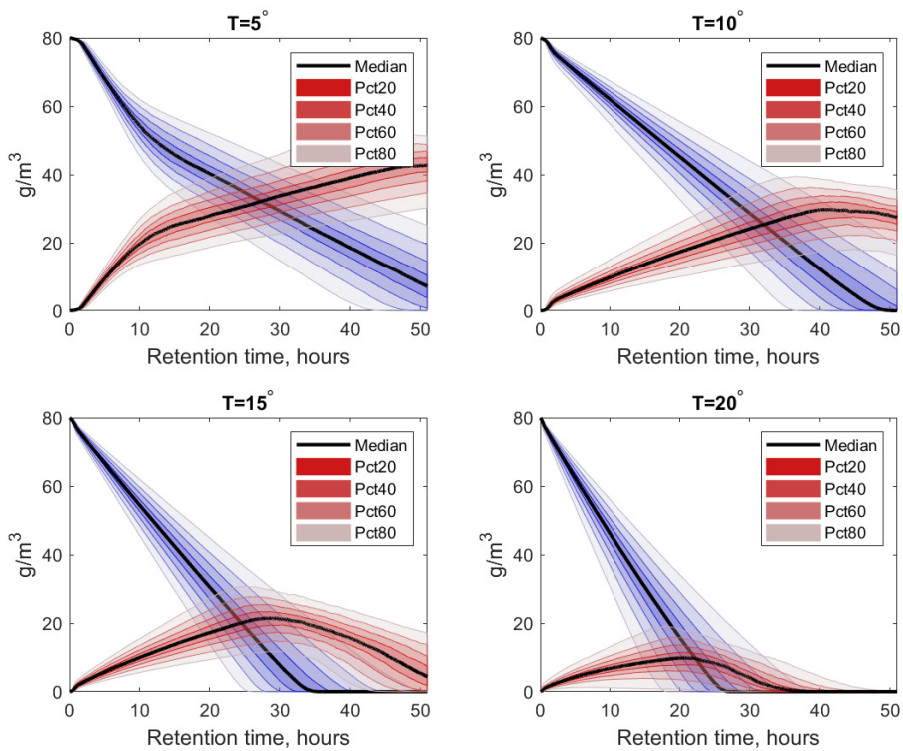
Figure 11.26: Nitrate nitrogen (blue) and nitrite nitrogen (red) concentrations. Sulfide control, nitrate injection of 80 g NO_3-N/m3, pH=7, dry conditions. Plots illustrate 20th to 80th percentiles from Monte Carlo simulations
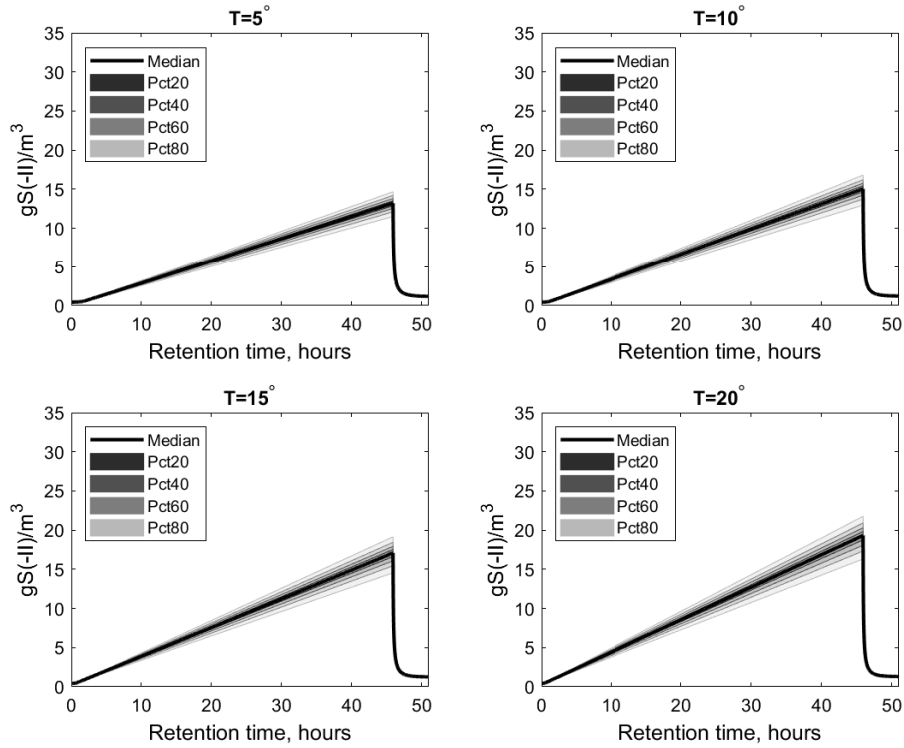
Figure 11.27: Sulfide control, precipitation with Fe(II), ph=6, [Fe(II)]/[S(-II)] ratio = 2, dry conditions. Plots illustrate 20th to 80th percentiles from Monte Carlo simulations
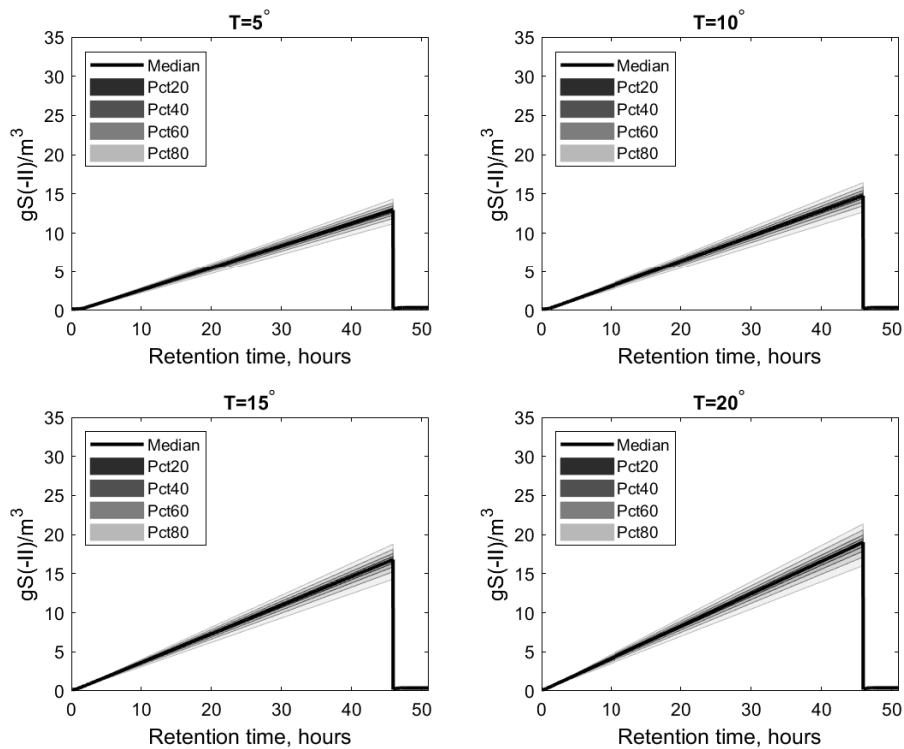
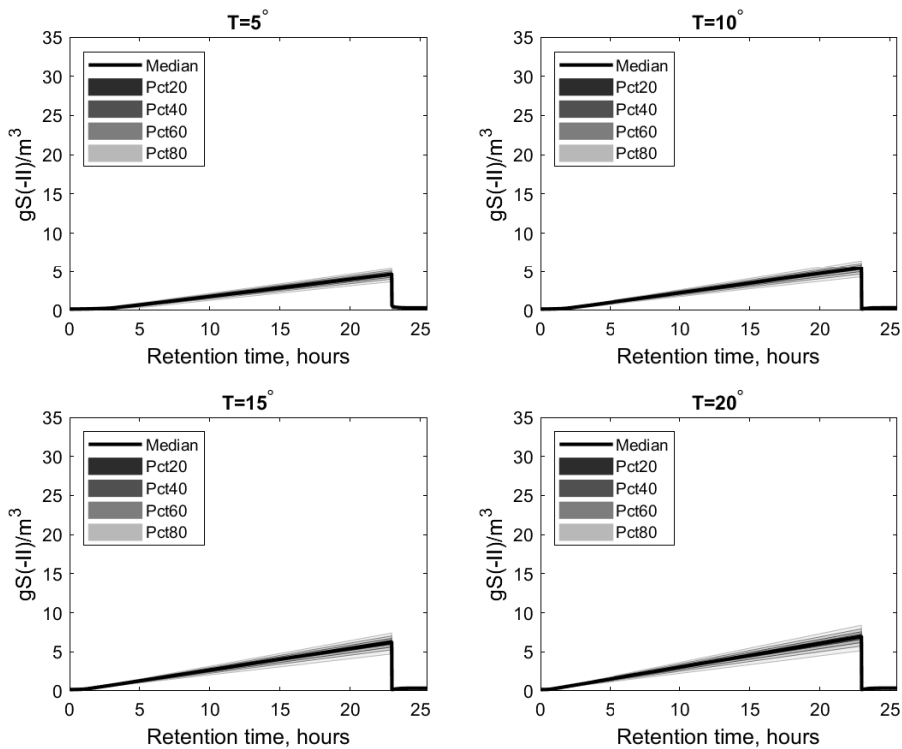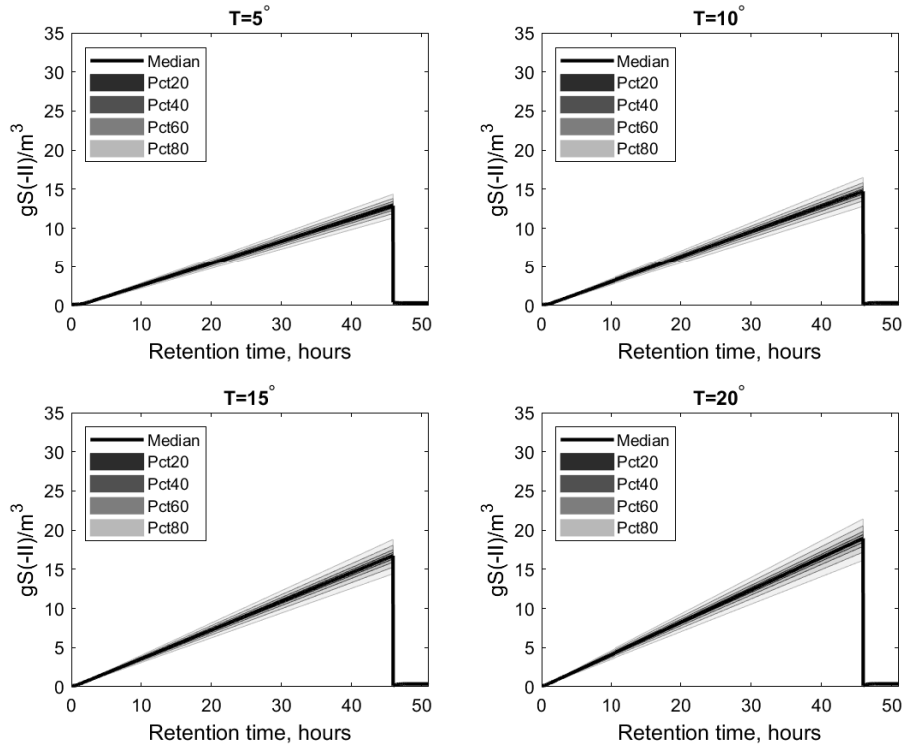Figure 11.28: Sulfide control, precipitation with Fe(II), ph=7, [Fe(II)]/[S(-II)] ratio = 2, dry conditions. Plots illustrate 20th to 80th percentiles from Monte Carlo simulations
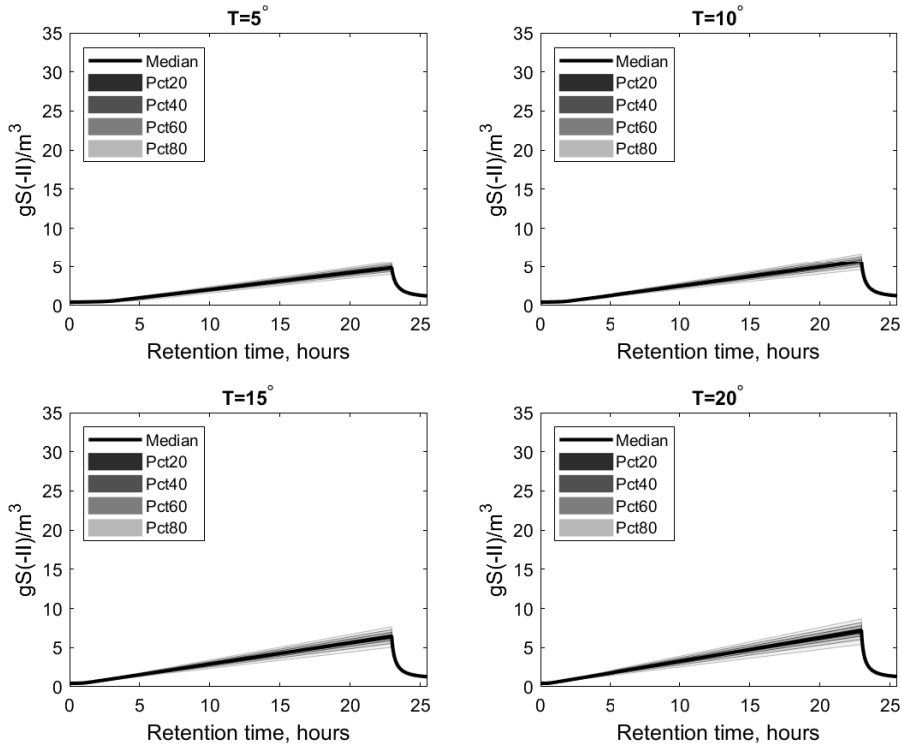
Figure 11.29: Sulfide control, precipitation with Fe(II), ph=6, [Fe(II)]/[S(-II)] ratio = 2, wet conditions. Plots illustrate 20th to 80th percentiles from Monte Carlo simulations

Figure 11.30: Sulfide control, precipitation with Fe(II), ph=7, [Fe(II)]/[S(-II)] ratio = 2, wet conditions. Plots illustrate 20th to 80th percentiles from Monte Carlo simulations

Figure 11.31: Sulfide control, precipitation with Fe(III), ph=6, [Fe(III)]/[S(-II)] ratio = 1.1, dry conditions. Plots illustrate 20th to 80th percentiles from Monte Carlo simulations
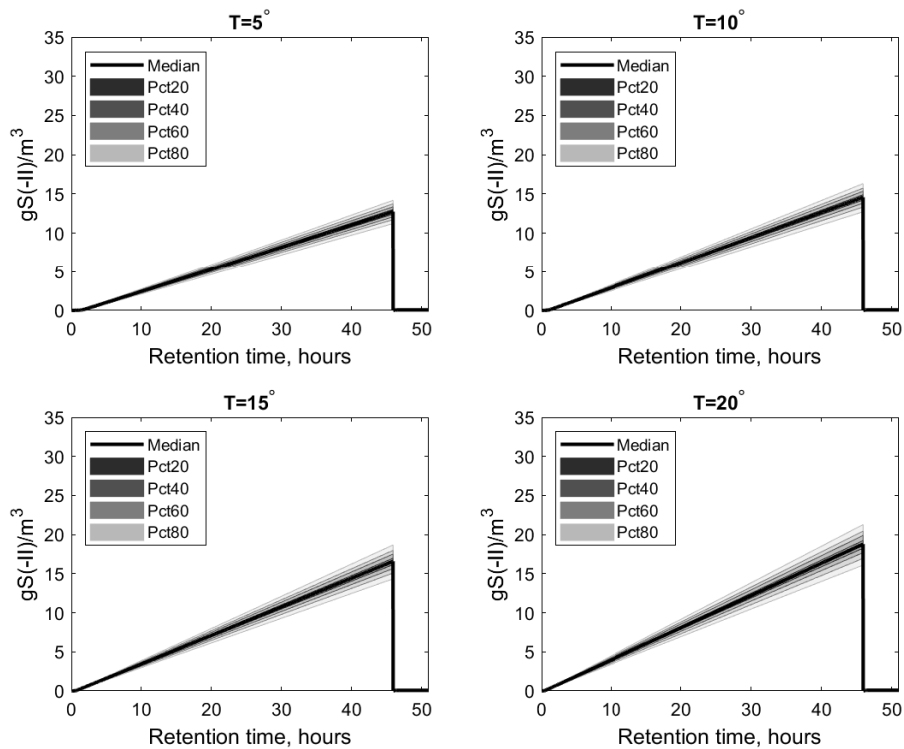

Figure 11.32: Sulfide control, precipitation with Fe(III), ph=7, [Fe(III)]/[S(-II)] ratio = 1.1, dry conditions. Plots illustrate 20th to 80th percentiles from Monte Carlo simulations
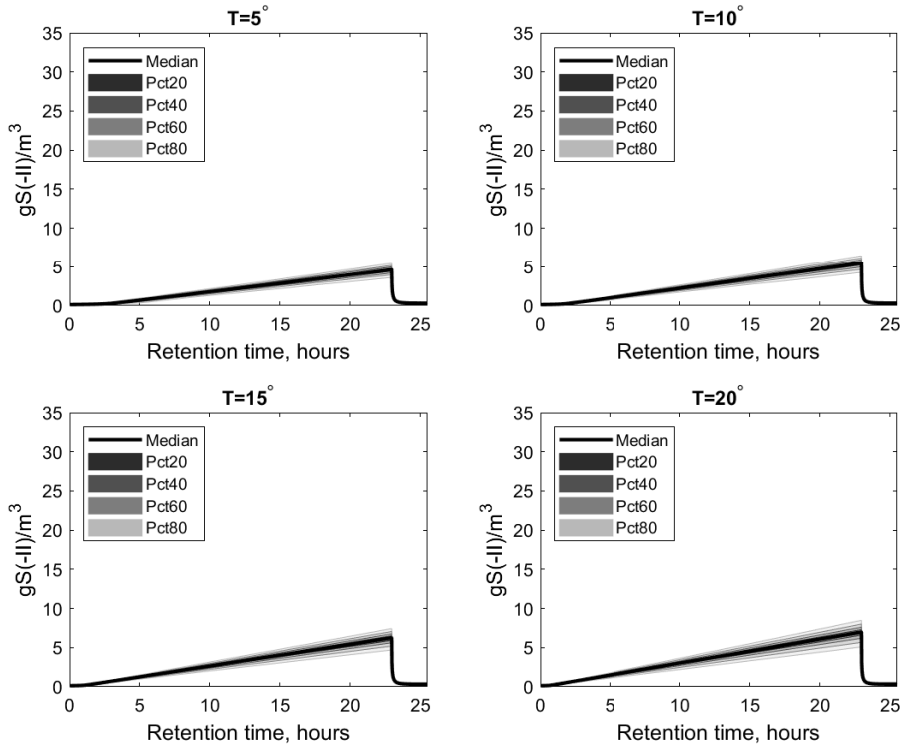
Figure 11.33: Sulfide control, precipitation with Fe(III), ph=6, [Fe(III)]/[S(-II)] ratio = 1.1, wet conditions. Plots illustrate 20th to 80th percentiles from Monte Carlo simulations
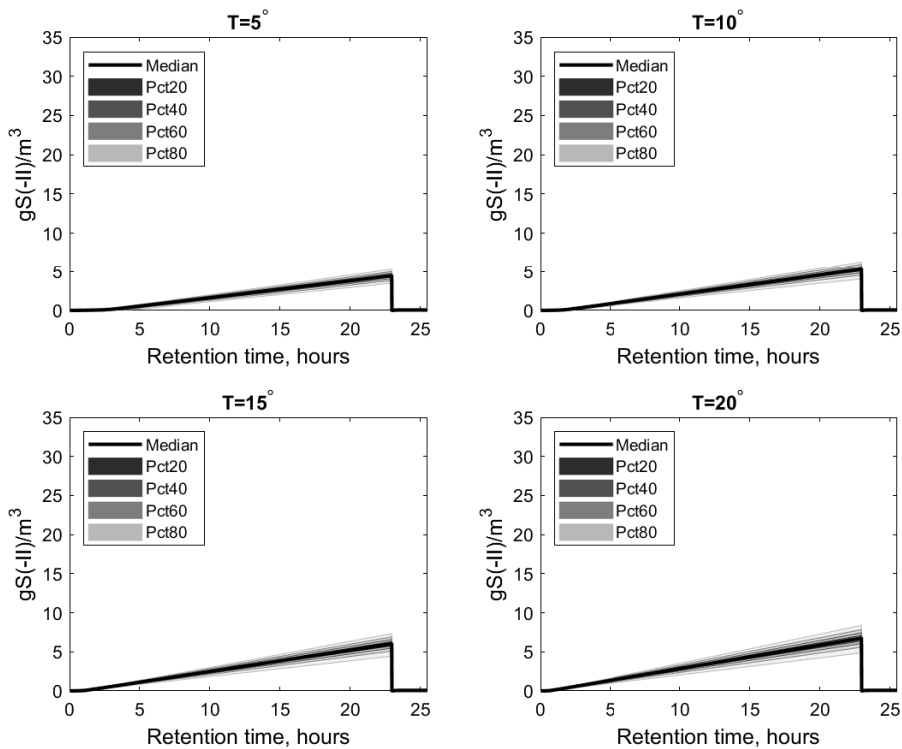

Figure 11.34: Sulfide control, precipitation with Fe(III), ph=7, [Fe(III)]/[S(-II)] ratio = 1.1, wet conditions. Plots illustrate 20th to 80th percentiles from Monte Carlo simulations
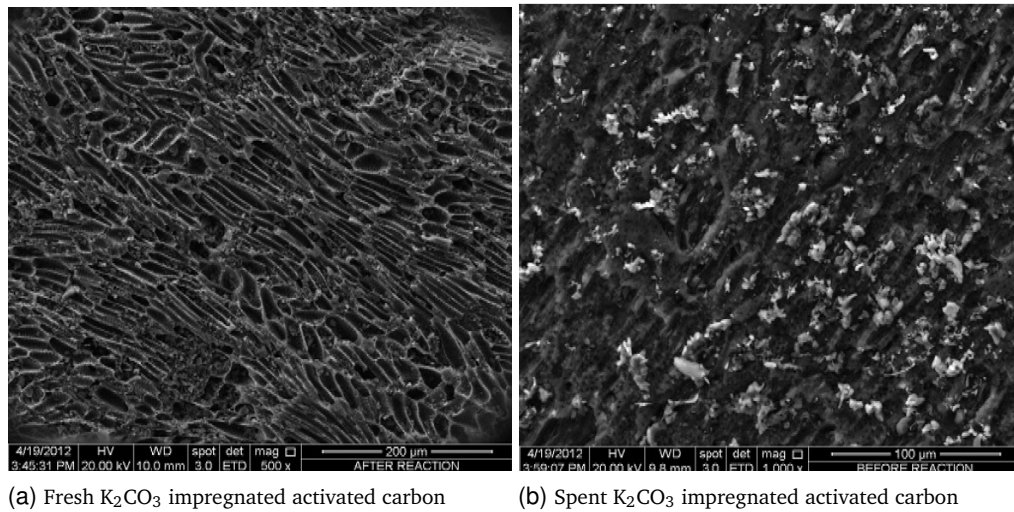
11.7 Scan of filter material for air filtering

(a) Fresh K$_2$CO$_3$ impregnated activated carbon   (b) Spent K$_2$CO$_3$ impregnated activated carbon

Figure 11.35: Scanning Electron Microscope (SEM) from filter material for air filtering, from Choo *et al.*, 2013

11.8 Net production of readily biodegradable substrate in the pressure main

Table 11.4: Concentrations of readily biodegradable substrates (S$_F$, S$_A$ and S$_S$) and change in net total readily biodegradable substrate (ΔS$_S$) from the start to the end of the pressure main. Initial concentrations under dry and wet conditions are as follows: S$_F$=23 g COD m^{-3}, S$_A$=13 g COD m^{-3} and S$_F$=13 g COD m^{-3}, S$_A$=7 g COD m^{-3} Data is based on medians from the plots presented in the appendix: Figure 11.15, Figure 11.16, Figure 11.17 and Figure 11.18

| T | Dry | | | | Wet | | | |
| C° | g COD m^{-3} | | | | g COD m^{-3} | | | |
	S$_F$	S$_A$	S$_S$	ΔS$_S$	S$_F$	S$_A$	S$_S$	ΔS$_S$
5	8	60	68	32	11	25	36	16
10	6	75	81	45	9	30	39	16
15	5	85	90	54	7	40	47	27
20	4	115	119	83	5	50	55	35

11.9 Supplementary data files

This thesis includes raw data used throughout the thesis in a .zip file, which is uploaded to the dedicated website of Aalborg University. Data is provided by the treatment plant, supervisor or collected during experiments and measurements.